Electronic Transport in Meso- and Nano-Scale Conductors

Prof. Gordey Lesovik

lesovik@phys.ethz.ch

HIT K 23.4

ETH Zürich

Herbstsemester 2008

For the latest (corrected!) version of the script please
visit our homepage:
http://www.itp.phys.ethz.ch/education/lectures_hs08/meso

If you find any mistakes please inform us (Fabian Hassler,
hassler@phys.ethz.ch or Ivan Sadovsky, sadovsky@phys.ethz.ch), such
that the quality of the script will increase.

Contents

Chapter 1

Introduction

This course is about electronic transport in meso- and nano-scale conductors. First, the words "meso" and "nano" will be defined. Then, we will provide specific examples of both fields (mostly mesoscopic physics). Nano-physics and nano-technology are very popular subjects nowadays. Nano-science deals with the creation and manipulation of objects whose size in at least one dimension is less than 100 nanometer ($1\,\mathrm{nm} = 10^{-9}\,\mathrm{m}$): for example, a graphene film is few nanometer thick whereas its other dimensions are of the order of a micrometer. Figure 1.1 shows typical length scales in meso- and nano-physics. According to this rule, various things got the name "nano". An old nano-device is the scanning tunneling microscope (STM), cf. Fig. 1.2, with a resolution down to a few Å ($= 10^{-10}\,\mathrm{m}$). The STM exhibits generic features of a nano-system: a atomic (nano-) scale object, the tip of the STM, can be manipulated at the macroscopic scale; therefore, the system is tunable and incorporates both quantum and classical motion. Further examples of nano-systems studied today in the context of electronic transport are carbon nano-tubes and carbon nano-films (graphene) which are typical nano-system. Generically, "nano" refers to a fixed length scale (nanometer) in physics, biology, chemistry or material science. Depending on temperature, interaction, ..., nano-physics can incorporate different effects. In total, nano-physics is not so well restricted as the traditional meso-physics, which is defined as transport physics for which quantum effects become important, i.e., when the typical size of the object L is less than the typical inelastic length scale $L_{\mathrm{inelastic}}$, $L \lesssim L_{\mathrm{inelastic}}$, which may be the coherence length L_ϕ or the energy relaxation length L_{relax} depending on the system studied. Figure 1.3 shows typical examples of micro-, meso-, and macro-systems. The size

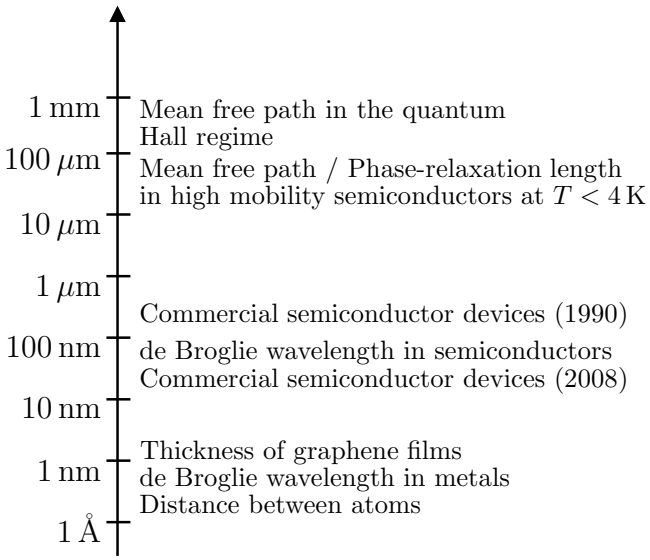

Figure 1.1: Typical length scales in meso- and nano-physics. Taken from S. Datta [1].

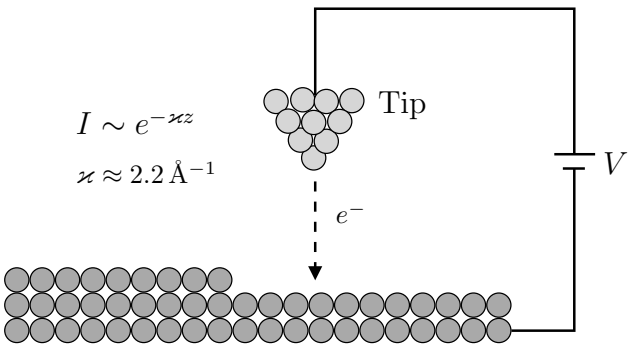

Figure 1.2: Sketch of an scanning tunneling microscope (STM). The STM probes the density of states of a material using the tunneling current which flows from the metal tip of the microscope to the surface. The tunneling current depends sensitively (exponential) from the distance of the tip to the surface; a resolution up to 0.1 nm is possible. For its development in 1981 The lateral resolution is limited by the size of the tip. The tip of a good STM is made of a single atom giving it a lateral resolution up to 1 nm. earned its inventors, Gerd Binnig and Heinrich Rohrer (at IBM Zürich), the Nobel Prize in Physics in 1986.

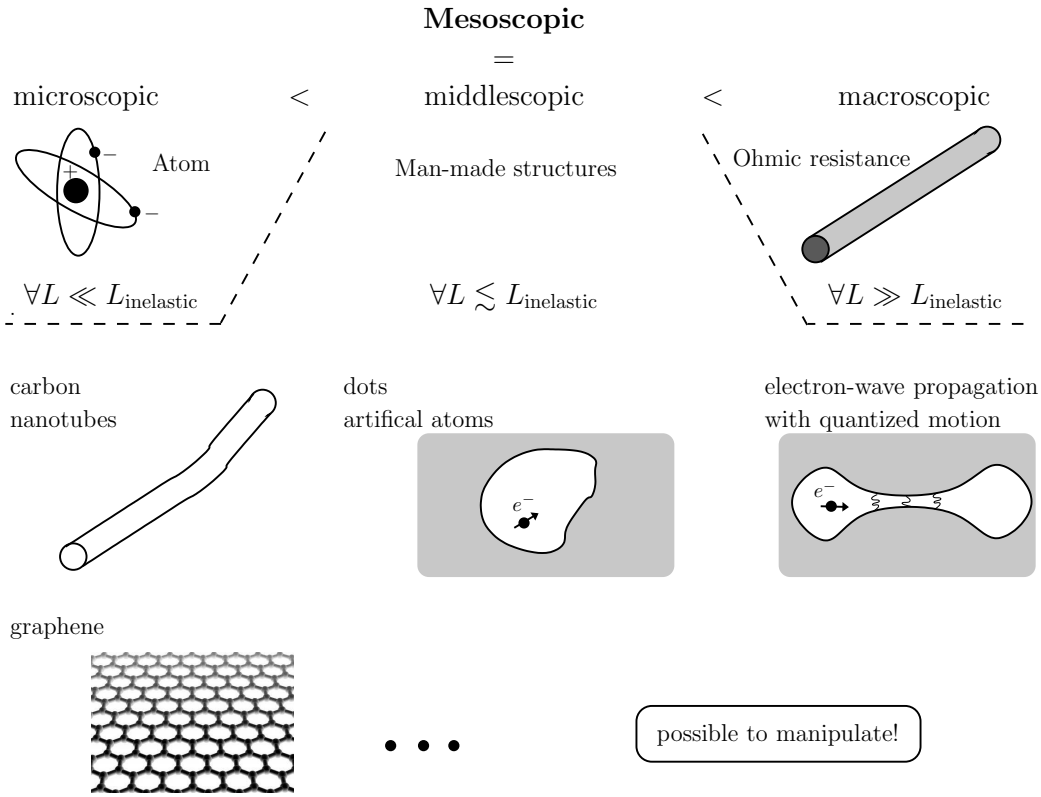

Figure 1.3: Length scale of micro-, meso-, and macro-scopic systems together with some examples.

of a meso-system is most of the time in the μm scale. However, sometimes mesoscopics crosses over to the new nano-physics.

Mesoscopic physics deals with subjects from quantum physics, e.g., interference, quantum statistics, and interaction. *Interference* plays a role in systems with continuous spectrum (complicated wave functions in dirty samples or in a chaotic dot). Furthermore, the discrete spectrum in quantum dots, metallic granule can be seen as an effect of interference. A famous example of interference is the Aharonov-Bohm ring with a possible which-path experiment. Unlike "classical" atomic physics, mesoscopic physics deals with many indistinguishable particles and, therefore, the consequences of the *quantum statistics* (Fermi, Bose, ...) become visible. In general, *interaction* effects play a more important role in mesoscopic systems which are essentially zero dimensional (0D) compared to physics in 2D and 3D bulk material. Moreover, new effective particles (quasiparticles) which appear in interacting

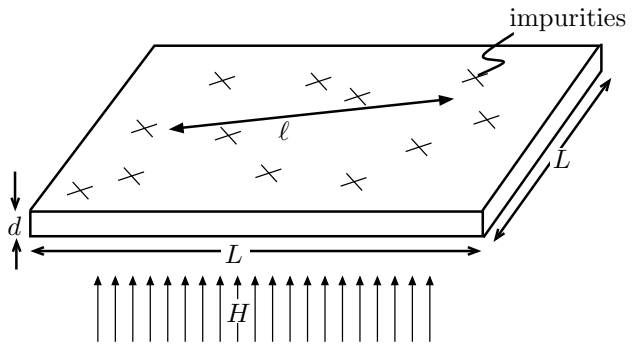

Figure 1.4: Dirty two-dimensional conductor. The crosses denote the position of the impurities which fluctuate from sample to sample. The mean free path is denoted by ℓ. An additional magnetic field H may be applied perpendicular to the sample.

many-body systems can be studied, e.g., spinons and holons in 1d Luttinger liquids or anyons in quantum Hall effect materials. Additionally, mesoscopic physics can shed light on fundamental problems in quantum mechanics, like the measurement problem (=interpretation of quantum mechanics) or nonlocality (Bell-type experiments). In the following, we will briefly discuss some interesting topics in meso- and nano-physics.

1.1 Conductance fluctuations

Mesoscopic physics, a relatively new subject, started in a narrow sense with the theoretical work by Altshuler who predicted strong fluctuations in the conductance G (in mesoscopic physics, the inverse resistance $G = 1/R$ and not the resistance R is the quantity which is typically studied) of quasi two-dimensional films [2], provided the conductor describes coherent transport of a dirty sample, i.e., quantum interference plays a role and the probability of an electron to reach the other side depends on the position of all impurities in the sample, cf. Fig. 1.4. Therefore, sample to sample fluctuations of the conductance are expected and the standard way to characterize fluctuations is by its variance

$$\langle \delta G^2 \rangle_{\rm im} = \langle (G - \langle G \rangle_{\rm im})^2 \rangle_{\rm im} \tag{1.1}$$

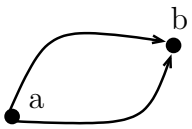

Figure 1.5: Two paths contributing to the conductance. The magnetic field induces an Aharonov-Bohm flux which changes the relative phase between these paths. The sensitivity with respect to the magnetic field (the change of the magnetic field which changes the conductance on the order G_0) is a magnetic flux quantum $\Phi_0 = hc/e$ over the area of the sample L^2.

where the subscript "im" denotes the average over all possible configurations of impurities and

$$\langle G \rangle_{\rm im} = dL\sigma/L \tag{1.2}$$

is the average conductance. Altshuler found that the standard deviation

$$\delta G = \sqrt{\langle \delta G^2 \rangle_{\rm im}} \approx G_0 \tag{1.3}$$

is universal and approximately given by the conductance quantum $G_0 = e^2/h$, with $h = 2\pi\hbar$. The relative fluctuations

$$\frac{\delta G}{\langle G \rangle_{\rm im}} \approx \frac{e^2}{h}\frac{1}{d\,\sigma} = \frac{3\pi}{2k_{\rm F}^2 d\,\ell} \tag{1.4}$$

do not depend on the system size L; here, we have inserted the Drude conductivity $\sigma = 2e^2k_{\rm F}^2\ell/3h\pi$ with ℓ the mean free path into Eq. (1.2). This result is surprising if one believes that quantum (or classical) self averaging should reduce relative fluctuations at large distances.

Nevertheless, it is a fact that self averaging is absent in a coherent mesoscopic sample. Soon, Lee and Stone considered fluctuations of the conductance as a function of the applied magnetic field or other external parameters [3]. The following argument provides an easy way to understand why the conductance will fluctuate with changing magnetic field: the conductance is proportional to the transfer probability $P_{a\to b}$ of an electron starting from the left side to reach the right side of the sample. The quantum mechanical probability (in the path integral picture) is the square of the sum of the amplitudes of all possible paths,

$$P_{a\to b} = |A_1 + A_2|^2 = |A_1|^2 + |A_2|^2 + A_1A_2^* + A_1^*A_2; \tag{1.5}$$

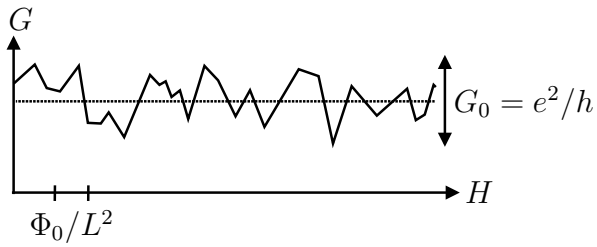

Figure 1.6: Conductance fluctuations due to changes in the applied magnetic field.

here, we consider for simplicity only two paths with amplitudes $A_{1,2}$, cf. Fig. 1.5. For the average probability $\langle P_{a\to b}\rangle_{\rm im}$, the cross-terms $A_1A_2^*$ and $A_1^*A_2$ vanish due to the fact that the relative phases are randomly distributed (except for special situations leading to the weak-localization corrections which we discuss later); the two probabilities simply add up $\langle P_{a\to b}\rangle_{\rm im} = |A_1|^2 + |A_2|^2 = P_1 + P_2$ without any interference. In the calculation of the second moment

$$\langle P_{a\to b}^2\rangle_{\rm im} \propto (P_1+P_2)^2 + 2|A_1|^2|A_2|^2 = \langle P_{a\to b}\rangle_{\rm im}^2 + 2P_1P_2, \tag{1.6}$$

terms with $A_1A_2^*$ and $A_1^*A_2$ also drop out while performing the impurity average. On the other hand, there is an additional term $2|A_1|^2|A_2|^2$ which does not average out. The standard deviation is given by

$$\delta P_{a\to b} = \sqrt{\langle (P_{a\to b} - \langle P_{a\to b}\rangle_{\rm im})^2\rangle_{\rm im}} = \sqrt{2P_1P_2}. \tag{1.7}$$

Now, if we apply even a weak magnetic field, the relative phases between all the paths change and the conductance changes. Thus, the conductance fluctuates in the same way as it would for different realizations of the impurity potential. A more detailed calculation shows that the standard deviation of the conductance fluctuation is of the order of the conductance quantum $G_0 = e^2/h$, cf. Fig. 1.6. Similar fluctuations in the conductance also appear as a function of voltage bias, cf. Fig. 1.7 [4].

1.1.1 Weak localization

The study of localization was pioneered by P.W. Anderson already in 1958 [5], i.e., long before the discovery of the conductance fluctuations. Depending on the strength of the disorder, one talks about strong or weak localization.

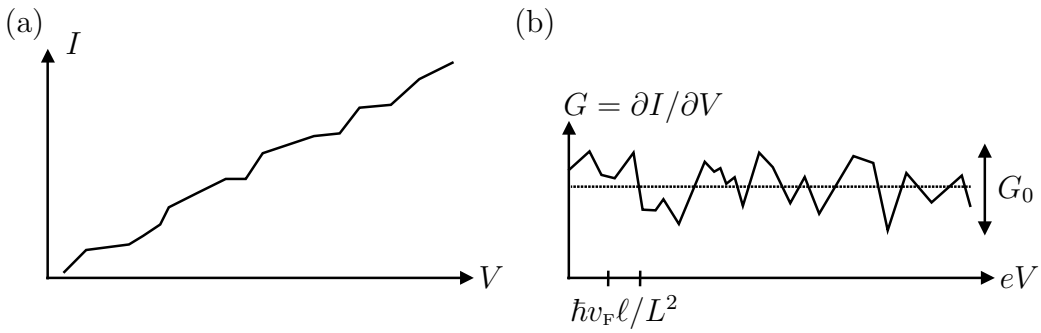

Figure 1.7: Fluctuations in the differential conductance due to variations of the applied voltage.

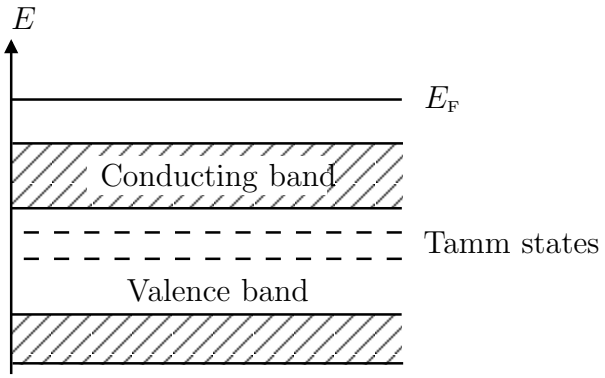

Figure 1.8: Typical band structure of a semiconductor. In the conduction and valence band, electronic states are extended (conducting). The Fermi level lies within the band gap where no bulk states exist. Nevertheless, there may by some surface- (Tamm-) state even within the band gap.

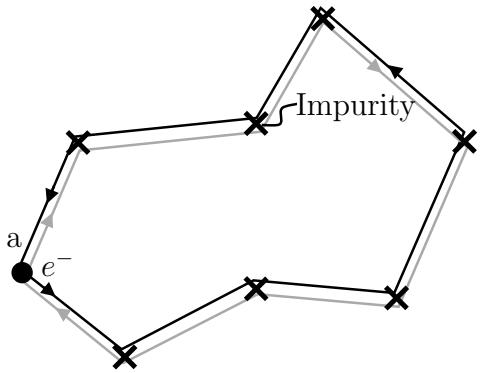

Figure 1.9: Paths responsible for weak localization.

Localization is an effect in dirty noninteracting electronic systems. In quasi three-, two-, or one-dimensional sample where the impurity potential is periodic (a crystal), a band structure appears as known from condensed matter physics, cf. Fig. 1.8. Electrons with energies lying in one of the bands propagate freely through the crystal, whereas electrons with energies in the gap do not propagate at all [except possible surface- (Tamm-) states]. What happens now if we randomly shift all these impurities a bit? In quasi one-dimensional systems, all states become localized. In three dimension a mobility edge forms, i.e., localized states appear only at the boundaries of the band. If we increase the disorder, more and more states become localized until, for strong disorder, all states become localized.

There are also corrections to transport due to localization physics before the system turns insulating, weak localization. Here, we are interested in the return probability $P_{a\to a}$ for an electron starting at the position a returning back after a certain time. The probability is the square of the sum of the amplitudes of all path. For simplicity, we consider again only two path (black and gray in Fig. 1.9): the black path goes counterclockwise (with amplitude $A_{\circlearrowleft}$), whereas the gray path is its time reversed analog which goes clockwise through the same set of impurities (with amplitude $A_{\circlearrowright}$). If time inversion symmetry is not broken, i.e., without an applied magnetic field, both amplitudes are the same $A_{\circlearrowleft} = A_{\circlearrowright} = A$. Hence, the return probability is given by (coherent backscattering)

$$P_{a\to a} = |A_{\circlearrowleft} + A_{\circlearrowright}|^2 = 4|A|^2, \tag{1.8}$$

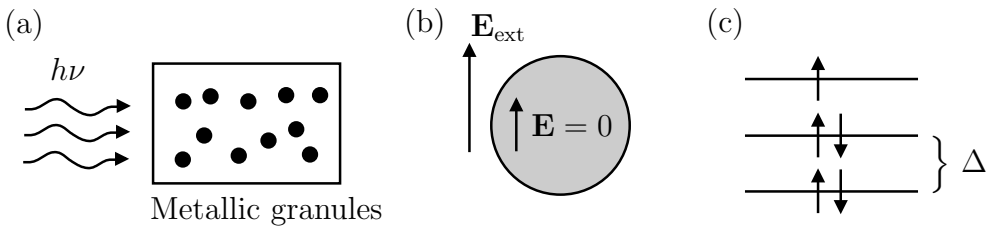

Figure 1.10: (a) Granules absorbs photons. (b) Vanishing electric field inside granule. (c) Energy levels in the granule.

while classically, one could expect (incoherent backscattering)

$$P_{a\to a}^{\text{classical}} = |A_{\circlearrowleft}|^2 + |A_{\circlearrowright}|^2 = 2|A|^2, \tag{1.9}$$

without any interference. To that effect, the usual diffusion is suppressed and the material less conducting. The application of a magnetic field breaks time reversal symmetry and the conductance rises. For a field $B \approx \Phi_0/\ell^2$, the backscattering is incoherent and the classical Drude result holds.

1.2 Complex systems with random level distribution

1.2.1 Absorption of radiation by metallic granules

Even before the discovery of localization, people studied systems which today may be called mesoscopic or nano-systems; an example is the polarizability of small metallic granules. It is known for a long time that an ultra dispersed media absorbs low-frequency radiation well, cf. Fig. 1.10(a). One may think about ultra dispersed media in terms of small metallic granules which are plugged into some nonconducting matrix. The reason for the absorption was (and still is in some respect) a big puzzle. Gorkov and Eliashberg (well-known for their work about superconductors) studied this system. Their idea was that each electrons moves quasiclassically in a granule occupying one of a set of discrete levels. The problem is that each level should be accounted for and it is difficult (if not impossible) to predict the location of the levels. They suggested to use the so-called Wigner-Dyson distribution for the levels (a result of random matrix theory [6, 7]) which was already successful in describing of the level distribution of big molecules, a nucleus,

or other complicated quantum objects where the spectrum is impossible to calculate from first principles. In the random matrix theory, the probability $P(\epsilon)$ to find two levels spaced by ε is given by

$$P(\varepsilon) \propto \left(\frac{\varepsilon}{\Delta}\right)^{\beta}, \tag{1.10}$$

where Δ is the mean level spacing [Fig. 1.10(c)] and the parameter β depends on the universality class: $\beta = 1$ if both time-reversal symmetry and spin-rotation symmetry are present, $\beta = 2$ if time reversal symmetry is broken, $\beta = 4$ if time-reversal symmetry is present and spin-rotation symmetry is absent [8]. Gorkov and Eliashberg predicted a large polarizability. It took the physics community several years to realize that they made a simple mistake: screening was neglected, and each electron was assumed to respond to the total applied electric field, cf. Fig. 1.10(b). However, if the granule is polarized completely, the electric field in this granule will be (almost) zero. Assuming that each electron would still feel the initial electric field, a huge dipole moment was obtained. Even though the theory was wrong, the idea to use random matrix theory was very stimulating. Evetov proved using his supersymmetric method that the level statistics indeed follows Eq. (1.10). In the middle of the 90s, Altshuler and Spivak reconsidered this problem. They solved it purely quantum mechanically, i.e., they did not assume that the electrons move quasiclassically and even the absorption process was taken into account quantum mechanically. Their calculation matches the experiment up to a reasonable accuracy.

1.2.2 Conductance fluctuations and Dorokhov distribution function

Having introduced the random matrix theory with the corresponding distribution of energy levels in the last section, we now take a look at the conductance and the conductance fluctuations of a diffusive quantum wire from a different perspective. As will be shown later, the conductance G of a quantum wire (waveguide) with N_{ch} channels (or propagating modes) is given by

$$G = N_{\mathrm{ch}} \frac{2e^2}{h} \langle T \rangle, \tag{1.11}$$

where $G_0 = e^2/h$ is the conductance quantum and the factor of 2 originates in the spin degeneracy. The transmission probability $\langle T \rangle$ is averaged over all

channels. The classically Drude conductance

$$G = \frac{S}{L}\sigma, \tag{1.12}$$

depends on the length L and the cross-section S of the wire; the conductivity σ is given by Kubo formula at zero frequency $\sigma = e^2\nu D$ [9, 10] with $-e$ the charge of an electron, ν the density of states at the Fermi energy, and $D = v_{\rm F}\ell/3$ the diffusion constant. Substituting the density of state of a free electron gas $\nu = mk_{\rm F}/\pi^2\hbar^2$ into Eq. (1.12), we obtain

$$G = \frac{S}{L}\, e^2 \frac{mk_{\rm F}}{\pi^2\hbar^2}\frac{v_{\rm F}\ell}{3} = \frac{2e^2}{h}\frac{Sk_{\rm F}^2}{\pi^2}\frac{\pi\ell}{3L}. \tag{1.13}$$

Note that number of channels in the wave-guide can be estimated quasiclassically as $N_{\rm channels} = Sk_{\rm F}^2/\pi^2$ (i.e., one channel per area $\pi^2/k_{\rm F}^2 = (\lambda_{\rm F}/2)^2$). Comparing Eq. (1.11) to Eq. (1.13), the average transmission probability is given by

$$\langle T\rangle = \frac{\pi\ell}{3L}, \tag{1.14}$$

i.e., the average transmission probability is of the order of ℓ/L, a quantity which approaches zero for $L \to \infty$. Does this mean that a typical transmission probability is of the order ℓ/L?. The answer is "no". Typically most channels are closed $T \approx 0$. Only $n = N_{\rm channels}\,\ell/L$ channels which are completely open with $T \approx 1$ carry most of the charge. The transmission probability T itself is distributed according to the Dorokhov distribution function [11, 12]

$$P(T) \propto \frac{1}{T\sqrt{1-T}}, \tag{1.15}$$

see Fig. 1.11. This result is general for a quasi one-dimensional diffusive wire with the total length smaller then localization length $L \ll L_{\rm loc}$, where the localization length can be estimated as $L_{\rm loc} \approx N_{\rm channel}\ell$, i.e., when the conductance becomes of the order of the conductance quantum $G_0 = e^2/h$. The switching between of the channels between *on* and *off* state is characterized by the standard deviation [2]

$$\delta G \approx \frac{e^2}{h}. \tag{1.16}$$

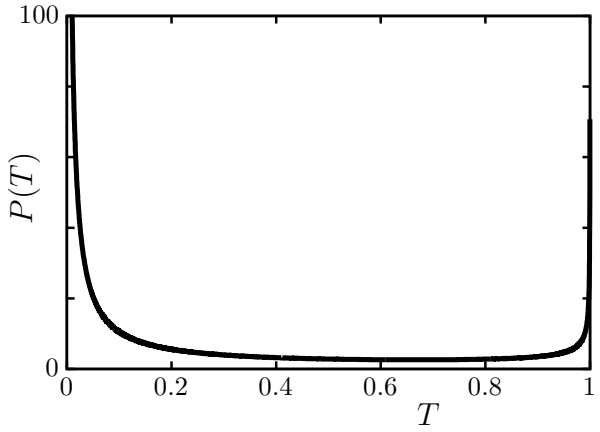

Figure 1.11: The Dorokhov $P(T)$ distribution is a bimodal distribution where T is most likely either 0 or 1.

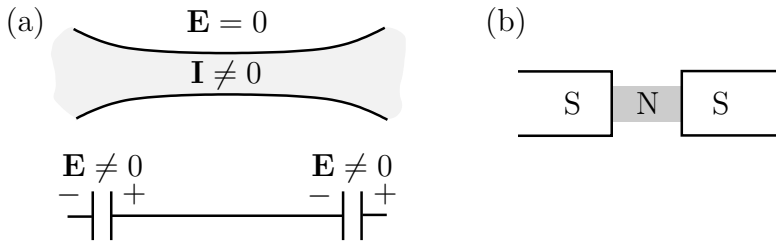

Figure 1.12: (a) A ballistic conductor, i.e., an adiabatic channel with voltage drops at the entry and exit. (b) A Josephson junction, i.e., a superconductor-normalconductor-superconductor interface. The current I through the Josephson junction is proportional to $\sin(\Delta\phi)$ where $\Delta\phi$ is the order-parameter phase- difference between the two superconductors, see [13].

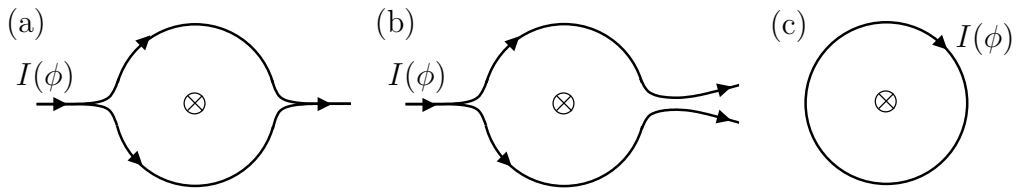

Figure 1.13: Setup of the Aharonov-Bohm effect with the magnetic flux Φ penetrating the ring: (a) With unavoidable back reflections at the second fork, (b) Without back reflections at the second fork due to the reflectionless four lead geometry. The picture (c) sketches the persistent current effect which appears in the same loop geometry without bias.

1.3 Nonlocality of quantum transport

1.3.1 Coherent conductors

Another important feature of mesoscopic transport and quantum transport in general is nonlocality. On the one hand, in classical transport theory, Ohm's law works and the local current density $\mathbf{j}$ is proportional to the local electric field $\mathbf{E}$

$$\mathbf{j}(\mathbf{E}) = \sigma \mathbf{E} \tag{1.17}$$

with the proportionality constant given by the conductivity σ. In particular, there is no response (current) without a driver (electric field). On the other hand, in quantum systems, it can well be that, even without electric field, there is a finite current flowing. In a sense this is trivial as electrons move ballistically; accelerating an electron at some point in the wire, it will move on forever. For a ballistic wire, the voltage drops at the entrance and the exit of the one dimensional wire where the electrons are accelerated, cf. Fig. 1.12(a). Nonetheless, there is a finite current flowing in the conductor. Another example in condensed matter are Josephson junctions (weak links) in superconductors, Fig. 1.12(b), where a current flows between two superconductors without an applied driving field (a gradient of the order parameter in this case).

1.3.2 Aharonov-Bohm effect

Another aspect of the nonlocality of quantum transport is the well-known Aharonov-Bohm effect [14]. In this case, the nonlocality enters via the fact

that the current depends on the total flux threaded by the loop. If two quantum wires enclose a solenoid producing a magnetic flux Φ, as shown in Fig. 1.13, a vector potential $\mathbf{A}$, but no driving forces ($\mathbf{E} = 0$, $\mathbf{H} = 0$) act at the location of the wire. The net effect of the vector potential on the electron wave-function is to accumulate phase ϕ_{A} on the path A and a different phase ϕ_{B} for the path B with $\Delta\phi = \phi_{\mathrm{A}} - \phi_{\mathrm{B}} = 2\pi\Phi/\Phi_0$ and $\Phi_0 = hc/e$ the magnetic flux quantum. In the simplest model, the current

$$I = |I_{\mathrm{A}} \cos\phi_{\mathrm{A}} + I_{\mathrm{B}} \cos\phi_{\mathrm{B}}| = \sqrt{I_{\mathrm{A}}^2 + I_{\mathrm{B}}^2 + 2I_{\mathrm{A}} I_{\mathrm{B}} \cos\Delta\phi} \tag{1.18}$$

is a superposition of the individual currents $I_{\mathrm{A,B}}$ with the corresponding phases $\phi_{\mathrm{A,B}}$. Figure 1.13 shows two possible experimental setups: in Fig. 1.13(a) back reflections at the second fork cannot be avoided and therefore some spurious resonances appear. This setup was realized experimentally [15, 16]. The situation in Fig. 1.13(b) is easier to analyze as back reflection are suppressed due to the four lead geometry in the second fork. Aharonov and Bohm were studying this setup exactly due to the fact that it shows nonlocal physics, a thing which is absent in classical mechanics.

1.3.3 Persistent current

Another nonlocal effect in mesoscopic physics is the persistent-current effect: applying simply a magnetic field through a ring, current starts to flow, see Fig. 1.13(c). Theoretically, this is expected, but in early experiments decoherence was strong enough to suppress this effect. In the case of a ballistic quantum wire, theory predicts the current to be given by

$$I \approx \frac{e v_{\mathrm{F}}}{L}, \tag{1.19}$$

with L is circumference of the ring which matches with experiments. For the diffusive case, the current is theoretically expected to be given by

$$I \approx \frac{e}{\tau_{\mathrm{D}}}, \tag{1.20}$$

where $\tau_{\mathrm{D}} = L^2/v_{\mathrm{F}}\ell$ is the diffusive traveling time around the ring. Interestingly, the value obtained experimentally [17] is much larger than the theoretical prediction. Over ten years, this discrepancy was tried to resolve without success. Recently, Schechter, Imry, *et al.* [18] have attempted to explain the magnitude of the persistent current with attractive pairing-interacting known from BCS superconductivity.

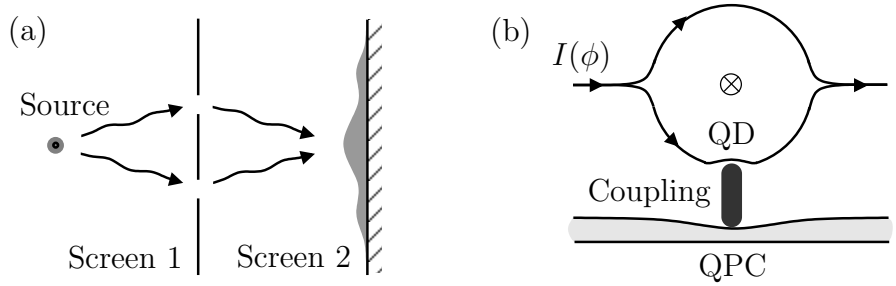

Figure 1.14: (a) Interference of the electrons in the double-slit experiment. (b) Mesoscopic which-path detector.

1.3.4 Which-path detector for electrons

A variation of the Aharonov-Bohm interferometer, closely related to the measurement theory, is the which-path detector. The version in the double-slit setup, is well-explained by Feynman in Ref. [13]: imagine a screen with two holes through which photons propagate behind which another screen is placed detecting the photons. If we assume that there is no decoherence and we do not detect through which slit the photon passes, an interference pattern will reveal itself on the detection screen. In contrast, if we detect through which hole the photons have passed, the interference is gone, i.e., only a single intensity maximum is observed. This Gedanken experiment, which is quite important for the development of quantum mechanics, was first checked in an experiment performed at Weizmann, Israel using the mesoscopic setup of an Aharonov-Bohm interferometer, cf. Fig. 1.13 [19]. The experiment was performed in a quasi two-dimensional electron gas which is realized in a GaAs-GaAlAs heterostructure. Applying an additional electrostatic potential by top gates, certain areas of the gas can be depleted such that the motion of the electrons can be further confined. To check the quantum coherence, the Aharonov-Bohm effect was measured, corresponding to the interference pattern in the double-slit experiment. In a next step, a quantum dot was introduced in one arm to detect the electron passing by using a capacitive coupling to a nearby quantum point contact; the current through the quantum point contact depends on the fact whether the electron is located in the dot or not. While performing the experiment, the Weizmann group observed that if the charge detector in the dot is sensitive enough to be sure that the electrons are detected then the interference pattern disappears.

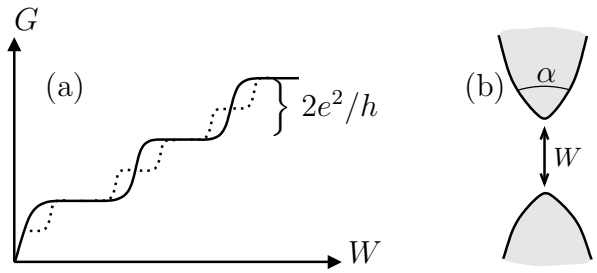

Figure 1.15: (a) Differential conductance as a function of the width of the quantum point contact. The width can be tuned by changing the gate voltage. The conductance rises in steps of $2e^2/h$ as more and more channels become conducting. Breaking the spin-degeneracy by introducing some Zeeman splitting half-plateaus are also observed (b) The quasiclassical approximation works for opening angles $\alpha \gg 1/\pi^2 \approx 2.5°$.

1.4 Conductance quantization in a quantum point contact

The conductance quantization in a quantum point contact (a constriction in a quantum conductor) is another interesting subject which will be treated later in this lecture in more detail. Here, we will present only the main ideas. The effect of the quantization of the conductance in a quantum point contact was first observed in 1988 [20, 21]. The quantization of the conductance appears due to the fact that when opening the constriction more an more by applying a gate voltage one channel after the other becomes transmitting. As each channel which is fully transmitting carries the conductance $2G_0 = 2e^2/h$ (the factor of two is due to the spin degeneracy), we expect steps in the conductance as a function of the width of the constriction [solid line in Fig. 1.15(a)].

This reasoning remains valid as long as we can treat the conductor quasiclassically, i.e., as long as the width of the sample acts as an effective potential on the motion of the particle along the wire. Interestingly, in the experiments the constriction was relatively short like in Fig. 1.15(b). Therefore, one might expect the quasiclassical approximation to break down. Regardless, in the experiments clear steps were observed. The puzzle was solved by Glazman, Lesovik, *et al.* [22] shortly after the experiments where published: the quasiclassical approximation is valid as long as the opening angle α is larger than

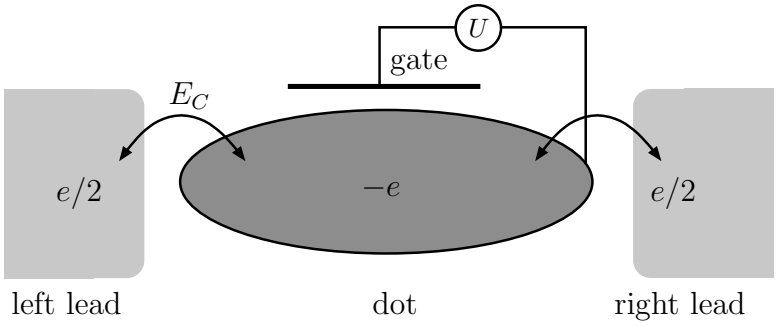

Figure 1.16: Setup leading to Coulomb blockade physics. The charge transport from the left to the right lead is blocked at certain values of the gate voltage.

$1/\pi^2$ and not larger than 1 as one might naïvely expect. When applying additionally an in-plane magnetic field, such that the orbital motion is not disturbed but a Zeeman splitting breaks the spin degeneracy, also steps of e^2/h were observed [dashed line in Fig. 1.15(a)] [21].

1.5 Coulomb blockade

Coulomb blockade was found in the 1980s by K.K. Likharev and co-workers. The effect is due to interaction of electrons and cannot be explained in a simple one particle picture. The Coulomb blockade describes the disappearance of current across a small object (quantum dot, granule, ...) with a large capacitance C because of a large charging energy $E_C = e^2/2C$ ($-e$ is the charge of the electron) on the island: the large charging energy suppresses the adding or removing of charge carriers on the island blocking the charge transport. The Coulomb blockade requires the charging energy E_C to be larger than other energy scales important for transport like the voltage bias eV or the temperature T.

Applying additionally a bias U, the number of particles can be tuned. Furthermore, it is possible to remove the Coulomb blockade electrostatically and thereby creating a single electron transistor (SET). A transistor is a device where the current across it depends sensitively on the applied gate voltage U. The electrostatic energy of n electrons on the island biased with

Figure 1.17: Scattering of an electron at a potential barrier.

a voltage U is given by

$$E_C(n, U) = \frac{(ne)^2}{2C} - neU. \tag{1.21}$$

It is possible to choose $U = U^*$ such that $E_C(n, U^*) = E_C(n+1, U^*)$, i.e., the electrostatic energy for n and $n+1$ particles is the same. Solving the equation for U^*, we obtain

$$U^* = \frac{e(2n+1)}{2C}. \tag{1.22}$$

At this value of the gate voltage, charges can flow. The sensitivity of the SET is given by $|\delta U| = e/2C$. It depends on the discrete nature of the charge. For vanishing charge quantization, $e \to 0$, the resistance would be just the sum of the two tunneling resistances combined in series. Already, this simple theory manages to explain the experimental results up to a reasonable accuracy.

1.6 Noise and the statistics of charge transport

In any conductor current and voltage fluctuate, the so-called noise. A fundamental source of noise is thermal (or Nyquist-Johnson) noise determined by the fluctuation-dissipation theorem. In nonequilibrium or in quantum systems, there are more sources of noise, shot-noise, flicker-noise, ...

Consider the quantum mechanical problem of scattering of an electron at a potential. In general, one part of the wave function is reflected (with amplitude r) and another is transmitted (with amplitude t). Probability conservation implies that the particle is either reflected (with probability $R = |r|^2$) or transmitted (with probability $T = |t|^2$), i.e., $R + T = 1$. It is important to note that quantum mechanics inevitably has a randomness associated with it; a single electron is either transmitted or reflected and quantum mechanics provides us with the probabilities for these events. Of course, this randomness produces noise the so-called shot (or partitioning) noise. Around 1989, Lesovik [23] and others [24–26] were able to derive the

spectral density at small frequencies and temperatures

$$S(0) = \int dt \, \langle I(t)I(0) - \langle I \rangle^2 \rangle = e\frac{2e^2}{h} VT(1-T) = e\langle I \rangle (1-T), \qquad (1.23)$$

of the current fluctuation induced by partitioning in a two-terminal conductor; here, V is the voltage applied across the conductor. The result was later on generalized to the multichannel and multilead case [25]. In Eq. (1.23) for shot noise, the charge quantum e appears explicitly, i.e., one can infer the value of the charge by measuring $S(0)$ and $\langle I \rangle$ knowing the transmission probability T. This fact was used to observe the fractional charge $e^* = e/3$ in the quantum Hall effect at filling $1/3$ as well as the charge $2e$ in superconducting systems.

For a ballistic two-terminal conductor, it is even possible to calculate the full probability distribution $P(Q_t)$ of the charge $Q_t = -ne$ transmitted during a given time t. Levitov and Lesovik demonstrated that the distribution (named full counting statistics) is given by

$$P(Q_t) = \binom{N}{n} T^n (1-T)^{N-n}, \qquad (1.24)$$

a result which is valid for long times where $N = eVt/h \gg 1$ [27, 28]. The distribution function is called binomial distribution. It can be obtained by a simple Bernoulli (coin tossing) process, where N is the number of attempts and T is the success probability. For dirty sample which are coherent, we can use Eq. (1.24) and averaging the transmission probabilities using the Dorokhov distribution Eq. (1.15) for the transmission eigenvalues.

1.7 Entanglement – Bell's inequality

Soon after the invention of the quantum mechanic, Einstein, Podolsky, and Rosen thought about a paradox which reveals strange correlations inherent in quantum mechanics which cannot be explained in classical terms [30]. We will present here Bohm's version of the Einstein-Podolsky-Rosen paradox: consider two particles (photons or electrons) with a spin degree of freedom created in singlet state. If these particles fly away from each other (particle 1 to position L and particle 2 to position R, see Fig. 1.18), their finale state is described by

$$|\Psi\rangle_{\mathrm{EPR}} = \frac{1}{\sqrt{2}} (|\uparrow\rangle_{\mathrm{L}} |\downarrow\rangle_{\mathrm{R}} - |\downarrow\rangle_{\mathrm{L}} |\uparrow\rangle_{\mathrm{R}}). \qquad (1.25)$$

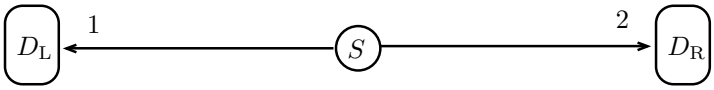

Figure 1.18: Bohm's version of the Einstein-Podolsky-Rosen experiment. Two particles are emitted from the source S in opposite directions residing in a singlet state. Later, their spin degree of freedom is detected along an arbitrary direction in the two detectors D_L and D_R. The correlation predicted by quantum mechanics and measured experimentally [29] cannot be explained by any local hidden-variable theory.

Performing a measurement on the first particle and measuring it at the location L in state $\uparrow$ ($\downarrow$), we know for sure that the second particle is in state $\downarrow$ ($\uparrow$). This correlation by itself could be produced by a classical fluctuating magnetic field which always acts in opposite direction along the measurement basis at the two position of the particles. The crucial point is that the quantum mechanical state described by Eq. (1.25) produces correlation in any measurement basis (the singlet is rotationally invariant) whereas the classical fluctuating magnetic field can reproduce the nonlocal correlations only in one basis. Bell proved that the quantum mechanical correlation cannot be obtained by any local hidden-variable theory. The state $|\Psi\rangle_{\mathrm{EPR}}$ is an entangled state. Entangled states are the reason for the increased power of quantum computers with respect to their classical analogues. It is used, e.g., for cracking classical codes by factoring large prime number or generating quantum codes which are secure.

Bibliography

[1] S. Datta, *Electronic Transport in Mesoscopic Systems* (Cambridge University Press, 1995).

[2] B. L. Al'tshuler, *Fluctuations in the extrinsic conductivity of disordered conductors*, JETP Lett. **41**, 648 (1985).

[3] P. A. Lee and A. D. Stone, *Universal conductance fluctuations in metals*, Phys. Rev. Lett. **55**, 1622 (1985).

[4] A. I. Larkin and D. E. Khmelnitsky, *Mesoscopic fluctuations of the current-voltage characteristic*, Sov. Phys. JETP **91**, 1815 (1986).

[5] P. W. Anderson, *Absence of diffusion in certain random lattices*, Phys. Rev. **109**, 1492 (1958).

[6] E. P. Wigner, *On the statistical distribution of the widths and spacings of nuclear resonance levels*, Proc. Cambridge Philos. Soc. **47**, 790 (1951).

[7] F. J. Dyson, *Statistical theory of energy levels of complex systems*, J. Math. Phys. **3**, 140 (1962).

[8] C. W. J. Beenakker, *Random-matrix theory of quantum transport*, Rev. Mod. Phys. **69**, 731 (1997).

[9] R. Kubo, *Statistical-mechanical theory of irreversible processes. 1. general theory and simple applications to magnetic and conduction problems*, J. Phys. Soc. Jpn. **12**, 570 (1957).

[10] D. A. Greenwood, *The Boltzmann equation in the theory of electrical conduction in metals*, Proc. Phys. Soc. London **71**, 585 (1958).

[11] O. N. Dorokhov, *Transmission coefficient and the localization length of an electron in n bound disordered chains*, JETP Lett. **36**, 318 (1982).

[12] O. N. Dorokhov, *On the coexistence of localized and extended electronic states in the metallic phase*, Solid State Commun. **51**, 381 (1984).

[13] R. P. Feynman, R. B. Leighton, and M. Sands, *The Feynman Lectures on Physics*, vol. 3 (Addison-Wesley, Reading, Massachusetts, 1965).

[14] Y. Aharonov and D. Bohm, *Significance of electromagnetic potentials in the quantum theory*, Phys. Rev. **115**, 485 (1959).

[15] A. Yacoby, M. Heiblum, V. Umansky, H. Shtrikman, and D. Mahalu, *Unexpected periodicity in an electronic double slit interference experiment*, Phys. Rev. Lett. **73**, 3149 (1994).

[16] R. Schuster, E. Buks, M. Heiblum, D. Mahalu, V. Umansky, and H. Shtrikman, *Phase measurement in a quantum dot via a double-slit interference experiment*, Nature **385**, 417 (1997).

[17] L. P. Lévy, G. Dolan, J. Dunsmuir, and H. Bouchiat, *Magnetization of mesoscopic copper rings: Evidence for persistent currents*, Phys. Rev. Lett. **64**, 2074 (1990).

[18] M. Schechter, Y. Imry, Y. Levinson, and Y. Oreg, *Magnetic response of disordered metallic rings: Large contribution of far levels*, Phys. Rev. Lett. **90**, 026805 (2003).

[19] E. Buks, R. Schuster, M. Heiblum, D. Mahalu, and V. Umansky, *Dephasing due to which path detector*, Nature **391**, 871 (1998).

[20] B. J. van Wees, H. van Houten, C. W. J. Beenakker, J. G. Williamson, L. P. Kouwenhoven, D. van der Marel, and C. T. Foxon, *Quantized conductance of point contacts in a two-dimensional electron gas*, Phys. Rev. Lett. **60**, 848 (1988).

[21] D. A. Wharam, T. J. Thornton, R. Newbury, M. Pepper, H. Ahme, J. E. F. Frost, D. G. Hasko, D. Peacock, and D. A. Ritchie, *One-dimensional transport and the quantization of the ballistic resistance*, J. Phys. C **21**, L209 (1988).

[22] L. I. Glazman and A. V. Khaetskii, *Nonlinear quantum conductance of a point contact*, JETP Lett. **48**, 591 (1988).

[23] G. B. Lesovik, *Excess quantum noise in 2D ballistic point contacts*, JETP Lett. **49**, 592 (1989).

[24] V. A. Khlus, *Current and voltage fluctuations in microjunctions of normal and superconducting metals*, Sov. Phys. JETP **66**, 1243 (1987).

[25] M. Büttiker, *Scattering-theory of thermal and excess noise in open conductors*, Phys. Rev. Lett. **65**, 2901 (1990).

[26] Th. Martin and R. Landauer, *Wave-packet approach to noise in multichannel mesoscopic systems*, Phys. Rev. B **45**, 1742 (1992).

[27] L. S. Levitov and G. B. Lesovik, *Charge distribution in quantum shot noise*, JETP Lett. **58**, 230 (1993).

[28] L. S. Levitov, H. W. Lee, and G. B. Lesovik, *Electron counting statistics and coherent states of electric current*, J. Math. Phys. **37**, 4845 (1996).

[29] A. Aspect, J. Dalibard, and G. Roger, *Experimental test of bell's inequalities using time- varying analyzers*, Phys. Rev. Lett. **49**, 1804 (1982).

[30] A. Einstein, B. Podolsky, and N. Rosen, *Can quantum-mechanical description of physical reality be considered complete?*, Phys. Rev. **47**, 777 (1935).

Chapter 2

Scattering problems in one dimension

2.1 Plane waves – Scattering states

In one dimension, the Schrödinger equation is given by

$$\left[-\frac{\hbar^2}{2m}\frac{d^2}{dx^2} + V(x)\right]\Psi(x) = E\,\Psi(x), \tag{2.1}$$

with m the mass of the particle and $V(x)$ the potential energy. For a free particle with $V(x) = 0$ at energy $E > 0$, the solution can be written as $\Psi(x) = a_{\mathrm{L}}e^{ikx} + a_{\mathrm{R}}e^{-ikx}$ with the wave vector $k = \sqrt{2mE}/\hbar$: this corresponds to two plane waves, one (with the amplitude a_{L}) incoming from the left and the other (with the amplitude a_{R}) incoming from the right. Adding a potential $E \to E - V(x)$ with $V(x) \to 0$ for $|x| \to \infty$, the plane-wave solutions $e^{\pm ikx}$ develop into scattering states of the form

$$\Psi_{\mathrm{L}}(x) = \begin{cases} e^{ikx} + r_{\mathrm{L}}e^{-ikx} & x \to -\infty \\ t_{\mathrm{L}}e^{ikx} & x \to \infty \end{cases} \tag{2.2}$$

for the right moving part and

$$\Psi_{\mathrm{R}}(x) = \begin{cases} t_{\mathrm{R}}e^{-ikx} & x \to -\infty \\ e^{-ikx} + r_{\mathrm{R}}e^{ikx} & x \to \infty \end{cases} \tag{2.3}$$

for the left moving part; here, $t_{\mathrm{L/R}}$ ($r_{\mathrm{L/R}}$) are transmission (reflection) amplitudes of the scattering problem.

2.1.1 Unitarity

Due to the fact that Eqs. (2.2) and (2.3) are stationary states, no charge accumulation can happen and the current

$$I(x) = -i\frac{q\hbar}{2m}[\Psi(x)^*\Psi'(x) - \Psi'(x)^*\Psi(x)] \tag{2.4}$$

has to be constant, $I(x) = \text{const}$. Assuming the system to be in state Ψ_L, the condition for constant current implies

$$1 - |r_\text{L}|^2 = |t_\text{L}|^2, \tag{2.5}$$

where the right (left) hand side is the current for the asymptotic scattering state for $x \to \pm\infty$. Analogously, the condition for the right scattering state reads

$$1 - |r_\text{R}|^2 = |t_\text{R}|^2. \tag{2.6}$$

In general, the condition of constant current should also hold for arbitrary linear superpositions $\Psi(x) = a_\text{L}\Psi_\text{L}(x) + a_\text{R}\Psi_\text{R}(x)$ of the two scattering eigenstates. Setting the current on the asymptotic left side $x \to -\infty$ equal to the current on the asymptotic right side $x \to \infty$ yields

$$-a_\text{L}^* a_\text{R}\, r_\text{L}^* t_\text{R} - a_\text{R}^* a_\text{L}\, t_\text{R}^* r_\text{L} = a_\text{L}^* a_\text{R}\, t_\text{L}^* r_\text{R} + a_\text{R}^* a_\text{L}\, r_\text{R}^* t_\text{L}, \tag{2.7}$$

where we already used Eqs. (2.5) and (2.6) to get rid of the terms proportional to $|a_{\text{L/R}}|^2$. Equation (2.7) for all $a_{\text{L/R}}$ implies

$$r_\text{L}^* t_\text{R} = -t_\text{L}^* r_\text{R}. \tag{2.8}$$

This condition leads to the fact that $T = |t_\text{L}|^2 = |t_\text{R}|^2$, i.e., the transmission probability T is the same for both right and left moving scattering states; even more, for a time-reversal invariant Schrödinger equation of the form (2.1) without a vector potential, it can be shown that the transmission amplitudes themselves are equal,

$$t_\text{L} = t_\text{R}. \tag{2.9}$$

On the other hand, for a symmetric potential with $V(x) = V(-x)$ the reflection amplitudes agree, $r_\text{L} = r_\text{R}$. In general, all the amplitudes can be collected in a scattering matrix

$$S = \begin{pmatrix} r_\text{L} & t_\text{R} \\ t_\text{L} & r_\text{R} \end{pmatrix}, \tag{2.10}$$

which connects the ingoing to the outgoing parts of the scattering states at energy E. The conditions Eq. (2.5) to (2.8) simply mean that S is unitary.

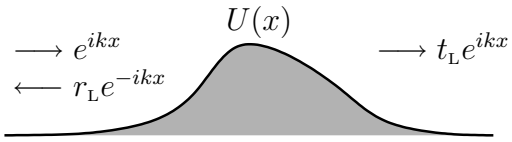

Figure 2.1: Quasiclassical scattering problem.

2.1.2 Current eigenstates

As the current is independent on the position x, it is also possible to find eigenstates of the current operator at a given energy E. Introducing the shorthand notation

$$\langle m|\tilde{I}|n\rangle = \frac{1}{2ik}[\Psi_m(x)^*\Psi_n'(x) - \Psi_m'(x)^*\Psi_n(x)] \tag{2.11}$$

for the dimensionless current $\tilde{I} = (m/\hbar k)I$, the task is to diagonalize the Hermitian matrix

$$\langle \mathrm{L,R}|\tilde{I}|\mathrm{L,R}\rangle = \begin{pmatrix} T & t_{\mathrm{L}}^* r_{\mathrm{R}} \\ r_{\mathrm{R}}^* t_{\mathrm{L}} & -T \end{pmatrix}, \tag{2.12}$$

which is $\tilde{I}$ expressed in the basis $\Psi_{\mathrm{L/R}}$. The eigenvalues, given by

$$\tilde{I}_0 = \pm\sqrt{T} \tag{2.13}$$

belong to the eigenstates $\Psi_\pm$; the $\Psi_\pm(x)$ are the normalized states with the maximal (minimal) currents possible.

2.1.3 Quasiclassical Approximation

The quasiclassical or WKB (Wentzel-Kramers-Brillouin) method is a way to solve the Schrödinger Eq. (2.1) for slowly varying potentials $V(x) = U(x)$, cf. Fig. 2.1; for one dimensional problems it assumes a particularly simple form. To derive it, we plug the Ansatz $\Psi(x) = A(x)\exp[iS(x)/\hbar]$ into Eq. (2.1), and obtain (for the real and imaginary part)

$$S'(x)^2 - 2m[E - U(x)] = \hbar^2 \frac{A''(x)}{A(x)} \quad \text{and} \quad [A(x)^2 S'(x)]' = 0. \tag{2.14}$$

The latter equation is easily integrated, $A(x) = \mathrm{const}/\sqrt{S'(x)}$. Inserting this solution into the former equation, yields

$$S'(x)^2 - 2m[E - U(x)] = \hbar^2 \left[\frac{3}{4}\left(\frac{S''(x)}{S'(x)}\right)^2 - \frac{1}{2}\left(\frac{S'''(x)}{S'(x)}\right)\right] \tag{2.15}$$

To obtain the WKB approximation, we expand $S(x)$ in $\hbar^2$,

$$S = S_0 + \hbar^2 S_1 + \hbar^4 S_2 + \ldots, \tag{2.16}$$

and insert this expansion into Eq. (2.15). To 0^{th} order, we obtain

$$S_0'(x)^2 = 2m[E - U(x)] \rightarrow S_0(x) - S_0(x_0) = \pm \int_{x_0}^{x} dx\, p(x) \tag{2.17}$$

where the local momentum is given by $p(x) = \sqrt{2m[E - U(x)]}$. Calculating the next order, one can check that the quasiclassical approximation is valid whenever $|\partial_x[\hbar/p(x)]| \ll 1$, i.e., the wave length does not change considerably on the length of one period. To sum up, in quasiclassical approximation the wave function of a particle at energy E is given by

$$\Psi(x) = \frac{C}{\sqrt{|p(x)|}} e^{i\int^x dx\, p(x)/\hbar} \tag{2.18}$$

with C an undetermined constant fixed by the asymptotic (or normalization) condition.

2.1.4 Accounting for a vector potential

In classical mechanics, there is no effect of a magnetic field on a particle whose motion is restricted in one dimension. Similarly, in quantum mechanics, a time-independent vector potential $A(x)$ in the Schrödinger equation

$$\left\{ -\frac{1}{2m}\left[-i\hbar\frac{d}{dx} - \frac{q}{c}A(x) \right]^2 + V(x) \right\} \Psi(x) = E\Psi(x) \tag{2.19}$$

can be gauged away; here, q (m) is the charge (mass) of the particle and c is the speed of light. Let $\Psi^{(0)}(x)$ be a solution of Eq. (2.19) with $A(x) = 0$, then

$$\Psi(x) = \exp\left[i\frac{q}{\hbar c} \int^x dx'\, A(x') \right] \Psi^{(0)}(x) \tag{2.20}$$

is a solution with $A(x) \neq 0$. Therefore, the application of a magnetic field yields only an additional phase. The transmission and reflection probabilities remain unchanged.

2.1.5 Linear spectrum and scalar potential

The one dimensional Fermi sea has the particular property that low-energy excitations moving to the right follow the dispersion $E = v_{\mathrm{F}}p$ with v_{F} the Fermi velocity. With certain restrictions, this approximation on the spectrum is valid. Assuming a linear spectrum, we can write down the time-dependent Schrödinger equation

$$[i\hbar\frac{\partial}{\partial t} - q\,\varphi(x,t)]\Psi(x,t) = v_{\mathrm{F}}[-i\hbar\frac{\partial}{\partial x} - \frac{q}{c}A(x,t)]\Psi(x,t) \tag{2.21}$$

for a particle in a dynamical electric- (φ) and magnetic- (A) potential. Knowing the solution $\Psi^{(0)}(x,t) = \exp[ik(x - v_{\mathrm{F}}t)]$ for $\varphi = A = 0$, the wave function

$$\Psi(x,t) = \exp\left\{\frac{iq}{\hbar c}\int_{x-v_{\mathrm{F}}t}^{x} dx'\left[A\Big(x', t - \frac{x-x'}{v_{\mathrm{F}}}\Big) - \frac{c}{v_{\mathrm{F}}}\varphi\Big(x', t - \frac{x-x'}{v_{\mathrm{F}}}\Big)\right]\right\} \times \Psi^{(0)}(x,t) \tag{2.22}$$

is a solution of Eq. (2.21), i.e., all effects of the vector- and scalar potential can be incorporated in a time-dependent phase; there is no backscattering at a potential for arbitrary fields.

2.2 Wave packets

Both traveling and spreading of a wave packets are usually exemplified for a Gaussian packet as this is one of the only cases where all the integrals can be calculated exactly. Here, we want to present some general result which are valid for a wave packet with arbitrary shape. The motion of a wave packet is given by Ehrenfest theorem which implies that for average $\langle x\rangle$ of the position operator x the quantum version of Newton equation

$$m\frac{d^2\langle x\rangle}{dt^2} = -\Big\langle\frac{dU(x)}{dx}\Big\rangle. \tag{2.23}$$

is valid [1]. If we consider the time evolution of a wave packet, a wave function Ψ which is nonzero only in a small region around the average value $\langle x\rangle$. The average value of x changes in accordance with Eq. (2.23). Assuming that the shape of the packet does not change in time, the motion of the packet could be equalized with the motion of a classical particle and quantum mechanics would map trivially on classical mechanics. In general, this kind of reasoning

is wrong. Firstly, because the wave packet broadens and, secondly, in order that the motion of the center of the wave packet coincides with the motion of the classical particle, the following condition

$$\left\langle \frac{dU(x)}{dx} \right\rangle = \frac{dU(\langle x \rangle)}{d\langle x \rangle}, \tag{2.24}$$

should be satisfied.

Let us now consider the motion and broadening of a wave packet in details. The width of the packet is characterized by the variance $\langle (\Delta x)^2 \rangle = \langle x^2 \rangle - \langle x \rangle^2$ with $\Delta x = x - \langle x \rangle$. Expanding the right hand side of Eq. (2.23) around $\langle x \rangle$ for a small packet size $\langle (\Delta x)^2 \rangle$ up to second order, we obtain

$$m\frac{d^2\langle x \rangle}{dt^2} = -\frac{dU(\langle x \rangle)}{d\langle x \rangle} - \frac{1}{2}\frac{d^3U(\langle x \rangle)}{d\langle x \rangle^3}\langle (\Delta x)^2 \rangle - \dots \tag{2.25}$$

If the potential is changing slowly and the size of the packet is small,

$$\left| \frac{d^3U(\langle x \rangle)}{d\langle x \rangle^3}\langle (\Delta x)^2 \rangle \right| \ll \left| \frac{dU(\langle x \rangle)}{d\langle x \rangle} \right| \tag{2.26}$$

we can retain only the first term on the right hand side of Eq. (2.25). The equation of motion for the average $\langle x \rangle$ is then equal to the equation of motion of a classical particle,

$$m\frac{d^2\langle x \rangle}{dt^2} = -\frac{dU(\langle x \rangle)}{d\langle x \rangle}; \tag{2.27}$$

for example, in free space with $U(x) = 0$, the center of mass of the package moves inertially with a velocity $\langle v \rangle$ which does not change with time, that is

$$\langle x \rangle_t = \langle x \rangle_0 + \langle v \rangle t. \tag{2.28}$$

Next, we are interested in the time evolution of the spreading $\langle (\Delta x)^2 \rangle_t$: the Heisenberg equation of motion for the operator $(\Delta x)^2$ reads

$$\frac{d(\Delta x)^2}{dt} = \frac{\partial (\Delta x)^2}{\partial t} + \frac{i}{\hbar}[H, (\Delta x)^2] = -\frac{d\langle x \rangle^2}{dt} + \frac{i}{\hbar}[H, x^2]. \tag{2.29}$$

where $[A, B] = AB - BA$ is the commutator. Using the free particle Hamiltonian $H = p^2/2m$ with $[p, x] = i\hbar$ to evaluate the commutator

$$[H, x^2] = \frac{1}{2m}[p^2, x^2] = \frac{1}{2m}(p^2x^2 - x^2p^2) = \frac{\hbar}{im}(xp + px), \tag{2.30}$$

we obtain for first derivative with respect to time

$$\frac{d(\Delta x)^2}{dt} = \frac{xp+px}{m} - \frac{d\langle x\rangle^2}{dt} = \frac{xp+px}{m} - 2\langle v\rangle\langle x\rangle. \tag{2.31}$$

Writing down the Heisenberg evolution for the operator in Eq. (2.31)

$$\begin{aligned}\frac{d^2(\Delta x)^2}{dt^2} &= \frac{\partial}{\partial t}\left(\frac{d(\Delta x)^2}{dt}\right) + \frac{i}{\hbar}\left[H, \frac{d(\Delta x)^2}{dt}\right] \\ &= -\frac{d^2\langle x\rangle^2}{dt^2} + \frac{i}{\hbar}\left[H, \frac{xp+px}{m}\right].\end{aligned} \tag{2.32}$$

gives the second time derivative of the variance $(\Delta x)^2$. Inserting the commutator

$$\left[H, \frac{xp+px}{m}\right] = \frac{1}{2m^2}[p^2(xp+px) - (xp+px)p^2] = \frac{2\hbar p^2}{im^2}, \tag{2.33}$$

we obtain

$$\frac{d^2(\Delta x)^2}{dt^2} = \frac{2p^2}{m^2} - \frac{d^2\langle x\rangle^2}{dt^2} = \frac{2p^2}{m^2} - 2\langle v\rangle^2. \tag{2.34}$$

Now, as p^2 commutes with H, all higher order derivatives with respect to time vanish,

$$\frac{d^n(\Delta x)^2}{dt^n} = 0 \tag{2.35}$$

for all $n > 2$. The operator for the width of the wave packet evolves like

$$(\Delta x)_t^2 = (\Delta x)_0^2 + \left(\frac{xp+px}{m} - 2\langle v\rangle\langle x\rangle\right)t + \left(\frac{p^2}{m^2} - \langle v\rangle^2\right)t^2. \tag{2.36}$$

Taking the average yields

$$\langle(\Delta x)^2\rangle_t = \langle(\Delta x)^2\rangle_0 + \left(\frac{\langle xp\rangle + \langle px\rangle}{m} - 2\langle v\rangle\langle x\rangle\right)t + \left(\frac{\langle p^2\rangle}{m^2} - \langle v\rangle^2\right)t^2. \tag{2.37}$$

As $\langle(\Delta x)^2\rangle_t$ must be positive for all times, the coefficient of the linear term in t cannot be large; for typical initial wave packets, the term even vanishes and the expression simplifies to

$$\langle\Delta x^2\rangle_t = \langle\Delta x^2\rangle_0 + \langle(\Delta v)^2\rangle t^2, \tag{2.38}$$

with the velocity dispersion $\langle(\Delta v)^2\rangle = \langle v^2\rangle - \langle v\rangle^2$. Note that there is a part of the time evolution $t < 0$ where the wave packet shrinks and a part

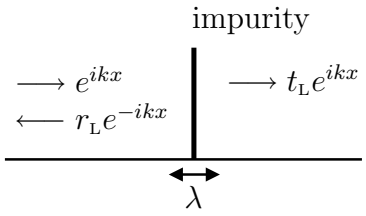

Figure 2.2: Delta-scattering potential. A potential can be approximated by a Dirac delta function when its range is smaller than the wavelength λ of the incident particle.

$t > 0$ where the wave packet expands. The only reason why one usually talks about the fact that wave packets smear out in time is the problem of preparing wave packets which contract. As stated before, quite generally, the initial condition corresponds to $t = 0$ and the wave packet will expand in time. The smearing of the wave packet coincides with smearing of a set of classical particles given an initial distribution with the same $\langle(\Delta x)^2\rangle_0$ and $\langle(\Delta v)^2\rangle$.

2.3 Scattering potentials

2.3.1 Delta scatterer – Impurity potential

To calculate the transmission amplitude through a delta scattering potential of the form $V(x) = V_0\delta(x)$ with $\delta(x)$ the Dirac delta function, the Schrödinger equation

$$\left[-\frac{\hbar^2}{2m}\frac{d^2}{dx^2} + V_0\delta(x)\right]\Psi(x) = E\Psi(x) \tag{2.39}$$

has to be solved. Away from $x = 0$, the solutions are of the form $e^{\pm ikx}$ with $k = \sqrt{2mE}/\hbar$. Thus, we make the Ansatz

$$\Psi(x) = \begin{cases} e^{ikx} + r_{\mathrm{L}} e^{-ikx} & x < 0 \\ t_{\mathrm{L}} e^{ikx} & 0 < x \end{cases}, \tag{2.40}$$

with t_{L} (r_{L}) the transmission (reflection) amplitude, cf. Fig. 2.2. The Schrödinger equation (2.39) implies the continuity of the solution $\Psi(0^-) = \Psi(0^+)$, i.e.,

$$1 + r_{\mathrm{L}} = t_{\mathrm{L}}. \tag{2.41}$$

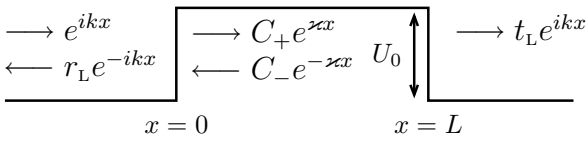

Figure 2.3: Tunneling under a rectangular barrier of length L and height U_0.

Different from the situation in Sec. 2.3.2, the first derivative of Ψ is not continuous due to the fact that the potential has a delta-function singularity; integrating Eq. (2.39) from 0^- to 0^+ yields the condition

$$-\frac{\hbar^2}{2m}\left[\Psi'(0^+) - \Psi'(0^-)\right] + V_0\Psi(0) = 0, \tag{2.42}$$

which implies

$$\frac{\hbar^2}{2m} ik(t_{\mathrm{L}} - 1 + r_{\mathrm{L}}) + V_0 t_{\mathrm{L}} = 0. \tag{2.43}$$

Together with Eq. (2.41), the transmission amplitude of the impurity

$$t_{\mathrm{L}} = \frac{ik}{ik + mV_0/\hbar^2}. \tag{2.44}$$

can be obtained. The transmission amplitude of the delta scatterer approaches zero for $k \to 0$; this a generic feature of the transmission for all scattering potentials.

2.3.2 Rectangular barrier

To describe the tunneling of a particle with energy E under a rectangular potential barrier of length L and height U_0, Fig. 2.3, we make the piecewise Ansatz

$$\Psi(x) = \begin{cases} e^{ikx} + r_{\mathrm{L}} e^{-ikx} & x < 0 \\ C_+ e^{\varkappa x} + C_- e^{-\varkappa x} & 0 < x < L \\ t_{\mathrm{L}} e^{ikx} & L < x \end{cases} \tag{2.45}$$

for the scattering wave function of the particle; here, $k = \sqrt{2mE}/\hbar$ and $\varkappa = \sqrt{2m(U_0 - E)}/\hbar$ are wave vectors in the appropriate regions. To find the solution of the tunneling problem, we have to match the wave functions and their derivatives at at $x = 0$

$$\Psi(0^-) = \Psi(0^+) \quad \longrightarrow \quad 1 + r_{\mathrm{L}} = C_+ + C_-, \tag{2.46}$$

$$\Psi'(x)|_{x=0^-} = \Psi'(x)|_{x=0^+} \quad \longrightarrow \quad ik(1 - r_{\mathrm{L}}) = \varkappa(C_+ - C_-), \tag{2.47}$$

and at $x = L$

$$\Psi(L^-) = \Psi(L^+) \quad \longrightarrow \quad C_+ e^{\varkappa L} + C_- e^{-\varkappa L} = t_{\mathrm{L}} e^{ikL} \tag{2.48}$$

$$\Psi'(x)|_{x=L^-} = \Psi'(x)|_{x=L^+} \quad \longrightarrow \quad \varkappa(C_+ e^{\varkappa L} - C_- e^{-\varkappa L}) = ikt_{\mathrm{L}} e^{ikL}. \tag{2.49}$$

By eliminating r and t from systems of equations (2.46) to (2.49), we obtain for coefficients C_+ and C_- in between,

$$C_\pm = \frac{2ik(\varkappa \pm ik)e^{\mp \varkappa L}}{(\varkappa + ik)^2 e^{-\varkappa L} - (\varkappa - ik)^2 e^{\varkappa L}}. \tag{2.50}$$

Inserting into $C_\pm$ into Eq. (2.49), we obtain the transmission amplitude

$$t_{\mathrm{L}} = \frac{4ik\varkappa}{(\varkappa + ik)^2 e^{-\varkappa L} - (\varkappa - ik)^2 e^{\varkappa L}} \, e^{-ikL}. \tag{2.51}$$

For long barriers, $\varkappa L \gg 1$, we can neglect the term proportional to $e^{-\varkappa L}$ in denominator of (2.51) and we obtain

$$t_{\mathrm{L}} = -\frac{4ik\varkappa}{(\varkappa - ik)^2} \, e^{-(\varkappa + ik)L}. \tag{2.52}$$

The transparency (transmission probability) $T = |t_{\mathrm{L}}|^2$ of the barrier is in this limit given by

$$T = \frac{16k^2\varkappa^2}{(k^2 + \varkappa^2)^2} \, e^{-2\varkappa L}. \tag{2.53}$$

Note that a quasiclassical analysis would only yield $e^{-2\varkappa L}$; the prefactor $16k^2\varkappa^2/(k^2 + \varkappa^2)^2$ is due to sharp edges of the barrier which violate the quasiclassical assumption.

Hartman effect

The Hartman effect describes the fact that the time a particle needs for tunneling through a long tunneling barrier does not depend on the length of the constriction [2]. Consider the propagation of a wave packet

$$\Psi(x,t) = \int \frac{dk}{2\pi} f(k) e^{ikx - i\hbar k^2 t/2m}, \tag{2.54}$$

where $f(k)$ is a function localized around k_0 and normalized according to $\int (dk/2\pi)|f(k)|^2 = 1$. The wave packet can be approximately written as

$$\Psi(x,t) \approx \int \frac{dk}{2\pi} f(k) e^{ikx - iv_0(k-k_0)t - i\hbar k_0^2 t/2m} \tag{2.55}$$

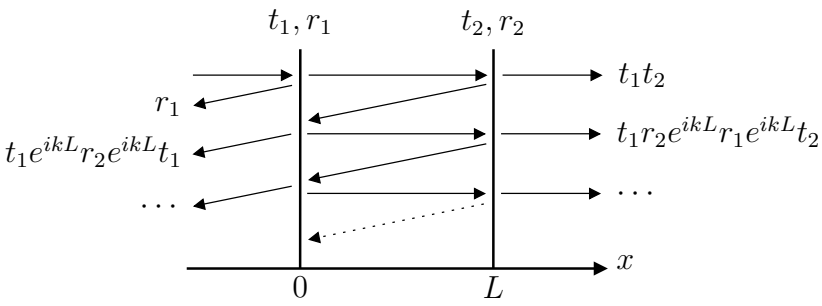

Figure 2.4: The double barrier (two potentials in series) can be thought of as an analog to the Fabry-Pérot interferometer in optics. The interference leads to resonances whenever $kL \approx \pi\mathbb{Z}$.

with $v_0 = \hbar k_0/m$. Thus

$$\Psi(x,t) \approx \Psi(x - v_0 t, 0) e^{i\hbar k_0^2 t/2m} \tag{2.56}$$

After the scattering ($t \to \infty$) at a potential with the transmission probabilities t_{L}, the transmitted part of the wave packet will have the form

$$\Psi(x,t) \approx \int \frac{dk}{2\pi} f(k) t_{\text{L}} e^{ikx - i\hbar k^2 t/2m} \tag{2.57}$$

Inserting the expression (2.52) for the rectangular barrier

$$t_{\text{L}} \approx -\frac{4ike^{-(\varkappa + ik)L}}{\varkappa} \tag{2.58}$$

in the limit ($k \ll \varkappa$, $\varkappa L \gg 1$), we may write

$$\Psi(x,t) \approx -\frac{4ike^{-\varkappa L}}{\varkappa} \Psi(x - vt - L, 0) e^{i\hbar k_0^2 t/2m}, \tag{2.59}$$

i.e., the particle tunneled through the barrier with length L without using any time. This effect is also tagged paradox, as traveling with a speed larger than light seems to be possible. The solution of this paradox can be seen due to the fact that still no fast information transfer is possible, as the probability that the particle actually tunnels through the barrier is exponentially suppressed.

2.3.3 Double barrier – Fabry-Pérot

The double barrier structure consists of two scattering potential in series. Because of the coherent nature of the transport, interference appears which

lead to transmission resonances (quasibound states). The transmission characteristics could be calculated using the formalism of last Section, i.e., wave function matching. Here, we want to employ a different approach and sum up the amplitudes of the different paths the particle can take. The setup is sketched in Fig. 2.4. The transmission amplitude is given by the series

$$t_{\text{L}} = t_1 t_2 + t_1 (r_2 e^{ikL} r_1 e^{ikL}) t_2 + t_1 (r_2 e^{ikL} r_1 e^{ikL})^2 t_2 + \dots \tag{2.60}$$

where the first term corresponds to a path traversing both barriers without being reflected, the second term corresponds to a path involving an additional round trip (bracket), and so on. Summing up the geometric series yields the transmission amplitude

$$t_{\text{L}} = \frac{t_1 t_2}{1 - r_1 r_2 e^{2ikL}}. \tag{2.61}$$

Note that $t_{\text{R}} = t_{\text{L}}$, as t_{R} can be obtained from Eq. 2.61 by swapping t_1 and t_2 and t_{L} is symmetric in t_1 and t_2. An interesting feature of the transmission amplitude is the fact that for a symmetric barrier with $t_1 = t_2$ the resonances at $kL \approx \pi\mathbb{Z}$ are perfect with $t_{\text{L}} = 1$; that is, even though the individual barriers are not perfectly transmitting, the whole device is. This effect is due to interference and serves as a clear feature of coherence. As soon as the coherence is lost, we expect $T \approx T_1 T_2$ which can be much less than unity. This effect is used in the experimental for checking of the coherence. Note that when $T < 1$, one can not decide, if the system coherent or not. The case $T = 1$ is the indication of coherence. Out of resonance

$$t_{\text{L}} = \frac{t_1 t_2}{1 + |r_1 r_2|}. \tag{2.62}$$

At $|t_{1,2}| \ll 1$ it gives $T \approx T_1 T_2/4$ so we see the effect of the destructive coherence in compare to incoherent case $T \approx T_1 T_2$.

In the same way, we can sum up the paths waves for the left reflection amplitude

$$r_{\text{L}} = e^{-ikL} r_1 + e^{-ikL} t_1 e^{ikL} r_2 e^{ikL} t_1 + e^{-ikL} t_1 e^{ikL} (r_2 e^{ikL} r_1 e^{ikL}) r_2 e^{ikL} t_1 + \dots \tag{2.63}$$

which yields

$$r_{\text{L}} = r_1 e^{-ikL} + \frac{t_1^2 r_2 e^{ikL}}{1 - r_1 r_2 e^{2ikL}} = \frac{r_1 e^{-ikL} + r_2 e^{ikL}(t_1^2 - r_1^2)}{1 - r_1 r_2 e^{2ikL}}. \tag{2.64}$$

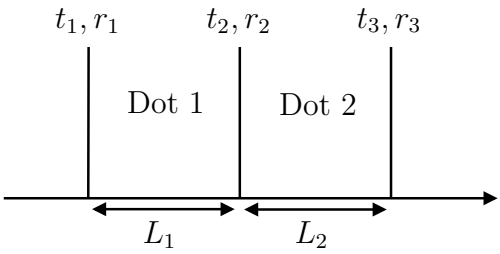

Figure 2.5: A double barrier can also be thought of as a quantum dot. Having three barriers in series models to a double dot system.

Using the unitarity relation $t_1^* r_1 = -t_1 r_1^*$ to rewrite the expression

$$t_1^2 - r_1^2 = -t_1 t_1^* \frac{r_1}{r_1^*} - r_1^2 = -\frac{r_1}{r_1^*}(t_1 t_1^* r_1 + r_1 r_1^*) = -\frac{r_1}{r_1^*}.$$

Inserting the result into Eq. (2.64), we obtain the reflection amplitude

$$r_{\text{L}} = \frac{1}{r_1^*} \frac{R_1 e^{-ikL} - r_1 r_2 e^{ikL}}{1 - r_1 r_2 e^{2ikL}} \tag{2.65}$$

The right reflection amplitude can be obtained from (2.65) by the replacement $1 \leftrightarrow 2$

$$r_{\text{R}} = \frac{1}{r_2^*} \frac{R_2 e^{-ikL} - r_1 r_2 e^{ikL}}{1 - r_1 r_2 e^{2ikL}} = \frac{1}{r_2^*} \frac{R_2 e^{-ikL} - r_1 r_2 e^{ikL}}{1 - r_1 r_2 e^{2ikL}}. \tag{2.66}$$

2.3.4 Double dot

A double dot system can be modeled by two resonances in series, cf. Fig. 2.5. This can be done in a similar fashion as in the last section. The idea is to use the result for the transmission $\tilde{t}_{23}$ and reflection $\tilde{r}_{23,\text{L}}$ amplitudes for 2nd and 3rd scatterers together

$$\tilde{t}_{23} = \frac{t_2 t_3}{1 - r_2 r_3 e^{2ikL_2}}, \quad \tilde{r}_{23,\text{L}} = \frac{1}{r_2^*} \frac{R_2 - r_2 r_3 e^{2ikL_2}}{1 - r_2 r_3 e^{2ikL_2}} \tag{2.67}$$

as a single object and insert them into the formula Eq. (2.61) for the double barrier, replacing t_2 and r_2, i.e.,

$$t_{\text{L}} = \frac{t_1 \tilde{t}_{23}}{1 - r_1 \tilde{r}_{23,\text{L}} e^{ikL_2} e^{2ikL_1}}, \tag{2.68}$$

where additional factor e^{ikL_2} in the denominator corresponds to the shift of the center of the effective barrier composed by 2nd and 3rd barriers. Note that we do not need for $\tilde{r}_{23,\mathrm{R}}$. Performing the substitution, we see that the transmission amplitude of the double dot t_{L} is given by

$$t_{\mathrm{L}} = \frac{t_1 t_2 t_3}{1 - r_1 r_2 e^{2ikL_1} - r_2 r_3 e^{2ikL_2} + r_1 r_3 (r_2/r_2^*) e^{2ik(L_1+L_2)}}. \tag{2.69}$$

2.4 Lippmann-Schwinger equation

In general, solving the scattering problem involves finding of a solution to the Schrödinger equation

$$\left[-\frac{\hbar^2}{2m}\Delta + U(x) + V(x)\right]\psi(x) = E\psi(x) \tag{2.70}$$

at the energy E in a potential $U(x)+V(x)$ with a given asymptotic form of the extended (nonnormalizable) wave function as the boundary condition. We take $U(x)$ to be a potential where we can solve the scattering problem exactly and think of $V(x)$ as a perturbation. In general, we assume that the potential $U(x) + V(x)$ goes to zero for $|x| \to \infty$ rapidly enough such that we can define an asymptotic wave vector $k = \sqrt{2mE}/\hbar$. The differential equation Eq. (2.70) with the appropriate boundary conditions can be formulated as an integral equation, called Lippmann-Schwinger equation. Rewriting Eq. (2.70) as

$$(E - H_0)\psi(x) = V(x)\psi(x), \tag{2.71}$$

with $H_0 = -\hbar^2\Delta/2m + U(x)$, we see that $V(x)\psi(x)$ can be treated as a inhomogeneity to the homogeneous Schrödinger equation $(E - H_0)\Psi(x) = 0$. Solving the fundamental equation

$$(E - H_0)G(x, x') = \delta(x - x') \tag{2.72}$$

for the outgoing Green's function $G(x, x')$ with $G(x, x') \sim e^{ik|x|}$ for $|x| \to \infty$, we can write the solution as

$$\psi_{\mathrm{L}}(x) = \Psi_{\mathrm{L}}(x) + \int dx'\, G(x, x')V(x')\psi_{\mathrm{L}}(x'), \tag{2.73}$$

where $\Psi_{\mathrm{L}}(x)$ is a scattering state (incoming from the left) of the unperturbed Schrödinger equation with $V(x) = 0$. For 1D systems, the Green's function

Figure 2.6: (a) Quantum point contact which is treated as unperturbed potential $U(x)$ for the Lippmann-Schwinger problem. (b) Quantum point contact with an additional delta scatterer. (c) Quantum point contact with a quantum dot (resonance).

is given by

$$G(x,x') = \frac{2m}{\hbar^2 w} \begin{cases} \Psi_{\rm L}(x)\Psi_{\rm R}(x') & x > x' \\ \Psi_{\rm R}(x)\Psi_{\rm L}(x') & x < x' \end{cases}, \tag{2.74}$$

and the Wronskian is given by

$$w = \Psi'_{\rm L}(x)\Psi_{\rm R}(x) - \Psi_{\rm L}(x)\Psi'_{\rm R}(x) = 2ikt_{\rm L}, \tag{2.75}$$

independent on x; the second equality $w = 2ikt_{\rm L}$ was obtained using the asymptotic form of the scattering states, Eqs. (2.2) and (2.3). In the free-particle case with $U(x) = 0$, the wave functions are given by $\Psi_{\rm L(R)}(x) = e^{\pm ikx}$ and $G(x,x') = me^{ik|x-x'|}/i\hbar^2 k$.

2.4.1 Impurity on a rectangular barrier

As an example, we study the situation in Fig. 2.6, i.e., a delta-scattering potential (impurity) at position x_0 on top of a constriction, cf. Fig. 2.6(b), i.e., long rectangular barrier of the form as in Fig. 2.3. Let $V = V_0\delta(x - x_0)$ and $U(x)$ be the potential of the constriction, see Fig. 2.6(a): the Lippmann-Schwinger equation (2.73) in this case reads as

$$\psi_{\rm L}(x) = \Psi_{\rm L}(x) + G(x,x_0)V_0\psi_{\rm L}(x_0). \tag{2.76}$$

which can be solved for $\psi_{\rm L}(x_0) = \Psi_{\rm L}(x_0)/[1 - V_0 G(x_0,x_0)]$. Thereby, the scattering wave function assumes the form

$$\psi_{\rm L}(x) = \Psi_{\rm L}(x) + \frac{G(x,x_0)V_0\Psi_{\rm L}(x_0)}{1 - V_0 G(x_0,x_0)}. \tag{2.77}$$

with $\Psi_{\mathrm{L}}(x)$ as in Eq. (2.45) and $\Psi_{\mathrm{R}}(x) = e^{-ikL}\Psi_{\mathrm{L}}(L-x)$. Inserting (2.74) and restricting to $x > x_0$, we obtain

$$\begin{aligned}\psi_{\mathrm{L}}(x) &= \left[1 + \frac{V_0\Psi_{\mathrm{R}}(x_0)\Psi_{\mathrm{L}}(x_0)}{\hbar^2 w/2m - V_0\Psi_{\mathrm{R}}(x_0)\Psi_{\mathrm{L}}(x_0)}\right]\Psi_{\mathrm{L}}(x) \\ &= \frac{1}{1-(2mV_0/\hbar^2 w)\Psi_{\mathrm{R}}(x_0)\Psi_{\mathrm{L}}(x_0)}\Psi_{\mathrm{L}}(x) \end{aligned} \tag{2.78}$$

Knowing the asymptotics of the wave function for the rectangular barrier, $\Psi_{\mathrm{L}}(x \to \infty) \sim t_{\mathrm{L}} e^{ikx}$, Eqs. (2.45), and defining the transmission amplitude $\tilde{t}$ as $\psi(x \to \infty)_{\mathrm{L}} \sim \tilde{t}_{\mathrm{L}} e^{ikx}$, we obtain a result for the transmission amplitude

$$\tilde{t}_{\mathrm{L}} = \frac{t_{\mathrm{L}}}{1 + i(mV_0/\hbar^2 k t_{\mathrm{L}})\Psi_{\mathrm{R}}(x_0)\Psi_{\mathrm{L}}(x_0)}, \tag{2.79}$$

where we set $w = 2ikt_{\mathrm{L}}$ and t_{L} is given by Eq. (2.51). To calculate $\tilde{t}_{\mathrm{L}}$ explicitly, we need to know t_{L} and $\Psi_{\mathrm{R}}(x_0)\Psi_{\mathrm{L}}(x_0)$. Starting from Eq. (2.52), the following results can be obtained easily in the limit $\varkappa L \gg 1$ and $\varkappa \gg k$:

$$t_{\mathrm{L}} = -\frac{4ik}{\varkappa}\, e^{-(\varkappa + ik)L},$$

and

$$\Psi_{\mathrm{L}}(x_0) = -\frac{2ik}{\varkappa}[e^{-\varkappa x_0} + e^{-\varkappa(2L - x_0)}]$$

Inserting these results into Eq. (2.79) and using the fact that $\Psi_{\mathrm{R}}(x_0) = e^{-ikL}\Psi_{\mathrm{L}}(L - x_0)$, we obtain

$$\tilde{t}_{\mathrm{L}} = \frac{t_{\mathrm{L}}}{1 + (mV_0/\hbar^2\varkappa)(1 + e^{-2\varkappa x_0} + e^{-2\varkappa(L-x_0)})}. \tag{2.80}$$

The transmission shows almost no dependence on the position of the resonance whenever x_0 in neither close to 0 nor L.

2.4.2 Rectangular potential and two impurities

The transmission through two impurities, cf. Fig. 2.6(c) can be calculated similar to the method in the last section. The potential assumes the form

$$V(x) = V_1\delta(x - x_1) + V_2\delta(x - x_2). \tag{2.81}$$

The Lippmann-Schwinger equation (2.73) simplifies to

$$\psi_{\mathrm{L}}(x) = \Psi_{\mathrm{L}}(x) + G(x, x_1)V_1\psi_{\mathrm{L}}(x_1) + G(x, x_2)V_2\psi_{\mathrm{L}}(x_2). \tag{2.82}$$

Which we will solve approximately by performing perturbation theory up to 2nd order (in V_1 and V_2). The zero order solution is given by the solution involving only the rectangular barrier,

$$\psi_{\mathrm{L}}^{(0)}(x) = \Psi_{\mathrm{L}}(x). \tag{2.83}$$

To first order, we plug (2.83) into the right hand side of the Lippmann-Schwinger equation (2.82), which yields

$$\psi_{\mathrm{L}}^{(1)}(x) = G(x, x_1)V_1\Psi_{\mathrm{L}}(x_1) + G(x, x_2)V_2\Psi_{\mathrm{L}}(x_2). \tag{2.84}$$

Going to second order, we obtain the solution, $x > L$,

$$\psi_{\mathrm{L}}^{(2)}(x) = \Psi_{\mathrm{L}}(x)\left(V_1\frac{2m\Psi_{\mathrm{R}}(x_1)}{\hbar^2 w}\psi_{\mathrm{L}}^{(1)}(x_1) + V_2\frac{2m\Psi_{\mathrm{R}}(x_2)}{\hbar^2 w}\psi_{\mathrm{L}}^{(1)}(x_2)\right), \tag{2.85}$$

for the particle incoming from the left.

Bibliography

[1] P. Ehrenfest, *Bemerkung üer die angenäerte Gütigkeit der klassischen Mechanik innerhalb der quantenmechanik*, Z. Phys. A **45**, 455 (1927).

[2] T. E. Hartman, *Tunneling of a wave packet*, J. Appl. Phys. **33**, 3427 (1962).

Chapter 3

Waveguides – Multi-channel scattering problems

Quasi one-dimensional systems are built by constricting the motions of the particles in the lateral dimensions (y, z) such that only the motion along x is allowed, cf. Fig. 3.1. The plane wave of last chapter are then replace by modes, i.e., plane waves with a lateral structure of a bound state. A waveguide can in general carry many modes. For low temperatures and strong constriction, only the lowest mode becomes important and we enter the regime of pure 1D transport discussed in the last section. In general, more than one mode needs to be taken into account.

3.1 Mode quantization

We will show in a simple example of a translation-invariant system (along x) how this mode quantization comes about. The problem to solve is the

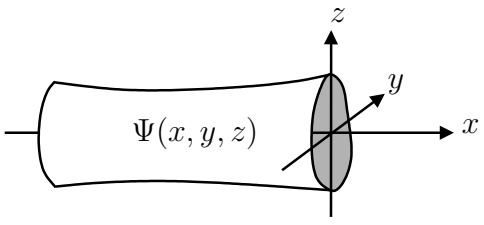

Figure 3.1: A waveguide, elongated along x, with an adiabatically changing shape.

stationary Schrödinger equation

$$\left[-\frac{\hbar^2}{2m}\Delta + V(x,y,z)\right]\Psi(x,y,z) = E\Psi(x,y,z), \tag{3.1}$$

where, at first, the potential $V(x,y,z) = V(y,z)$ and the boundary conditions are translation-invariant. Therefore, we can make the Ansatz $\Psi(x,y,z) = \chi(y,z)e^{ikx}$. Plugging this Ansatz in Eq. (3.1), the equation separates and the eigenvalue equation for the transversal part reads

$$\left[-\frac{\hbar^2}{2m}(\partial_y^2 + \partial_z^2) + V(y,z)\right]\chi_n(y,z) = E_n\chi_n(y,z) \tag{3.2}$$

with n the mode index and $\chi_n(y,z)$ the corresponding wave function. The eigenenergies E_n (the quantization energy) can be interpreted as the energy which is needed to generate the transversal structure. The transversal modes $\chi_n(y,z)$ form in general a complete

$$\sum_n \chi_n(y,z)\chi_n^*(y',z') = \delta(y-y')\delta(z-z') \tag{3.3}$$

and orthonormal

$$\int dydx\, \chi_m^*(y,z)\chi_n(y,z) = \delta_{mn} \tag{3.4}$$

set. Therefore, the general solution of Eq. (3.1) can be expanded in this set and is given by

$$\Psi(x,y,z) = \sum_n c_n\chi_n(y,z)e^{ik_nx}, \tag{3.5}$$

where $k_n = \sqrt{2m(E-E_n)}/\hbar$ is the wave vector of the n-th mode and c_n are constants. Depending on the energy E, the modes with $E_n > E$ do not propagate as the energy supplied is not enough for the transversal structure. These modes become evanescent modes which decay according to $e^{-\varkappa_n x}$ with $\varkappa_n = \sqrt{2m(E_n-E)}/\hbar$.

3.2 Scattering problems in waveguides

We consider a system which for $x \to \pm\infty$ is given by a regular (translational invariant) waveguide; the asymptotic states are given by Eq. (3.5). In the case there is an additional potential (or a change in boundary condition, as for example a constriction) around some position $x \approx x_s$ along the waveguide, we

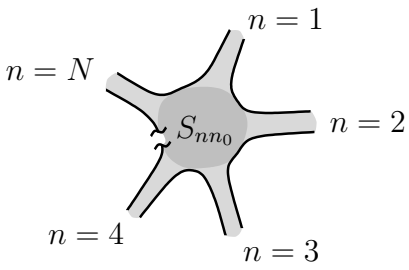

Figure 3.2: Multilead setup.

can formulate the problem as a scattering problem. Assuming an incoming state of the form

$$\Psi^{\text{in}}(x, y, z) = \chi_{n_0}(y, z)e^{ik_{n_0}x}, \tag{3.6}$$

the outgoing wave will have the general form

$$\Psi^{\text{out}}(x, y, z) = \sum_n S_{nn_0}\sqrt{\frac{k_{n_0}}{|k_n|}}\,\chi_n(y, z)e^{ik_n x} \tag{3.7}$$

where the sum over n runs of both the left-moving, transmitted states ($n > 0$, k_n) and the right-moving, reflected states ($n < 0$, $k_n = -k_{|n|}$). The additional factor $\sqrt{k_{n_0}/|k_n|}$ has been introduced to render the scattering matrix S_{nn_0} unitary; they normalize the asymptotic states $\chi_n(y, z)e^{ik_n x}/\sqrt{k_n}$ to carry unit current. In a similar fashion (replacing modes by leads) it is possible to discuss the multilead setup Fig. 3.2.

3.3 Adiabatic changing waveguides

In general, the boundary condition and the potential in Eq. (3.1) are not fully translational invariant. Nevertheless, in many cases the changes in the boundary condition or in the potential are slow compared to the length given by the wave length. In these cases, one can employ the so-called adiabatic approximation: we separate the motion in a fast (transversal) and a slow (longitudinal) part. The fast part is the eigenvalue equation

$$\left[-\frac{\hbar^2}{2m}(\partial_y^2 + \partial_z^2) + V(x, y, z)\right]\chi_n(x, y, z) = E_n(x)\chi_n(x, y, z); \tag{3.8}$$

for each cross section, cf. Fig. 3.1; the transversal quantization energy $E_n(x)$ becomes (slightly) x dependent. Assuming adiabaticity, we make the Ansatz

$$\Psi(x, y, z) = c_n\chi_n(x, y, z)\phi_n(x) \tag{3.9}$$

where $\phi_n(x)$ solves the equation

$$\left[-\frac{\hbar^2}{2m}\frac{d^2}{dx^2} + E_n(x)\right]\phi_n(x) = E\phi_n(x) \tag{3.10}$$

for the motion along the wire; note, that the eigenenergies $E_n(x)$ for the transversal (fast) mode serve as an effective potential for the motion along x (slow). Equation (3.9) serves as an approximate solution to the Schrödinger equation as long as we can neglect mode mixing.

As an example, we study the case of a two-dimensional electron gas (2DEG) (extended into x, y plane) which is furthermore confined in the y direction with the help of some gate voltages. In order to have a clear distinction between propagating and evanescent modes, we model the confinement via the boundary conditions $\Psi[x, \pm d(x)/2] = 0$, i.e., the electrons are only allowed in the strip of width $d(x)$ around the x axis. Assuming a slow change of $d(x)$, we obtain a transversal mode of the form

$$\chi_n(x, y) = \sqrt{\frac{2}{d(x)}}\sin\left[n\pi\,\frac{y + d(x)/2}{d(x)}\right] \tag{3.11}$$

with $E_n(x) = \hbar^2\pi^2n^2/2md(x)^2$, $n \geq 1$. The last (1D) degree of freedom $\phi_n(x)$ obeys the equation (3.10) i.e., it moves in an effective potential $E_n(x)$. To model a quantum point contact, Fig. 1.15(b), we set

$$d(x) = \frac{W}{L}\sqrt{x^2 + L^2} \tag{3.12}$$

with W (L) the width (length) of the constriction and $\alpha = 2\arctan(W/2L)$ the opening angle. The effective potential

$$E_n(x) = \frac{\hbar^2\pi^2L^2n^2}{2mW^2(x^2 + L^2)} \approx E_n(0) - \frac{m}{2}\Omega_n^2x^2 \tag{3.13}$$

is approximately quadratic close to the top of the barrier ($x = 0$) with the expansion coefficients

$$E_n(0) = \frac{\hbar^2\pi^2n^2}{2mW^2} \quad \text{and} \quad \Omega_n = \frac{\hbar\pi n}{mWL}.$$

The tunneling problem in a inverted parabola can be solved exactly [1]. The transmission probability in (3.13) is given by the Kemble formula

$$T_n(E) = \left[e^{2\pi[E_n(0)-E]/\hbar\Omega_n} + 1\right]^{-1}, \tag{3.14}$$

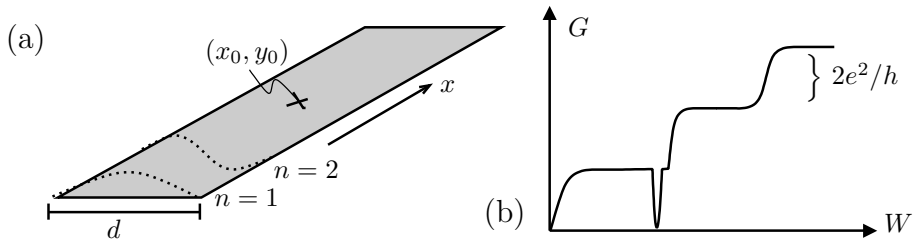

Figure 3.3: (a) A strip waveguide with an impurity scatterer at (x_0, y_0). (b) The transmission (conductance) of a quantum point contact showing a dip close to the opening of the second channel; this is due to resonant reflection by a quasibound state in the impurity potential.

a smeared step function which goes from 0 at $E < E_n(0)$ to 1 for $E > E_n(0)$ where the crossover happens in a range of the size of $\hbar\Omega_n/2\pi$. In order to observe steps in the conductance as a function of W, as depicted in Fig. 1.15, the width of the Kemble form $\hbar\Omega_n/2\pi$ should be much smaller than the separation between two steps $E_{n+1}(0) - E_n(0) \approx \hbar^2\pi^2 n/mW^2$, i.e.,

$$\frac{L}{W} \gg \frac{1}{2\pi^2} \approx 0.051. \tag{3.15}$$

Even for relatively short quantum point contacts, the quantization of the conductance is observable [2, 3].

3.4 Impurity in a waveguide

In this section, we consider an impurity in a 2D strip waveguide of size d, cf. Fig. 3.3(a). The goal is to qualitatively explain the dips below the conductance steps, cf. Fig. 3.3(b), in the measurement of the conductance through a quantum point contact. In order to have a clear distinction between propagating and evanescent modes, we model the quantum point contact as an infinite tube. We are interested in the situation where the electron has an energy E which is above the threshold for the first mode, but where the second mode is still evanescent, $E_1 < E < E_2$. The transverse modes are given by

$$\chi_n(y) = \sqrt{\frac{2}{d}} \sin\left[n\pi \frac{y + d/2}{d}\right], \tag{3.16}$$

with the threshold energies $E_n = \hbar^2\pi^2 n^2/2md^2$. The longitudinal wave functions assume the form

$$\phi_1(x) = e^{ik_1 x} \quad \text{and} \quad \phi_n(x) = e^{-\varkappa_n x}, n \geq 2 \tag{3.17}$$

where $k_1 = \sqrt{2m(E-E_1)}/\hbar$ and $\varkappa_n = \sqrt{2m(E_n - E)}/\hbar$. The Lippmann-Schwinger equation in 2D is the same as the one in Sec. 2.4,

$$\psi_{\mathrm{L}}(\mathbf{r}) = \Psi_{\mathrm{L}}(\mathbf{r}) + \int d^2r'\, G_E^{\mathrm{2D}}(\mathbf{r},\mathbf{r}')V(\mathbf{r}')\psi_{\mathrm{L}}(\mathbf{r}'), \tag{3.18}$$

with the 2D Green's function

$$G_E^{\mathrm{2D}}(\mathbf{r},\mathbf{r}') = \sum_{n\geq 1} \chi_n(y)\chi_n(y') G^{\mathrm{1D}}_{E-E_n}(x,x') \tag{3.19}$$

which separates in a projection on the transversal part and a 1D Green's function, cf. (2.72),

$$G^{\mathrm{1D}}_{E-E_1}(x,x') = \frac{m}{i\hbar^2 k_1} e^{ik_1|x-x'|} \text{ and } G^{\mathrm{1D}}_{E-E_n}(x,x') = -\frac{m}{\hbar^2\varkappa_n} e^{-\varkappa_n|x-x'|}. \tag{3.20}$$

As the delta potential in 2D leads to divergences, which are connected to the fact that it induces transitions to all modes, we take a regularized delta potential $V(\mathbf{r})$ which is V_0 for $\mathbf{r} \in [x_0 - a/2, x_0 + a/2] \times [y_0 - a/2, y_0 + a/2]$ and zero otherwise. Next, we plug the unperturbed wave function $\Psi_{\mathrm{L}}(\mathbf{r}) = \chi_1(y)\phi_1(x)$ together with the Ansatz

$$\psi_{\mathrm{L}}(\mathbf{r}) = \sum_{n\geq 1} c_n \chi_n(y)\phi_n(x) \tag{3.21}$$

(the transmission amplitude t_{L} is given by $t_{\mathrm{L}} = c_1$) into the Lippmann-Schwinger equation (3.18) with $x \to \infty$ and project it on the l-th mode (integrate against $\int dy\, \chi_l(y)\ldots$). As a result we obtain

$$c_l = \delta_{1l} + a^2 V_0 \sum_n \mathsf{A}_{ln} c_n, \tag{3.22}$$

where the matrix A is defined via

$$\begin{aligned}
\mathsf{A}_{1n} &= \frac{m}{i\hbar^2 k_1 a^2}\left[\int_{x_0-a/2}^{x_0+a/2} dx\, \phi_1(-x)\phi_n(x)\right]\left[\int_{y_0-a/2}^{y_0+a/2} dy\, \chi_1(y)\chi_n(y)\right], \\
\mathsf{A}_{ln} &= -\frac{m}{\hbar^2\varkappa_l a^2}\left[\int_{x_0-a/2}^{x_0+a/2} dx\, \phi_l(-x)\phi_n(x)\right]\left[\int_{y_0-a/2}^{y_0+a/2} dy\, \chi_l(y)\chi_n(y)\right].
\end{aligned} \tag{3.23}$$

The system of equation can be formally solved and we obtain

$$\mathbf{c} = [\mathbb{1} - a^2 V_0 \mathsf{A}]^{-1} \mathbf{c}^{(0)} \tag{3.24}$$

with $c_l^{(0)} = \delta_{1l}$, where the problem of inverting the infinite dimensional matrix A still remains. In the situation of Fig. 3.3(b) where the conductance shows a dip, a quasibound state in the second channel modifies the transmission through the first channel considerably [4]. For sake of simplicity, we take the energy to be close to the quantization energy in the second channel $E \lesssim E_2$. In this case only the first and second mode are important and the higher modes can be neglected. We retain only the 2×2 matrix

$$\mathsf{A} = \begin{pmatrix} \mathsf{A}_{11} & \mathsf{A}_{12} \\ \mathsf{A}_{21} & \mathsf{A}_{22} \end{pmatrix}$$

which can be easily inverted. Plugging it into Eq. (3.24), we obtain the transmission probability

$$t_{\text{L}} = c_1 = 1 - \frac{i\tilde{\Gamma}}{a^2 V_0 \mathsf{A}_{22} - 1 + i\tilde{\Gamma}} \tag{3.25}$$

with

$$i\tilde{\Gamma} = a^4 V_0^2 (\mathsf{A}_{12}\mathsf{A}_{21} - \mathsf{A}_{11}\mathsf{A}_{22}) + a^2 V_0 \mathsf{A}_{11}. \tag{3.26}$$

The bound state of the evanescent mode is given by the relation $a^2 V_0 \mathsf{A}_{22} = 1$. The approximate relation $\mathsf{A}_{22} \approx -m\chi_2(y_0)^2/\hbar^2 \varkappa_2$ yields the energy

$$E_{\text{B}} = E_2 - \frac{a^4 V_0^2 m \chi_2(y_0)^4}{\hbar^2} \tag{3.27}$$

for the bound state of the first evanescent mode; for weak potentials, the bound state is close to E_2. Expanding the transmission amplitude (3.25) around the position E_{B} of the bound state, we obtain

$$t = 1 - \frac{i\Gamma}{E - E_{\text{B}} + i\Gamma}. \tag{3.28}$$

which is a Breit-Wigner resonance with width

$$i\Gamma = \frac{a^4 V_0^2 m \chi_2(y_0)^4}{\hbar^2} [a^4 V_0^2 (\mathsf{A}_{12}\mathsf{A}_{21} - \mathsf{A}_{11}\mathsf{A}_{22}) + a^2 V_0 \mathsf{A}_{11}] \tag{3.29}$$

For $E = E_{\text{B}}$, the transmission vanishes $t = 0$ and the wave function is completely reflected which explains the dip in Fig. 3.3(b). Note that the bound state exists for arbitrary weak potentials as the motion is effectively 1D. The resonant reflection exists for a single impurity of arbitrary strength; only the width Γ of the resonance depends on the strength of the impurity.

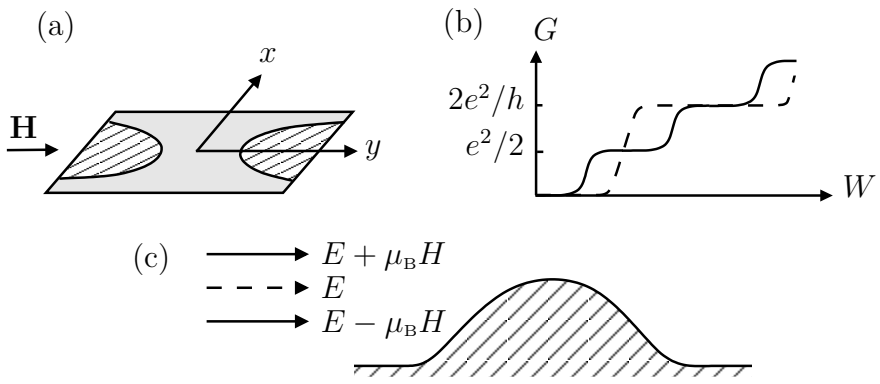

Figure 3.4: (a) Setup of a quantum point contact in a in-plane magnetic field. (b) The solid (dashed) line shows the conductance steps without (with) an applied magnetic. (c) Every scattering states at energy E is split into two scattering states at energies $E \pm \mu_B H$.

3.5 Waveguide in a magnetic field

The application of a magnetic field has two effects on the motion of an electron in a waveguide. First, the levels which where before doubly spin-degenerate split due to the Zeeman effect. Second, there are orbital effects in two and three dimensions which were absent in the one dimensional case, cf. Sec. 2.1.4, as any vector potential can be gauged away. In the following, we will show both the effects in specific examples.

3.5.1 Zeeman effect in a quantum point contact

A quantum point contact in a 2D electron gas (x, y-plane) with a magnetic field

$$\mathbf{H} = H\mathbf{e}_y, \tag{3.30}$$

in the plane defined by the electron gas cf. Fig. 3.4(a), is described by the Hamiltonian

$$\mathcal{H} = \frac{1}{2m}\left(\mathbf{p} + \frac{e}{c}\mathbf{A}\right)^2 + U(x,y) + \mu_B \mathbf{H}\cdot\boldsymbol{\sigma}, \tag{3.31}$$

where $-e$ is the charge of the electron, μ_B denotes Bohr's magneton, and $\boldsymbol{\sigma}$ are the three Pauli matrices. Note that in-plane magnetic field (3.30) does not change motion of the particle and we can reduce the Hamiltonian (3.31) to the Hamiltonian

$$\mathcal{H} = \mathcal{H}_0 + \mu_B H \sigma_y, \tag{3.32}$$

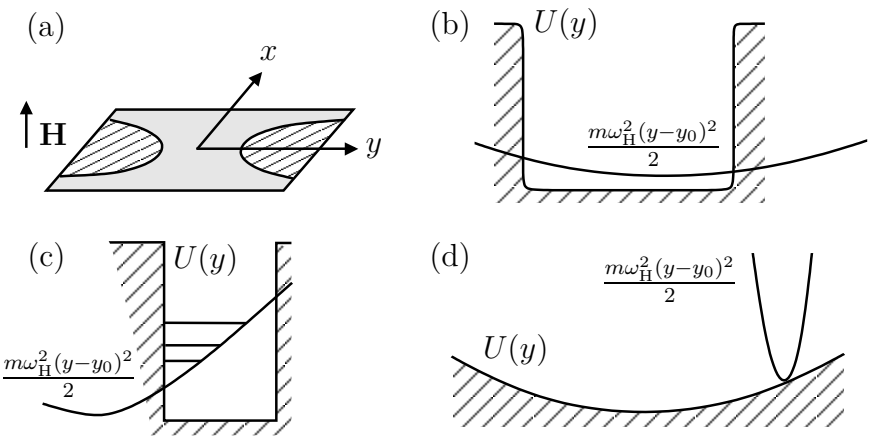

Figure 3.5: (a) Quantum point contact with a perpendicular magnetic field. (b) Week magnetic field in a tube. (c) Edge states for strong magnetic field in a sharp potential $U(y)$. (d) Edge states for strong magnetic field in a soft potential $U(y)$.

i.e., the Hamiltonian $\mathcal{H}_0 = p^2/2m + U(x, y)$ without the magnetic field plus the Zeeman term. To any solution (scattering or bound state) of the Hamiltonian $\mathcal{H}_0$ at energy E, there are two solutions of (3.36) with the kinetic energies $E \pm \mu_B H$, cf. Fig. 3.4. The spin-degeneracy is split and the conductance in a quantum point contact rises in steps of e^2/h while increasing the width W of the constriction, cf. Fig. 3.4(b).

3.5.2 Edge states in magnetic field perpendicular to the sample

If a magnetic field $\mathbf{H}$ is applied perpendicular to the plane, Fig. 3.4(a), there are both Zeeman and orbital effects. In order to keep the discussion simple, we neglect the Zeeman term and consider the simple situation of a translational invariant waveguide (tube). The Hamiltonian is given by

$$\mathcal{H} = \frac{1}{2m}\Big(\mathbf{p} + \frac{e}{c}\mathbf{A}\Big)^2 + U(y), \tag{3.33}$$

where the potential $U(y)$ does not depend on the position x along the wire. We assume a constant magnetic field as before but this time the magnetic field points perpendicular to the electron gas, i.e.,

$$\mathbf{H} = H\mathbf{e}_z. \tag{3.34}$$

This magnetic field can be implemented by a vector potential of the form

$$\mathbf{A} = -Hy\,\mathbf{e}_x, \tag{3.35}$$

which depends only on the y coordinate (Landau gauge). The Hamiltonian (3.33) assumes the form

$$\mathcal{H} = \frac{1}{2m}\left(p_x - \frac{eH}{c}y\right)^2 + \frac{p_y^2}{2m} + U(y). \tag{3.36}$$

The Schrödinger equation associated with (3.36) can be separated with the Ansatz

$$\Psi(x,y) = e^{ikx}\chi(y), \tag{3.37}$$

where the transversal mode $\chi(y)$ satisfies the following equation

$$\chi_n''(y) + \frac{2m}{\hbar^2}\left[E_n(k) - U(y) - \frac{m\omega_c^2}{2}(y-y_0)^2\right]\chi_n(y) = 0, \tag{3.38}$$

where $\omega_c = eH/mc$ is the cyclotron frequency and $y_0 = \ell_H^2 k$, with $\ell_H = \sqrt{c\hbar/eH}$ the magnetic length. Solving Eq. (3.38), we can obtain the energy band $E_n(k)$ and wave function in the presence of the magnetic field. In the absence of additional potential $U(y) = 0$, Eq. (3.38) reduces to the problem of an harmonic oscillator. The solution is given by the Landau levels

$$E_n(k) = \hbar\omega_c\left(n + \frac{1}{2}\right) \tag{3.39}$$

which are flat bands without dispersion [1].

For **weak magnetic fields**, we can consider the quadratic potential originating from H as a perturbation, cf. Fig. 3.4(b). The energy levels are given by

$$E_n(k) = E_n + \frac{\hbar^2 k^2}{2m} + \langle\chi_n^{(0)}|V(y)|\chi_n^{(0)}\rangle, \tag{3.40}$$

where E_n $[\chi^{(0)}(y)]$ is the quantization energy [transversal wave function] without magnetic field, and

$$V(y) = \frac{m\omega_c^2}{2}(y - 2y_0 y). \tag{3.41}$$

For a **strong magnetic field in sharp potential**, the transversal mode structure can be changed considerably for large k and H when the parabola involves a strong confinement and is shifted far away from the origin, e.g., in

the case of magnetic field in the box represented at the Fig. 3.4(c). States form at the boundary of the potential which are called edge states.

For a strong magnetic field and smooth potential, $U''(y_0)/m \ll \omega_c$, the effect of magnetic field is to confine the motion to the position y_0, i.e., $U(y)$ can be replaced by $U(y_0)$. The energy levels can be estimated as

$$E_n(k) = \hbar\omega_c\left(n+\frac{1}{2}\right) + U(y_0) + \frac{\hbar^2k^2}{2m}. \tag{3.42}$$

An exact solution can be found for **a parabolic confining potential** $U(y) = m\omega_0^2 y^2/2$, i.e,

$$\chi_n''(y) + \frac{2m}{\hbar^2}\left\{E_n(k) - \frac{m}{2}\left[\omega_0^2 y^2 + \omega_c^2(y-y_0)^2\right]\right\}\chi_n(y) = 0. \tag{3.43}$$

Introducing new variables

$$\tilde{\omega}^2 = \omega_c^2 + \omega_0^2, \quad \tilde{y}_0 = y_0\frac{\omega_c^2}{\omega_c^2+\omega_0^2}, \quad \tilde{E}_n(k) = E_n(k) - \frac{m\omega_c^2\omega_0^2}{2(\omega_c^2+\omega_0^2)}y_0^2.$$

this equation can be reduced to single harmonic oscillator

$$\chi_n''(y) + \frac{2m}{\hbar^2}\left[\tilde{E}_n(k) - \frac{m\tilde{\omega}^2(y-\tilde{y}_0)^2}{2}\right]\chi_n(y) = 0. \tag{3.44}$$

with the spectrum

$$\tilde{E}_n(k) = \hbar\tilde{\omega}\left(n+\frac{1}{2}\right) \tag{3.45}$$

without dispersion. Going back to the variables without tilde yields

$$E_n(k) = \hbar\sqrt{\omega_c^2+\omega_0^2}\left(n+\frac{1}{2}\right) + \frac{m\omega_c^2\omega_0^2}{2(\omega_c^2+\omega_0^2)}y_0^2. \tag{3.46}$$

where the k dependence enters through $y_0 = \ell_H^2 k$. Equation (3.44) shows that $\tilde{y}_0$ mark the position of the (edge) states. Let us fix the energy E and express the position of the edge state in terms of E and n,

$$\tilde{y}_0^2 = \frac{2\omega_c^2}{m\omega_0^2(\omega_c^2+\omega_0^2)}\left[E - \hbar\sqrt{\omega_c^2+\omega_0^2}\left(n+\frac{1}{2}\right)\right]; \tag{3.47}$$

the larger the energy E the more the state is located towards the edge of the sample.

Bibliography

[1] L. D. Landau and E. M. Lifshitz, *Quantum Mechanics*, vol. 3 of *Course of Theoretical Physics* (Pergamon Press, London, 1958).

[2] B. J. van Wees, H. van Houten, C. W. J. Beenakker, J. G. Williamson, L. P. Kouwenhoven, D. van der Marel, and C. T. Foxon, *Quantized conductance of point contacts in a two-dimensional electron gas*, Phys. Rev. Lett. **60**, 848 (1988).

[3] D. A. Wharam, T. J. Thornton, R. Newbury, M. Pepper, H. Ahme, J. E. F. Frost, D. G. Hasko, D. Peacock, and D. A. Ritchie, *One-dimensional transport and the quantization of the ballistic resistance*, J. Phys. C **21**, L209 (1988).

[4] S. A. Gurvitz and Y. B. Levinson, *Resonant reflection and transmission in a conducting channel with a single impurity*, Phys. Rev. B **47**, 10578 (1993).

Chapter 4

Many-particle systems

In this chapter, we describe systems where many fermionic particles are participating. For noninteracting particles, the total energy of the system is simply the sum of the individual one-particle energies. The only difficulty is that for fermionic particle Pauli's principle has to be fulfilled, i.e., a state can only be occupied by a single spinless Fermion (or two spin one-half Fermions). A possible electrochemical potential μ can be thought of as a particle reservoir which provides (accepts) particles with an energy μ.

4.1 Persistent current

The persistent current is the effect that a current flows around a ring geometry when we apply a magnetic flux through the loop without any electric field applied [1, 2]. Theoretically, this is not unexpected at all as we will see below. However, this effect needs coherence and in early experiments decoherence was still strong enough to mask the current.

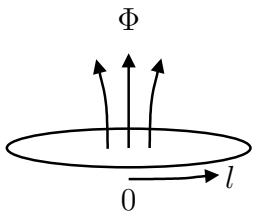

Figure 4.1: The loop of the length L with a persistent current flowing around it driven by a magnetic flux Φ threading the loop.

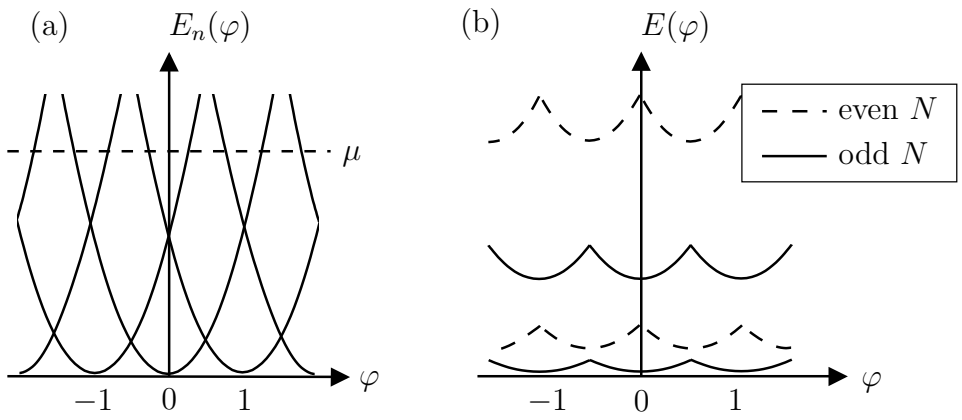

Figure 4.2: Single- (a) [and many- (b)] particle spectrum of the ring threaded by a magnetic flux $\Phi = \varphi\Phi_0$. The many particle spectrum shows even/odd alternation (even without taking into account the spin degree of freedom).

In our theoretical modeling of the ring geometry, let us first consider case with a fixed number of particles N in the system. For simplicity, we assume these particles to be spinless and noninteracting. We restrict the Hamiltonian of a single electron with charge $-e$

$$H = \frac{1}{2m}\left(\mathbf{p} + \frac{e}{c}\mathbf{A}\right)^2, \tag{4.1}$$

to the 1D Hilbert space around the ring, $l \in [0, L]$. Furthermore, we choose the gauge condition for the constant magnetic field to be $\mathbf{A} = A_n\mathbf{n}$ (with $\mathbf{n}$ is a unit tangent vector and $A_n = \Phi/L$). Rewriting (4.1) as a 1D problem involving only the cyclical coordinate l on the ring, cf. Fig. 4.1, we obtain

$$H = \frac{1}{2m}\left(-i\hbar\frac{\partial}{\partial l} + \frac{e}{c}A_n\right)^2 \tag{4.2}$$

The energy spectrum, cf. Fig. 4.2(a),

$$E_n = \frac{(2\pi\hbar)^2}{2mL^2}\left(n + \frac{\Phi}{\Phi_0}\right)^2, \tag{4.3}$$

can be obtained easily by using the Ansatz $\phi_n(l) = e^{i2\pi nl/L}$ for the wave function; here, $\Phi_0 = hc/e$ denotes the magnetic flux quantum. Filling in this single-particle levels to obtain the energy of a N particle state, we observe that the expression for the energy E_N of N particles is different whether N

is even or odd. Assuming N to be odd yields

$$E_{\text{odd}}(-1/2 < \varphi < 1/2) = \frac{h^2}{2mL^2} \sum_{n=-(N-1)/2}^{(N-1)/2} (\varphi + n)^2$$
$$= \frac{h^2 N}{2mL^2} \left[\frac{N^2 - 1}{12} + \varphi^2 \right], \tag{4.4}$$

with the dimensionless flux $\varphi = \Phi/\Phi_0$ between $-1/2 < \varphi < 1/2$ (with periodic continuation); note, that there exists a nondegenerate $n = 0$ state.For even N, we obtain

$$E_{\text{even}}(0 < \varphi < 1) = \frac{h^2}{2mL^2} \sum_{n=-N/2}^{N/2-1} (\varphi + n)^2$$
$$= \frac{h^2 N}{2mL^2} \left[\frac{N^2 + 2}{12} + \varphi(\varphi - 1) \right]. \tag{4.5}$$

The energies of Eqs. (4.4) and (4.5) are depicted in Figure 4.2(b). The persistent current is the derivative of the energy with respect to the flux,

$$I(\Phi) = -c \frac{\partial}{\partial \Phi} E(\Phi/\Phi_0). \tag{4.6}$$

On the one hand, for odd N, the current is given by

$$I_{\text{odd}}(-1/2 < \varphi < 1/2) = -\frac{h^2 cN}{mL^2 \Phi_0} \varphi, \tag{4.7}$$

on the other hand, for even N, we obtain

$$I_{\text{even}}(0 < \varphi < 1) = \frac{h^2 cN}{mL^2 \Phi_0} (1/2 - \varphi). \tag{4.8}$$

Next, we treat the case of a lead (reservoir) with an electrochemical potential μ attached to the loop. We assume that the connection is through a weak link such that the internal levels of the ring are only slightly perturbed, see Figure 4.3(a,b). The reservoir does not break the coherence in the ring, but fixes a chemical potential μ instead of the number of particles N. In this case, the energy is given by the sum of single particle energies (4.3) with $E_n \leq \mu$. This is equivalent to sum the the level index n over the range $n_{\min} \leq n \leq n_{\max}$, where

$$n_{\min} = -\left\lfloor \frac{\sqrt{2m\mu}}{h} L + \varphi \right\rfloor, \quad n_{\max} = \left\lfloor \frac{\sqrt{2m\mu}}{h} L - \varphi \right\rfloor; \tag{4.9}$$

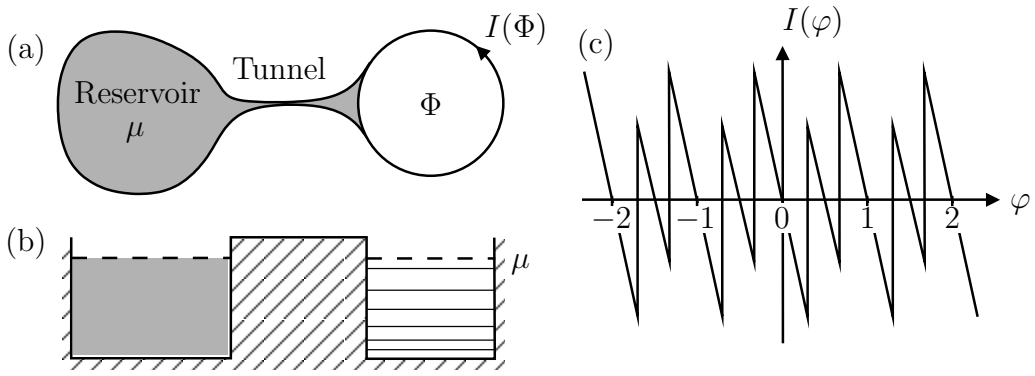

Figure 4.3: A ring connected through a weak tunnel junction to a reservoir with fixed electrochemical potential μ. Picture (a) shows a real-space and (b) an energy-space representations. In (c), the dependence of the current on the flux is plotted for fixed chemical potential.

here, $\lfloor x \rfloor$ denotes the floor function. The total energy is given by

$$E(\varphi) = \frac{(2\pi\hbar)^2}{2mL^2} \sum_{n=n_{\min}}^{n_{\max}} (n+\varphi)^2 \tag{4.10}$$

which yields a persistent current

$$\begin{aligned} I(\Phi) &= -\frac{h^2 c}{mL^2\Phi_0} \sum_{n=n_{\min}}^{n_{\max}} \left(n + \frac{\Phi}{\Phi_0} \right) \\ &= -\frac{h^2 c}{mL^2\Phi_0} (n_{\max} - n_{\min} + 1) \left[\frac{n_{\max} + n_{\min}}{2} + \frac{\Phi}{\Phi_0} \right] \end{aligned} \tag{4.11}$$

plotted in Figure 4.3(c). In reality, elastic (and inelastic) scattering lift the degeneracy of the levels at the crossing points smearing the sharpness of the $I(\Phi)$ curve in Fig. 4.3. Let us estimate the value of the current (4.11) in the limit of many particles, $|n_{\max}|, |n_{\min}| \gg 1$, and moderate magnetic fields, $\Phi/\Phi_0 \approx 1$. In this limit, we can estimate $n_{\max} - n_{\min} \approx 2k_{\mathrm{F}}L$ where we introduced the Fermi wave-vector $k_{\mathrm{F}} = \sqrt{2m\mu/\hbar^2}$ and $n_{\max} + n_{\min} \approx 1$. From Eq. (4.11), we obtain

$$|I| \approx \frac{h^2 c}{mL^2\Phi_0} 2k_{\mathrm{F}}L = \frac{hk_{\mathrm{F}}e}{mL} \approx \frac{v_{\mathrm{F}}e}{L} = \frac{e}{\tau}, \tag{4.12}$$

where $v_{\mathrm{F}} = \hbar k_{\mathrm{F}}/m$ is the Fermi velocity and $\tau = L/v_{\mathrm{F}}$ is the time of the round trip. This result for clean limit is in a good agreement with experiment.

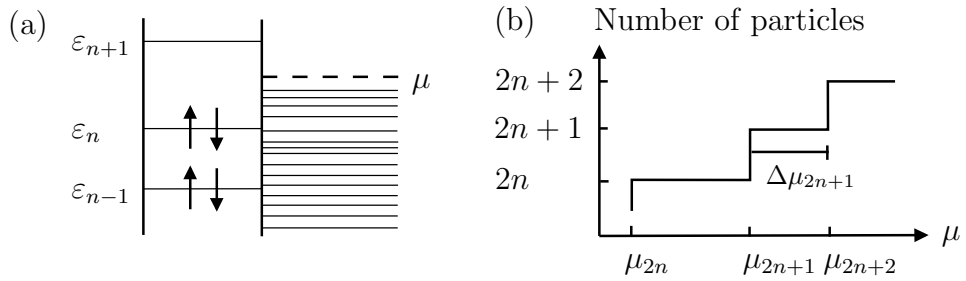

Figure 4.4: (a) Energy levels of a quantum dot coupled to a reservoir at electrochemical potential μ. The reservoir provides (accepts) particles with energy μ. (b) Number of particles in the dot as a function of the applied electrochemical potential μ.

In the dirty limit, theory predicts that the current is suppressed by the factor τ/τ_{D}, where $\tau_{\mathrm{D}} = L^2/v_{\mathrm{F}}\ell$ is the diffusive travelling time around the ring. Therefore, the magnitude of the persistent current is expected to be given by

$$|I_{\mathrm{D}}| \approx \frac{e}{\tau_{\mathrm{D}}}. \tag{4.13}$$

Experimentally [3], I_{D} is much larger than this. Over ten years, the discrepancy was tried to resolve without success. Recently, Schechter, Imry, *et al.* [4] explained the magnitude of the persistent current with attractive pairing-interacting known from BCS superconductivity.

4.2 Coulomb blockade in a quantum dot

For a system of noninteracting electrons, a electrochemical potential can only change the number of electrons in pairs of two as every level is doubly degenerate (an electron with spin-up has the same energy as an electron with spin-down in the same state). Coulomb interacting in a box lifts this degeneracy, cf. Fig. 4.4(a). In order to find the region of electrochemical potential μ where the ground state is given by an even number ($2n$) of particles, we calculate energy of the states with $2n-1$, $2n$, and $2n+1$ electrons in the box, taking into account charging effects. The energy of $2n+1$ electrons is given by

$$E_{2n+1} = 2\varepsilon_n + \varepsilon_{n+1} + \frac{e^2}{2C}(2n+1)^2 - (2n+1)eU + E_0. \tag{4.14}$$

where the first two terms denote the energy of the noninteracting particles $2n+1$, $2n$, and $2n-1$, the term involving the capacitance C of the box is the charging energy, $-(2n+1)eU$ denotes the electric energy in the potential U between the reservoir and the dot, and E_0 is all the additional energy of the electron reservoir and the $2n-2$ other particles. Moving one particle from the box to the reservoir, the energy is given by

$$E_{2n} = 2\varepsilon_n + \mu + \frac{e^2}{2C}(2n)^2 - 2neU + E_0, \tag{4.15}$$

involving the additional energy μ as well as the obvious changes in the charging terms. Similar considerations yield the following expression for the energy of $2n-1$ particles in the box,

$$E_{2n-1} = \varepsilon_n + 2\mu + \frac{e^2}{2C}(2n-1)^2 - (2n-1)eU + E_0. \tag{4.16}$$

In order that E_{2n} is the ground state, we need

$$E_{2n} < E_{2n-1}, \quad \text{and} \quad E_{2n} < E_{2n+1} \tag{4.17}$$

which can be rewritten as

$$\varepsilon_n + \frac{e^2}{2C}(4n-1) < \mu + eU < \varepsilon_{n+1} + \frac{e^2}{2C}(4n+1). \tag{4.18}$$

Changing μ, the ground state is given by a even number of particles over region of size

$$\Delta\mu_{2n} = \varepsilon_{n+1} - \varepsilon_n + \frac{e^2}{C}. \tag{4.19}$$

Performing the same analysis for an odd number $(2n+1)$ of particles, we have to compare the energies

$$E_{2n+2} = 2\varepsilon_n + 2\varepsilon_{n+1} + \frac{e^2}{2C}(2n+2)^2 - (2n+2)eU + E_0, \tag{4.20}$$

$$E_{2n+1} = 2\varepsilon_n + \varepsilon_{n+1} + \mu + \frac{e^2}{2C}(2n+1)^2 - (2n+1)eU + E_0, \tag{4.21}$$

$$E_{2n} = 2\varepsilon_n + 2\mu + \frac{e^2}{2C}(2n)^2 - 2neU + E_0. \tag{4.22}$$

In order that $2n+1$ particles are in the ground state, the conditions

$$\varepsilon_{n+1} + \frac{e^2}{2C}(4n+1) < \mu + eU < \varepsilon_{n+1} + \frac{e^2}{2C}(4n+3) \tag{4.23}$$

have to be fulfilled. Over a region of size

$$\Delta\mu_{2n+1} = \frac{e^2}{C} \tag{4.24}$$

in μ, the ground state is given by an odd number of particles. Note that when the charging energy goes to zero (by continuous charge $e \to 0$ or large box $C \to \infty$), the ground state involves always an even number of particles as $\Delta\mu_{2n+1} = 0$. When the electrochemical potential μ assumes the value

$$\begin{aligned}
\mu_{2n} &= \varepsilon_n + \frac{e^2}{2C}(4n-1) - eU, \\
\mu_{2n+1} &= \varepsilon_{n+1} + \frac{e^2}{2C}(4n+1) - eU, \\
\mu_{2n+2} &= \varepsilon_{n+1} + \frac{e^2}{2C}(4n+3) - eU,
\end{aligned}$$

an additional particle enters the dot, cf. Fig. 4.4(b).

Bibliography

[1] M. Büttiker, Y. Imry, and R. Landauer, *Josephson behavior in small normal one-dimensional rings*, Phys. Lett. A **96**, 365 (1983).

[2] M. Büttiker, *Small normal-metal loop coupled to an electron reservoir*, Phys. Rev. B **32**, 1846 (1985).

[3] L. P. Lévy, G. Dolan, J. Dunsmuir, and H. Bouchiat, *Magnetization of mesoscopic copper rings: Evidence for persistent currents*, Phys. Rev. Lett. **64**, 2074 (1990).

[4] M. Schechter, Y. Imry, Y. Levinson, and Y. Oreg, *Magnetic response of disordered metallic rings: Large contribution of far levels*, Phys. Rev. Lett. **90**, 026805 (2003).

Chapter 5

Scattering matrix approach

So far we were reviewing scattering problems. This is the natural starting point for the discussion of coherent transport. Nevertheless, the measurement of individual electrons being scattered in the conductor is hard to measure. In this chapter, we want to bridge over to a quantity which can be easily measured, the conductance G. As already mentioned before, it turns out that the conductance is given by the conductance quantum $G_0 = 2e^2/h$ weighted with transmission probability of the channels participating in the transport; here, the factor of 2 originates from the spin degeneracy.

5.1 Conductance in a 1D wire

Assume that an electron reservoir provides spinless electrons incoming from the left $k > 0$ up to the energy μ; an experimental realization would be a quantum wire being biased by a voltage $\mu = -eV_{\mathrm{B}}$. As the conductor is coherent, these electrons populate the Lippmann-Schwinger scattering states. Lippmann-Schwinger scattering state constitute a continuum such that there appears the problem of how to count these states. Usually, one introduces periodic boundary conditions putting the problem on a ring with circumference L making the spectrum discrete and then letting $L \to \infty$. Here, we want to pursue a different approach and form wave packets out of the extended states.

Partitioning the energy range $[0, \mu]$ into N sets of size $\Delta = \mu/N$, we form

the wave packets

$$\Psi_n(x,t) = c_n \int_{(n-1)\Delta}^{n\Delta} dE\, \Psi_{\mathrm{L},E}(x) e^{-iEt/\hbar} \tag{5.1}$$

with $n = 1, \ldots, N$ and $\Psi_{\mathrm{L},E}(x)$ is the Lippmann-Schwinger scattering state (2.2) at energy E. The normalization constant can be calculated using the relation ($k = \sqrt{2mE}/\hbar$)

$$\int dx\, \Psi^*_{\mathrm{L},E'}(x)\Psi_{\mathrm{L},E}(x) = 2\pi\delta(k' - k) \tag{5.2}$$

of the scattering states with the asymptotic form

$$\Psi_{\mathrm{L},E}(x) = \begin{cases} e^{ikx} + r_{\mathrm{L},E}e^{-ikx} & x \to -\infty \\ t_{\mathrm{L},E}e^{ikx} & x \to \infty \end{cases}. \tag{5.3}$$

Computing $\int dx\, |\Psi_n(x,t)|^2$ and setting it equal to 1 to normalize the wave packet yields

$$c_n = \frac{1}{\sqrt{h\Delta v_n}} \tag{5.4}$$

with $v_n = \sqrt{2n\Delta/m}$ the velocity of the n-th wave-packet; here, we have assumed Δ to be small. The wave packets in Eq. (5.1) are localized around $x = 0$ at time $t = 0$ with a spreading of approximately hv_n/Δ. In time, they are moving with a velocity v_n. For $\Delta \to 0$ (i.e., $N \to \infty$), the wave packets become broader and broader approaching the scattering states (5.3).

Next, we want to calculate the current I originating from the transport of these wave packets. The current is additive such that we can compute the current I_n of a single wave packet with index n, hereafter, summing up the contributions of the individual wave packets. In Sec. 2.1.1 it was shown that the current is independent on the position, such that the current

$$I_n = i\frac{e\hbar}{2m}\Big[\Psi_n(x)^*\Psi_n'(x) - \Psi_n'(x)^*\Psi_n(x)\Big] \tag{5.5}$$

can be obtained in the left asymptotic region with $\Psi_{\mathrm{L}}(x) \sim t_{\mathrm{L},E}e^{ikx}$ leading to ($\Delta \to 0$)

$$I_n = -c_n^2\Delta^2 e v_n\, T_{n\Delta} = -\frac{e}{h}\Delta T_{n\Delta}, \tag{5.6}$$

where $T_E = |t_{\mathrm{L},E}|^2$ is the transmission probability at energy E. Summing up the contributions of the different wave packets yields the total current

$$I = \sum_{n=1}^{N} I_n = -\frac{e}{h}\Delta \sum_{n=1}^{N} T_{n\Delta} \overset{(\Delta\to 0)}{\to} -\frac{e}{h}\int_0^{\mu} dE\, T_E \tag{5.7}$$

where in the limit $\Delta \to 0$ the sum of n becomes a Riemann integral. Therefore, the conductance, the ratio between current I and voltage $V_{\text{B}} = -\mu/e$, is given by

$$G = \frac{I}{V_{\text{B}}} = \frac{e^2}{h} \int_0^\mu \frac{dE}{\mu} T_E, \tag{5.8}$$

Landauer's formula for the conductance [1, 2].

The wave functions in the continuous spectrum are not normalizable. Therefore building many-body states out of the continuum, it is a priori not clear how much current a state carries. The trick to build wave packets out of the states in the continuous spectrum is a way to handle the question how to count the contribution of these states. Nevertheless, it is a bit awkward to follow the procedure outlined in this chapter—e.g., to form wave packets, normalize them, sum up their contributions and then let the size of the wave packets go to ∞—every time one has to work with a continuous spectrum. Luckily, there is a simple recipe which bypasses the formation of the wave packets. The relation (5.2) provides information about how to add up the contribution of the individual states: assuming the states $\psi_\xi(x)$ to form a continuum with the "normalization" relation

$$\int dx\, \psi_\xi(x)\psi_{\xi'}(x) = c(\xi)\delta(\xi - \xi') \tag{5.9}$$

the expectation value of the current operator (or any other operator which is additive) is given by

$$I = \int \frac{d\xi}{c(\xi)} n(\xi) I_\xi \tag{5.10}$$

where I_ξ is the current from a particle in the state $\psi_\xi(x)$ and $n(\xi)$ is the occupation function (either 0 or 1) which tells if the states with index ξ is occupied in the many-body state or not; for temperatures $\vartheta \neq 0$ $n(\xi)$ can assume any values between 0 and 1. For the case discussed above, $\xi = k$, $I_k = -e\hbar k T_E/m$, $c(k) = 2\pi$, and

$$n(k) = \begin{cases} 1 & \hbar^2 k^2/2m < \mu \\ 0 & \text{otherwise.} \end{cases}$$

Plugging these results in (5.10), we obtain

$$I = -\frac{e\hbar}{m} \int_0^{k(\mu)} \frac{dk}{2\pi}\, k T_E = -\frac{e}{h} \int_0^\mu dE\, T_E, \tag{5.11}$$

which agrees with Eq. (5.7). In the last step, we have changed the integration variable from the wave vector k to the energy E using the density of state (in 1D)

$$\nu(E) = \frac{dk}{dE} = \frac{m}{\hbar^2 k} \tag{5.12}$$

which canceled the factor k in the integral: each energy interval carries the same current, a curious feature of 1D ballistic transport which leads to the Landauer formula for the conductance.

5.2 Coherent conductor

So far, we discussed the simple model of spinless electrons incoming from the left to show the basic feature of 1D transport that each energy interval carries the same contribution to the current. In a more realistic situation, there are spin 1/2 electrons incoming from two reservoirs, one at the left with chemical potential $\mu_{\rm L}$ feeding $\Psi_{\rm L}(x)$ and one at the right $\mu_{\rm R}$ feeding $\Psi_{\rm R}(x)$. The total current is then the sum of the two currents

$$I_{\rm L} = -\frac{2e}{h}\int_0^{\mu_{\rm L}} dE\, T_E \tag{5.13}$$

and

$$I_{\rm R} = \frac{2e}{h}\int_0^{\mu_{\rm R}} dE\, T_E, \tag{5.14}$$

where a factor of two takes into account the spin degeneracy (each state is doubly occupied, once with spin up and once with spin down) and the current $I_{\rm R}$ generated by the state incoming from the right acquires a minus sign with respect to (5.7) as the wave vectors and velocities of $\Psi_{\rm R}(x)$ are opposite to $\Psi_{\rm L}(x)$, cf. Eqs. (2.2) and (2.3). In the total current

$$I = I_{\rm L} + I_{\rm R} = -\frac{2e}{h}\int_{\mu_{\rm R}}^{\mu_{\rm L}} dE\, T_E \tag{5.15}$$

the contributions of the energy interval present in both baths cancel and only the states which are biases from one side with respect to the other carry current.

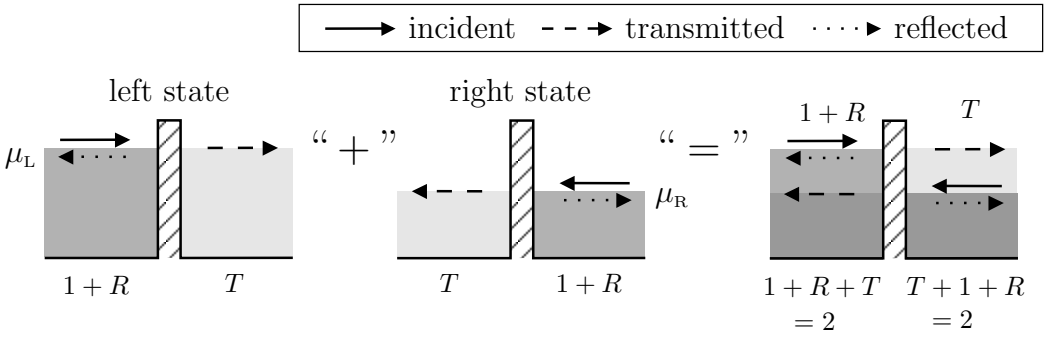

Figure 5.1: Particle density (shading) due to the Lippmann-Schwinger states originating from the left and right electron reservoir (averaged over several wavelength to get rid of Friedel oscillations). The densities due to the states below μ_{R} are equal (dark gray). Whereas for states between μ_{R} and μ_{L} there is a charge accumulation left of the scatterer (for $T \neq 1$).

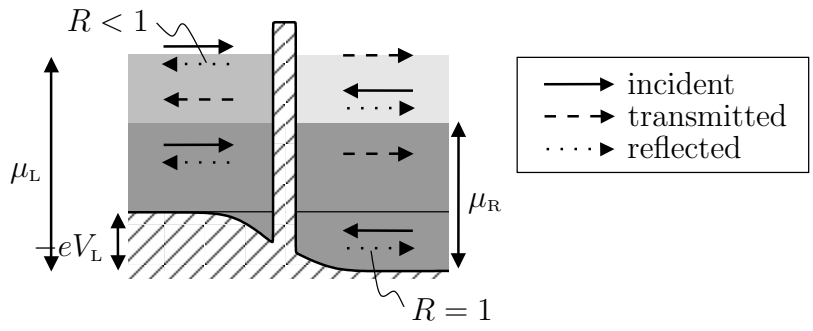

Figure 5.2: Appearance of the Landauer voltage drop V_{L} at the scatterer. Due to the bending of the band bottom, the states being emitted from the right reservoir between 0 and V_{L} are completely reflected.

5.3 Landauer dipole

After having discussed the current which is generated by a bias in the chemical potential between the left and right reservoir, we want to turn our attention to the charge density generated by this stationary situation; here, we assume $\mu_{\mathrm{L}} > \mu_{\mathrm{R}}$ to match with the figures. The left reservoir feeds states of the form (5.3) and the right reservoir the corresponding scattering states $\Psi_{\mathrm{R},E}$ at energy E which are incoming from the right. The total density at the right of the scatterer is given by the sum

$$\begin{aligned}\rho_{\mathrm{R}} &= 2\int_0^{k(\mu_{\mathrm{L}})}\frac{dk}{2\pi}|\Psi_{\mathrm{L},E}(x)|^2 + 2\int_0^{k(\mu_{\mathrm{R}})}\frac{dk}{2\pi}|\Psi_{\mathrm{R},E}(x)|^2 \\ &\approx 2\int_0^{k(\mu_{\mathrm{L}})}\frac{dk}{2\pi}T_E + 2\int_0^{k(\mu_{\mathrm{R}})}\frac{dk}{2\pi}(1+R_E)\end{aligned} \tag{5.16}$$

of the contributions of the left and right scattering states and the factor of 2 is due to the spin degeneracy; in the last step, we have averaged over a length $\propto \sqrt{2m\mu}/\hbar$ in order to get rid of the oscillations with period $2k(\mu)$ (Friedel oscillations). A calculation of the density to the left of the scatterer yields

$$\rho_{\mathrm{L}} \approx 2\int_0^{k(\mu_{\mathrm{L}})}\frac{dk}{2\pi}(1+R_E) + 2\int_0^{k(\mu_{\mathrm{R}})}\frac{dk}{2\pi}T_E. \tag{5.17}$$

For nonvanishing voltage bias $\mu_{\mathrm{L}} \neq \mu_{\mathrm{R}}$ and nonperfect transmission $T \neq 1$, the densities to the right is not equal to the density to the left. The change in density is given by

$$\rho_{\mathrm{L}} - \rho_{\mathrm{R}} = 4\int_{k(\mu_{\mathrm{R}})}^{k(\mu_{\mathrm{L}})}\frac{dk}{2\pi}R_E \tag{5.18}$$

where we used the fact that $R_E + T_E = 1$. The difference in particle density leads to a charge dipole (as the electrons are charged with charge $-e$) and therefore a voltage drop which will be built up in the stationary situation. The voltage drop bends the band bottom. The size of Landauer voltage drop V_{L} in the stationary situation can be obtained by the requirement that the incoming leads remain charge neutral, i.e., equal particle density on both sides of the scatterer, cf. Fig. 5.2. Assuming a voltage drop V_{L} over the scatterer, the left-incoming scattering state at energy E (measured from the

band bottom in the right part of the lead) assume the new form

$$\Psi_{\mathrm{L},E}(x) = \begin{cases} e^{ikx} + r_{\mathrm{L},E} e^{-ikx} & x \to -\infty \\ \sqrt{\frac{k}{\tilde{k}}}\, t_{\mathrm{L},E}\, e^{i\tilde{k}x}, & x \to \infty, \end{cases} \tag{5.19}$$

where $k(E) = \sqrt{2m(E + eV_{\mathrm{L}})}/\hbar$ ($\tilde{k}(E) = \sqrt{2mE}/\hbar$) is the wave vector in the left (right) asymptotic region. Similarly, the right scattering state is given by

$$\Psi_{\mathrm{R},E}(x) = \begin{cases} e^{-i\tilde{k}x} + r_{\mathrm{R},E} e^{i\tilde{k}x} & x \to \infty \\ \sqrt{\frac{\tilde{k}}{k}}\, t_{\mathrm{R},E}\, e^{-ikx}, & x \to -\infty. \end{cases} \tag{5.20}$$

As we discussed in Sec. 3.2, the factor $\sqrt{k/\tilde{k}}$ is required to render the scattering matrix unitary; note that the scattering problem has to be solved again with the bended band bottom due to V_{L}, e.g., right scattering states with energies $E < -eV_{\mathrm{L}}$, i.e., states which are below the band bottom in the left lead, are completely reflected $R_{E<-eV_{\mathrm{L}}} = 1$. The density due to the left scattering states at the left of the scatterer is given by (averaged over some wave lengths)

$$\rho_{\mathrm{LL}} = 2 \int_0^{k(\mu_{\mathrm{L}})} \frac{dk}{2\pi} (1 + R_E), \tag{5.21}$$

where the factor of two is due to the spin degeneracy. The density to the left of the scatterer originating from the right scattering states assumes the form

$$\rho_{\mathrm{LR}} = 2 \int_{\tilde{k}(-eV_{\mathrm{L}})}^{\tilde{k}(\mu_{\mathrm{R}})} \frac{d\tilde{k}}{2\pi} \frac{\tilde{k}}{k} T_E. \tag{5.22}$$

Similar, calculating the densities to the right of the scatterer yields

$$\rho_{\mathrm{RL}} = 2 \int_0^{k(\mu_{\mathrm{L}})} \frac{dk}{2\pi} \frac{k}{\tilde{k}} T_E, \tag{5.23}$$

$$\rho_{\mathrm{RR}} = 2 \int_{\tilde{k}(-eV_{\mathrm{L}})}^{\tilde{k}(\mu_{\mathrm{R}})} \frac{d\tilde{k}}{2\pi} (1 + R_E) + 2 \int_0^{\tilde{k}(-eV_{\mathrm{L}})} \frac{d\tilde{k}}{2\pi} (1 + 1), \tag{5.24}$$

where the last term appears due to the part below the left band bottom which is completely reflected.

It is not convenient to perform th integrations over k and $\tilde{k}$. Therefore, we make a change of variables and integrate over energies. For ρ_{LL}, we obtain

$[dk = (m/\hbar^2 k)dE]$

$$\rho_{\mathrm{LL}} = \frac{2}{\hbar}\sqrt{\frac{m}{2}}\int_{-eV_{\mathrm{L}}}^{\mu_{\mathrm{L}}} \frac{dE}{2\pi}\frac{1+R_E}{\sqrt{E+eV_{\mathrm{L}}}}. \tag{5.25}$$

Analogously, for ρ_{LR}, we have $[d\tilde{k} = (m/\hbar^2\tilde{k})dE]$

$$\rho_{\mathrm{LR}} = \frac{2}{\hbar}\sqrt{\frac{m}{2}}\int_{-eV_{\mathrm{L}}}^{\mu_{\mathrm{R}}} \frac{dE}{2\pi}\frac{T_E}{\sqrt{E+eV_{\mathrm{L}}}}. \tag{5.26}$$

A similar calculation for ρ_{RL} and ρ_{RR} yields

$$\rho_{\mathrm{RL}} = \frac{2}{\hbar}\sqrt{\frac{m}{2}}\int_{-eV_{\mathrm{L}}}^{\mu_{\mathrm{L}}} \frac{dE}{2\pi}\frac{T_E}{\sqrt{E}}, \tag{5.27}$$

$$\rho_{\mathrm{RR}} = \frac{2}{\hbar}\sqrt{\frac{m}{2}}\int_{-eV_{\mathrm{L}}}^{\mu_{\mathrm{R}}} \frac{dE}{2\pi}\frac{1+R_E}{\sqrt{E}} + \frac{2}{\hbar}\sqrt{\frac{m}{2}}\int_{0}^{-eV_{\mathrm{L}}} \frac{dE}{2\pi}\frac{2}{\sqrt{E}}. \tag{5.28}$$

Summing up the densities at the left $\rho_{\mathrm{L}} = \rho_{\mathrm{LL}} + \rho_{\mathrm{LR}}$ while using $T_E + R_E = 1$ yields

$$\rho_{\mathrm{L}} = \frac{2}{\hbar}\sqrt{\frac{m}{2}}\int_{-eV_{\mathrm{L}}}^{\mu_{\mathrm{R}}} \frac{dE}{2\pi}\frac{2}{\sqrt{E+eV_{\mathrm{L}}}} + \frac{2}{\hbar}\sqrt{\frac{m}{2}}\int_{\mu_{\mathrm{R}}}^{\mu_{\mathrm{L}}} \frac{dE}{2\pi}\frac{1+R_E}{\sqrt{E+eV_{\mathrm{L}}}}, \tag{5.29}$$

while the total density to the right is given by

$$\rho_{\mathrm{R}} = \frac{2}{\hbar}\sqrt{\frac{m}{2}}\int_{0}^{\mu_{\mathrm{R}}} \frac{dE}{2\pi}\frac{2}{\sqrt{E}} + \frac{2}{\hbar}\sqrt{\frac{m}{2}}\int_{\mu_{\mathrm{R}}}^{\mu_{\mathrm{L}}} \frac{dE}{2\pi}\frac{T_E}{\sqrt{E}}. \tag{5.30}$$

Assuming charge neutrality, the densities need to be equal, i.e.,

$$\int_{\mu_{\mathrm{R}}}^{\mu_{\mathrm{L}}} \frac{dE}{2\pi}\frac{1+R_E}{\sqrt{E+eV_{\mathrm{L}}}} = \int_{\mu_{\mathrm{R}}+eV_{\mathrm{L}}}^{\mu_{\mathrm{R}}} \frac{dE}{2\pi}\frac{2}{\sqrt{E}} + \int_{\mu_{\mathrm{R}}}^{\mu_{\mathrm{L}}} \frac{dE}{2\pi}\frac{T_E}{\sqrt{E}}. \tag{5.31}$$

This equation provides a way to calculate the Landauer voltage drop V_{L} for arbitrary energy dependent transmission and arbitrary large shifts in chemical potential. In order to solve for V_{L}, we assume the (linear case) of small $\Delta\mu \equiv \mu_{\mathrm{L}} - \mu_{\mathrm{R}} \ll \min\{\mu_{\mathrm{L}}, \mu_{\mathrm{R}}\}$; it follows that also the Landauer voltage $|eV_{\mathrm{L}}| \ll \min\{\mu_{\mathrm{L}}, \mu_{\mathrm{R}}\}$ is small. Let us assume that T_E is constant over the small energy interval $[\mu_{\mathrm{R}}, \mu_{\mathrm{L}}]$ interval. Then, we can replace $\sqrt{E+eV_{\mathrm{L}}}$ by $\sqrt{E}$ and take T_E and R_E out of the integral in (5.31). Finally, we obtain the Landauer voltage

$$-eV_{\mathrm{L}} = \Delta\mu R. \tag{5.32}$$

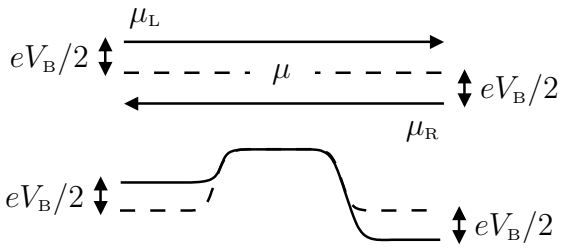

Figure 5.3: Initial (dashed lines) 1D potential (lower part) and initial electrochemical potential (upper part). Bias voltage modifies the potential and the electrochemical potential (solid line).

The voltage drop V_{L} is zero for perfect transmission and assumes its maximum value $-eV_{\mathrm{L}} = \Delta\mu$ when all electrons are reflected. The current is given by

$$I = -\frac{2e}{h} T \Delta\mu, \tag{5.33}$$

cf. (5.15) which leads to a Landauer resistance

$$R_{\mathrm{L}} = \frac{V_{\mathrm{L}}}{I} = \frac{2h}{e^2}\frac{R}{T}. \tag{5.34}$$

5.4 Contact resistance

The resistance in Eq. (5.34) is different than the one obtained by inverting G in the Landauer formula (5.8). One can think about (5.8) to be the conductance measured in a two-probe measurement while Eq. (5.34) is the resistance measured in a four-probe setup. The Landauer voltage only takes into account the voltage which drops immediately at the scatterer. Nevertheless, for coherent transport there is an additional voltage drop at the boundaries of the 1D conductor. This is the reason why the two formulas for the conductance do not match. If we subtract the Landauer voltage drop over the scatterer V_{L} from the total shift in the electrochemical potential $\Delta\mu = -eV_{\mathrm{B}}$, we obtain

$$\Delta\mu + eV_{\mathrm{L}} = \Delta\mu T.$$

Out of symmetry considerations, we expect this additional voltage drop to be split symmetrically between the contributions at both boundaries. At one of the boundaries there is an additional voltage $\Delta\mu T/2$ which corresponds to a resistance

$$R_{\mathrm{S}} = \frac{h}{4e^2}, \tag{5.35}$$

called Sharvin resistance. Figure 5.3 shows the example of a ballistic conductor ($T = 1$). If we apply a voltage, there appears a finite current of size $I = 2e^2/hV_{\rm B}$. Nevertheless, there cannot be any voltage drop within the 1D conductor (no back reflection). Therefore, we conclude that half of the voltage drops at the entrance and half of the voltage at the exit; for a detailed calculation supporting this argument, see Refs. [3, 4].

5.5 2D electron density

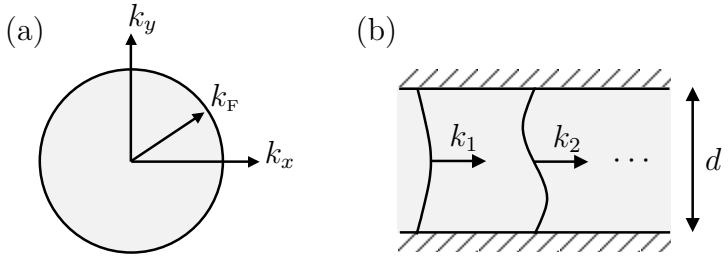

Figure 5.4: (a) 2D Fermi surface. (b) 1D conducting channel with a number N of modes. As the width $d \to \infty$, the quantization energy E_n of more and more modes lie below the Fermi energies and the 2D nature of the Fermi surface is restored.

Let us consider 2D reservoir and calculate the electron density given the electrochemical potential μ. Therefor, we integrate unity over the 2D wave vectors $\mathbf{k} = (k_x, k_y)$ inside the 2D Fermi circle

$$\rho^{\rm 2D} = \frac{2}{(2\pi)^2} \int_{|\mathbf{k}|<k_{\rm F}} dk_x dk_y = \frac{k_{\rm F}^2}{2\pi} \tag{5.36}$$

where the factor of two appears due to the spin degeneracy and $k_{\rm F} = \sqrt{2m\mu}/\hbar$ is the Fermi wave-vector.

As the reservoir feeds a 1D conductor, we can think about it as a 1D conductor whose lateral size d is very large. Let us see if we can restore the 2D Fermi surface while thinking about the reservoir as being a thick 1D conductor. As we have already seen before, in a 1D conductor with finite thickness modes appear. The electron density in the wire can be calculated by summing up all the 1D densities of the different modes. The electron

density in the first mode is given by

$$\rho_1^{\mathrm{1D}} = \frac{2k_1(\mu)}{\pi d} = \frac{2}{\pi d}\sqrt{k_{\mathrm{F}}^2 - \frac{\pi^2}{d^2}}. \tag{5.37}$$

Similarly, for nth mode, we obtain

$$\rho_n^{\mathrm{1D}} = \frac{2k_n(\mu)}{\pi d} = \frac{2}{\pi d}\sqrt{k_{\mathrm{F}}^2 - \frac{\pi^2 n^2}{d^2}}. \tag{5.38}$$

All modes with a quantization energy $E_n < \mu$ contribute. The total electron density is then given by

$$\rho^{\mathrm{2D}} = \sum_{n=1}^{n_{\mathrm{F}}} \rho_n^{\mathrm{1D}} = \frac{2}{\pi d}\sum_{n=1}^{n_{\mathrm{F}}} \sqrt{k_{\mathrm{F}}^2 - \frac{\pi^2 n^2}{d^2}}, \tag{5.39}$$

where $n_{\mathrm{F}} = \lfloor d\, k_{\mathrm{F}}/\pi \rfloor$ is the largest propagating mode number. In the limit of a wide conductor, many channel contribute $n_{\mathrm{F}} \gg 1$. The sum in (5.39) can be replace by an integral[1]

$$\rho^{\mathrm{2D}} = \frac{2}{\pi d}\int_0^{k_{\mathrm{F}}d/\pi} \sqrt{k_{\mathrm{F}}^2 - \frac{\pi^2 x^2}{d^2}} = \frac{2k_{\mathrm{F}}^2}{\pi^2}\int_0^1 \sqrt{1-\lambda^2}d\lambda = \frac{k_{\mathrm{F}}^2}{2\pi}, \tag{5.40}$$

which is the same as (5.36). The electron reservoir can be thought of as a 1D conductor with many channels. As the electrons enter the 1D part the constriction becomes narrower. All channels up to a few are then reflected. As we have seen reflection is connected to a voltage drop due to the Landauer dipole. That is a way to understand the voltage drop at the boundaries between the conductor and the reservoir.

5.6 Negative differential conductance

Here, we would like to discuss a experiment performed in 1989 [5], where back reflection over the barrier led to a negative differential resistance. Let us consider a quantum point contact whose transverse quantization induces a tunneling barrier of height E_1 (solid line in Fig. 5.5(a). Biasing the device with a voltage $\Delta\mu = -eV_{\mathrm{B}}$ a current given by Eq. (5.15) starts to flow. For moderate bias, the current behaves almost linear. Increasing the bias to the value

$$-eV_{\mathrm{B}}/2 > E_1, \tag{5.41}$$

[1] Here we use $\int_0^1 \sqrt{1-\lambda^2}d\lambda = \int_0^{\pi/2} \cos^2\phi\, d\phi = \pi/4$.

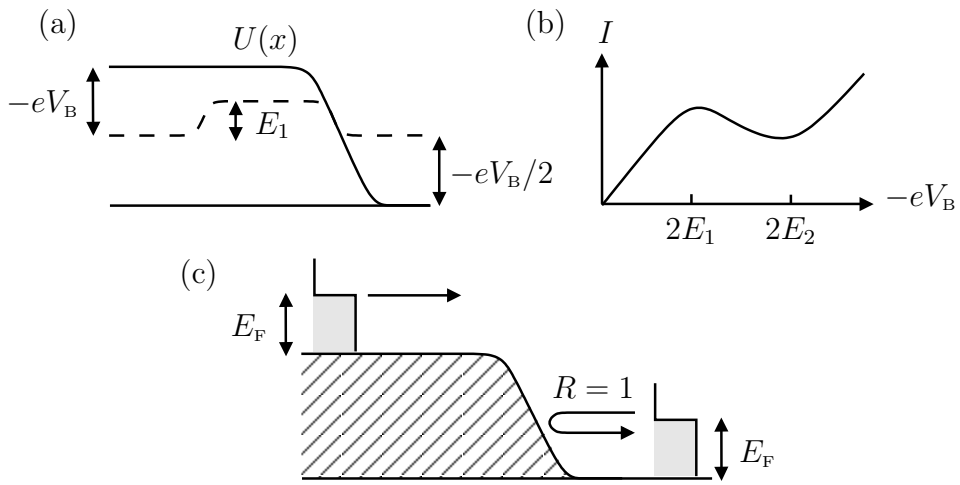

Figure 5.5: (a) A conductor involving a quantum point contact with quantization energy E_1 (dashed line). Applying a bias voltage $-eV_B > E_1$ the effective potential can be approximated by $U(x)$ (solid line). (b) Negative differential resistance appearing between $2E_1$ and $2E_2$. (c) Effective potential for the case when the bias is large; all electron from the right reservoir are reflected and do not contribute to the transport.

electrons only move from left to right as $R_{E<\mu_R} = 1$ (the energy is measured from the band bottom far to the right of the scatterer). In the situation, we the second mode does not participate in the transport, i.e.,

$$-eV_B/2 < E_2 = \frac{4\pi^2\hbar^2}{2md^2}. \tag{5.42}$$

The dashed potential in Fig. 5.5 can be approximated by

$$U(x) = -\frac{eV_B}{1+e^{\alpha x}}, \tag{5.43}$$

dashed line in Fig. 5.5(a), where the reflection probability

$$R = \frac{\sinh^2[\pi(k-\tilde{k})/\alpha]}{\sinh^2[\pi(k+\tilde{k})/\alpha]}, \qquad E > -eV_B \tag{5.44}$$

can be calculated exactly [6]: here, $k = \sqrt{2m(E+eV_B)}/\hbar$ and $\tilde{k} = \sqrt{2mE}/\hbar$ are the wave vectors left and right of the scattering region, respectively. Note, that the reflection coefficient is not vanishing for energies $E > -eV_B$ as one might expect; there appears a reflection above the barrier. An increase

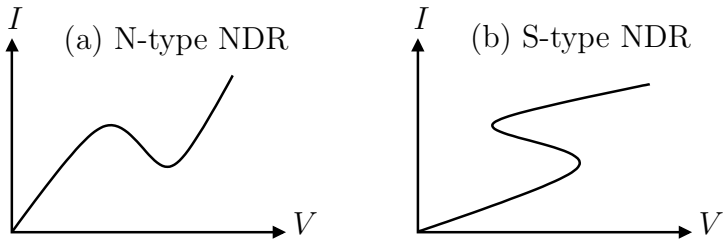

Figure 5.6: The current-voltage characteristics for (a) N-type or voltage-controlled and (b) S-type or current-controlled negative differential resistance (NDR).

in the bias voltage leads to an increase in k which tends to reduces the transmission probability and decreases the conductance, cf. Fig. 5.5(b). Only when the second mode becomes transmitting, the conductance rises again. The situation described above is called voltage-controlled negative differential resistance (or N-type nonlinearity, as the current-voltage characteristics is N shaped), cf Fig. 5.6(a). There exists also the current-controlled negative differential resistancs which is S shaped, cf Fig. 5.6(b).

5.7 Landauer current for a double barrier

In this section we calculate the Landauer current for the double barrier

$$I = -\frac{2e}{h}\int_{-\infty}^{\infty} dE\,[n_{\rm L}(E) - n_{\rm R}(E)]\,T(E). \tag{5.45}$$

where $n_{\rm L}$ ($n_{\rm R}$) are the occupation functions of the left (right) reservoir. In section 2.3.3, we obtained the transmission amplitude of the double barrier structure

$$t_{\rm L} = \frac{t_1 t_2}{1 - r_1 r_2 e^{2ikL}}, \tag{5.46}$$

where $k = \sqrt{2mE}/\hbar$ is the wave vector associated to the energy E, L is the distance between the two scatterers, and t_i, r_i are transmission and reflection amplitudes of the i-th barrier ($i = 1, 2$). The transparency of the barrier is given by

$$T \equiv |t_{\rm L}|^2 = \frac{T_1 T_2}{1 + R_1 R_2 - 2\sqrt{R_1 R_2}\cos(2kL + 2\varphi^r)}, \tag{5.47}$$

where $T_i = |t_i|^2$, $R_i = |r_i|^2$ are the transmission and reflection probabilities of the barriers, and $\varphi^r = (\varphi_1^r + \varphi_2^r)/2$ ($\varphi_i^r = \arg r_i$). The transmission probability $T(E)$ assumes its maximum (resonance) at wave vectors $k_n = (\pi n - \varphi^r)/L$ with corresponding energies

$$E_n = \frac{\hbar^2}{2mL^2}\big(\pi n - \varphi^r\big)^2, \tag{5.48}$$

cf Fig. 5.7(a). The maximal value of $T(E)$ is given by

$$T_{\max} = \frac{T_1 T_2}{(1 - \sqrt{R_1 R_2})^2}, \tag{5.49}$$

which is unity for a symmetric barrier with $T_1 = T_2$. Let us define the spacing between energy levels as

$$\Delta_n = \frac{|E_{n+1} - E_{n-1}|}{2} = 2\pi \frac{\hbar^2}{2mL^2}\big|\pi n - \varphi^r\big|, \tag{5.50}$$

cf. Eq. (5.48); note that the energies are not equidistant and that the continuous definition $\Delta_n = |\partial E_n/\partial n|$ would yield the same result. Next, we analyze the expression (5.47) near a resonance energy E_n (5.48). For that, we expand the cosine in the denominator up to the second order in the energy shift $\delta E_n = E - E_n$ and obtain

$$T = \frac{T_1 T_2}{1 + R_1 R_2 - 2\sqrt{R_1 R_2}\big[1 - mL^2(\delta E_n)^2/\hbar^2 E_n\big]}. \tag{5.51}$$

Rewriting this expression in the Breit-Wigner form

$$T_{\text{BW}} = \frac{\Gamma_n^2}{\Gamma_n^2 + (\delta E_n)^2}\, T_{\max}, \tag{5.52}$$

we introduce the half width of the resonance as

$$\Gamma_n = \sqrt{\frac{\hbar^2 E_n}{2mL^2}}\, \frac{1 - \sqrt{R_1 R_2}}{\sqrt[4]{R_1 R_2}} = \frac{\Delta_n (1 - \sqrt{R_1 R_2})}{2\pi \sqrt[4]{R_1 R_2}}. \tag{5.53}$$

For a sharp resonance $T_{1,2} \ll 1$, Eq. (5.53) can be rewritten in the simpler form

$$\Gamma_n = \frac{\Delta_n}{2\pi}\frac{T_1 + T_2}{2}; \tag{5.54}$$

note that the resonance becomes sharper the smaller T_1 and T_2.

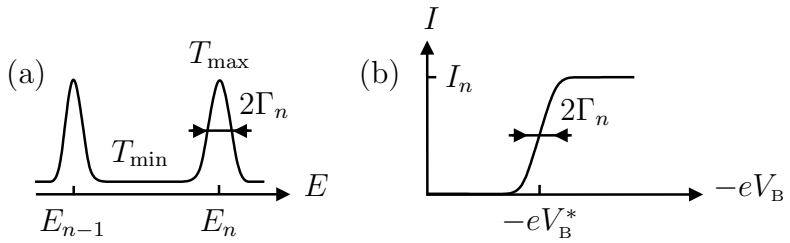

Figure 5.7: (a) Transmission probability $T(E)$ as a function of energy. (b) The Landauer current as a function of voltage bias V_{B}. Each resonance add to the current value $I_n = (2e^2/h)\pi\Gamma_n$

Next, we want to calculate the current (5.45) for a symmetric barrier $T_1 = T_2$ with sharp resonances $T_{1,2} \ll 1$ at zero temperature. Assuming a voltage bias V_{B} to be applied between the left and right reservoir, their electrochemical potentials are changed and assume the values $\mu_{\mathrm{L}} = \mu - eV_{\mathrm{B}}/2$ for the left reservoir and $\mu_{\mathrm{R}} = \mu + eV_{\mathrm{B}}/2$ for the right reservoir. The integration in the Landauer formula for the current 5.45 is restricted to energy interval $[\mu + eV_{\mathrm{B}}/2, \mu - eV_{\mathrm{B}}/2]$; the current assumes the form

$$I(V_{\mathrm{B}}) = -\frac{2e}{h} \int_{\mu+eV_{\mathrm{B}}/2}^{\mu-eV_{\mathrm{B}}/2} T(E)dE. \tag{5.55}$$

Only energies near one of the resonances E_n contribute to the current. Assuming that only the n-th resonance resides within the integration area, we can perform the substitution $\varphi = \varphi^r + L\sqrt{2mE}/\hbar$ to change from the energy variable E to φ, we obtain the current flowing through the n-th resonance

$$I_n(V_{\mathrm{B}}) = -\frac{2e}{h}\sqrt{\frac{\hbar^2}{2mL^2}\,E_n} \int \frac{d\varphi}{1 + (2/T_1)^2 \sin^2 \varphi/2a}. \tag{5.56}$$

we omit the integration limits for simplicity and replace E by E_n as slightly changed function; also we replace R_1 by unity. Making the integration we obtain[2]

$$I_n(V_{\mathrm{B}}) = \frac{2e}{h}\,\Gamma_n \arctan\left(\frac{4}{T_1^2}\tan\frac{1}{2}\sqrt{\frac{2mL^2}{\hbar^2 E_n}}(E - E_n)\right)\Bigg|_{E=\mu-eV_{\mathrm{B}}/2}^{\mu+eV_{\mathrm{B}}/2}. \tag{5.57}$$

[2]We use $\int \frac{d\varphi}{1+\lambda^2\sin^2\varphi} = \frac{2}{\sqrt{1+\lambda^2}} \arctan\left(\sqrt{1+\lambda^2}\tan\frac{\varphi}{2}\right) \approx \frac{2}{\lambda}\arctan\left(\lambda\tan\frac{\varphi}{2}\right)$ for $\lambda \gg 1$.

If all resonance (region $[E_n - \Gamma_n \dots E_n + \Gamma_n]$) hit in the region $[\mu - eV_B \dots \mu + eV_B]$ then we can expand the limits to $V_B \to -\infty$ and (5.57) gives the value

$$I_n = \frac{2e}{h}\,\pi\Gamma_n. \tag{5.58}$$

This current represents the additional current which appears at each resonance, cf Fig. 5.7(b).

5.8 Landauer current for a quantum point contact

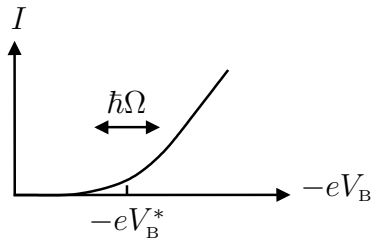

Figure 5.8: Current through a QPC versus the applied bias voltage V_B.

5.9 Thermoelectric current

Up to now, we have always considered the zero temperature situation. It is a result of statistical mechanics that the occupation function $n(E)$ which at zero temperature was either 0 or 1 dependent on the fact weather the state was occupied or not, has to be replaced by the Fermi distribution function

$$n(E) = \frac{1}{e^{(E-\mu)/\Theta} + 1}, \tag{5.59}$$

with $\Theta = k_B\vartheta$ the temperature ϑ in units of energy and k_B is the Boltzmann constant. Trivial effects of the finite temperature include the smearing in the steps in quantized conductance function $G(W)$ and of the sharp features of $I(V)$ near resonances.

To study the thermoelectric effects, we have to consider the case when the temperatures in the left Θ_L and in the right Θ_R reservoirs are different

from each other with a bias $\delta\Theta = \Theta_{\rm L} - \Theta_{\rm R}$. In this case a thermocurrent (= the electrical current induced by the temperature difference without an applied electric potential) of size

$$I(V) = -\frac{2e}{h}\int_{-\infty}^{\infty} dE\,[n_{\rm L}(E) - n_{\rm R}(E)]\,T(E). \tag{5.60}$$

will flow. It can be shown from the general formula (5.60) that for energy independent transmission probability with $\partial_E T(E) = 0$ now current will be induced.

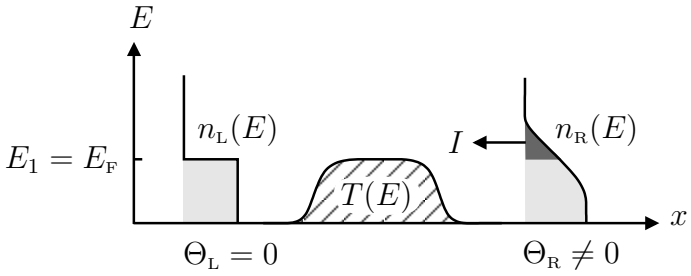

Figure 5.9: Explanation for thermocurrent appearance. Only electrons with energies $E > E_{\rm F}$ can propagate over the barrier from the right form thermocurrent.

At first, we study a simple example where we will show the basic principle for energy dependent transmittance. Let us for simplicity assume a quantum point contact with an ideal quantization

$$T(E) = \begin{cases} 0, & E < E_1, \\ 1, & E > E_1 \end{cases} \tag{5.61}$$

where the electrochemical potentials of the reservoirs is tuned to the quantization energy, $\mu = E_1$, such that μ is at threshold of opening the first channel. Setting the left reservoir to zero temperature $\Theta_{\rm L} = 0$, no particle will penetrate from the left and the part with $E > \mu$ of the electrons in the right reservoir will be able to overcome the barrier; the thermoelectric current is therefore given by

$$I = -\frac{2e}{h}\int_{-\infty}^{\infty} dE\,[n_{\rm L}(E) - n_{\rm R}(E)]\,T(E) = \frac{2e}{h}\int_{0}^{\infty} d\varepsilon\,\frac{1}{e^{\varepsilon/\Theta_{\rm R}}+1}, \tag{5.62}$$

with $\varepsilon = E - \mu$. Performing the integration over ε, we obtain[3]

$$I = \frac{2e}{h}\Delta\Theta. \tag{5.63}$$

If the circuit is not open, a voltage should compensate the temperature gradient such that no current flows. Applying both a temperature difference $\Delta\Theta$ and a voltage $V_{\rm B}$, the general expression (5.60) assumes the form

$$I(\Delta\Theta, V) = -\frac{2e}{h}\int_{-\infty}^{\infty} dE \left\{ \frac{1}{e^{(E-\mu+eV_{\rm B})/(\Theta+\Delta\Theta)}+1} - \frac{1}{e^{(E-\mu)/\Theta}+1} \right\} T(E). \tag{5.64}$$

If the temperature difference $\Delta\Theta$ is small and $T(E)$ depends only weakly on energy E, the Fermi functions can be expanded and the condition that no current flows $I(\Delta\Theta, V_{\rm B}) = 0$ yields

$$\begin{aligned} 0 = &-\frac{2e^2}{h}V_{\rm B}\int_{-\infty}^{\infty} dE\, \frac{\partial n(E)}{\partial E}\, T(\mu) \\ &+ \frac{2e}{h}\Delta\Theta \int_{-\infty}^{\infty} dE\, \frac{\partial n(E)}{\partial E}\frac{E-\mu}{\Theta}\left[T(\mu) + (E-\mu)\frac{\partial T(\mu)}{\partial E}\right]. \end{aligned} \tag{5.65}$$

The voltage $eV_{\rm B}$ which builds up due to the temperature difference is called the thermoelectric voltage. The linear coefficient $\alpha = V_{\rm B}/\Delta\vartheta$ is called thermopower. Rewriting Eq. (5.65), we obtain the Cutler-Mott formula $[\zeta = (E-\mu)/\Theta]$[4]

$$\alpha = -\frac{k_{\rm B}\Theta}{e}\frac{\partial \log T(\mu)}{\partial E}\int_{-\infty}^{\infty} \zeta^2 \frac{\partial n}{\partial \zeta} d\zeta = \frac{\pi^2}{3}\frac{k_{\rm B}^2\vartheta}{e}\frac{\partial \log T(\mu)}{\partial E}. \tag{5.66}$$

5.10 Joule heat

As we have already seen, in a quantum conductor a current may flow in region where no electric field is applied. Another unusual fact is that heat is produced not in the region where the voltage drops. The energy relaxation actually takes place in the reservoirs via the emission of bosonic degrees of

[3] We use $\int_0^\infty \frac{d\zeta}{e^\zeta+1} = \int_1^\infty \frac{d\lambda}{\lambda(\lambda+1)} = \int_1^\infty \left(\frac{1}{\lambda} - \frac{1}{\lambda+1}\right)d\lambda = \log\frac{\lambda}{\lambda+1}\Big|_1^\infty = \log 2.$

[4] We use $\int_{-\infty}^{\infty} \zeta^2 \frac{\partial n}{\partial \zeta} d\zeta = -\frac{\pi^2}{3}.$

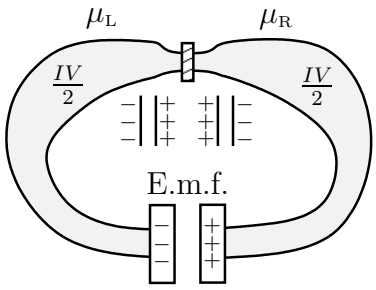

Figure 5.10: Explanation for Joule heat. The contact has characteristic length L much smaller than inelastic length $\ell_{\rm in}$ and coherence length ℓ_φ.

freedom (phonons, photons). Let us estimate the rate of the energy dissipation. For that we subdivide the relevant energy range $\Delta\mu = \mu_{\rm L} - \mu_{\rm R}$ into N distinct intervals of size $\Delta\mu/N$. In each of these intervals $(\Delta\mu/N)(2/h)T$ electrons are transfered per unit of time. The energy which each of it emits is given by $\Delta\mu\, n/N$, where n labels the energy interval. Summing up the contributions of all intervals yields to total emitted heat per unit time

$$P = \sum_{n=1}^{N} \Delta\mu\, n \frac{\Delta\mu}{N^2} \frac{2}{h} T = \frac{(\Delta\mu)^2}{2} \frac{2}{h} T = \frac{(eV_{\rm B})^2}{2} \frac{2}{h} T = \frac{V_{\rm B} I}{2}. \tag{5.67}$$

5.11 Heat current – Wiedemann-Franz law

For an applied temperature difference $\Delta\Theta \neq 0$, no thermoelectric current flows without an appreciable dependence of T on the energy around the chemical potential μ. But even without an electric current flowing, the heat flux

$$I_Q = \frac{2}{h} \int_{-\infty}^{\infty} dE\, [n_{\rm L}(E) - n_{\rm R}(E)]\, T(E)(E-\mu). \tag{5.68}$$

is still nonzero; as motivated in Sec. 5.10 the factor $2/h$ originates from the amount of electrons transferred in unit time and the factor $E-\mu$ measures the energy which each of the electrons transports. For the case of $\alpha = 0$ $(\partial_E T(\mu) = 0)$, the thermal current is given by

$$I_Q = \frac{G}{e^2} \int_{-\infty}^{\infty} dE\, [n_{\rm L}(E) - n_{\rm R}(E)](E-\mu). \tag{5.69}$$

with the electric conductance $G = (2e/h)T$. By assuming a small temperature bias ΔT and expanding $n_{\mathrm{L}}(E) - n_{\mathrm{R}}(E)$, we obtain

$$I_Q = \Delta\Theta \frac{G}{e^2}\Theta \int_{-\infty}^{\infty} \zeta^2 \frac{\partial n}{\partial \zeta} d\zeta \tag{5.70}$$

with $\zeta = (E-\mu)/\Theta$. Performing the integration as in Sec. 5.9, we obtain the Wiedemann-Franz law

$$\varkappa = \frac{\pi^2}{3}\left(\frac{k_{\mathrm{B}}}{e}\right)^2 G\,\vartheta \tag{5.71}$$

with the thermal conductivity $\varkappa = I_Q/\Delta\vartheta$.

5.12 Violation of the Wiedemann-Franz law

In the case where the transmission probability around the chemical potential μ is strongly energy-dependent, an additional thermoelectric voltage

$$V_{\mathrm{B}} = \alpha \Delta\vartheta \tag{5.72}$$

develops which also leads to a heat flow; in this situation the Wiedemann-Franz law (5.71) can be violated. Inserting Eq. (5.72) into the formula for the heat current (5.68), we obtain

$$I_Q = \frac{2}{h}\int_{-\infty}^{\infty} dE \left\{ \frac{1}{e^{(E-\mu+e\alpha\Delta\vartheta)/(\Theta+\Delta\Theta)}+1} - \frac{1}{e^{(E-\mu)/\Theta}+1} \right\} T(E)(E-\mu). \tag{5.73}$$

Expanding this expression as usual in $\Delta\Theta$, we obtain

$$I_Q = \frac{2}{h}\int_{-\infty}^{\infty} dE \left[\frac{e\alpha}{k_{\mathrm{B}}}\frac{\partial T(\mu)}{\partial E} - \frac{T(\mu)}{\Theta} \right] (E-\mu)^2 \frac{\partial n(E)}{\partial E}\,\Delta\Theta. \tag{5.74}$$

Performing the integration, we have

$$I_Q = G\vartheta \left[-\alpha^2 + \frac{\pi^2}{3}\left(\frac{k_{\mathrm{B}}}{e}\right)^2 \right] \Delta\vartheta. \tag{5.75}$$

Thus, only if $\alpha \ll (\pi/\sqrt{3})(k_{\mathrm{B}}/e)$, the Wiedemann-Franz law is correct. On the other hand it is even possible that $\alpha > (\pi/\sqrt{3})(k_{\mathrm{B}}/e)$; but even in the case of a large thermopower, $\varkappa$ will still be positive as a more careful calculation shows.

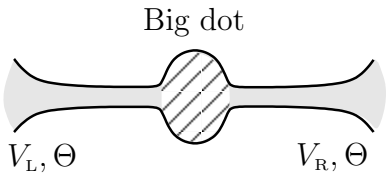

Figure 5.11: Setup for Peliter heating/cooling.

5.13 Large thermopower

As an example for a situation where $\alpha > (\pi/\sqrt{3})(k_{\rm B}/e)$ consider the case of the scattering at a quantum point contact where the difference $U_0 = E_1 - \mu$ of the quantization energy of the first mode E_1 to the electrochemical potential is much larger than the temperature, $U_0 \gg \Theta$. In the situation of perfect quantization, the thermoelectric voltage is obtained by the relation

$$\begin{aligned} 0 = I &= -\frac{2e}{h}\int_{E_1}^{\infty} dE \left\{ \frac{1}{e^{(E-\mu+eV_{\rm B})/(\Theta+\Delta\Theta)}+1} - \frac{1}{e^{(E-\mu)/\Theta_{\rm R}}+1} \right\} \\ &\approx -\frac{2e}{h}\left\{ eV_{\rm B}\int_{E_1}^{\infty} dE \frac{\partial n(E)}{\partial E} - \int_{E_1}^{\infty} dE \frac{E-\mu}{\Theta}\frac{\partial n(E)}{\partial E}\Delta\Theta \right\}; \end{aligned} \quad (5.76)$$

or equivalently, introducing $\zeta = (E-\mu)/\Theta$ as before,

$$eV_{\rm B}\int_{U_0/\Theta}^{\infty} \frac{\partial n}{\partial \zeta} d\zeta = \Delta\Theta \int_{U_0/\Theta}^{\infty} \zeta \frac{\partial n}{\partial \zeta} d\zeta. \quad (5.77)$$

For $U_0/\Theta \gg 1$, we can estimate n as $e^{-\zeta}$ and obtain

$$V_{\rm B} = \frac{U_0}{e\Theta}\Delta\Theta \quad (5.78)$$

which yields

$$\alpha = \frac{U_0}{e\vartheta} \gg \frac{k_{\rm B}}{e}, \quad (5.79)$$

and therefore in this system the Wiedemann-Franz law is not valid.

5.14 Peltier heating/cooling

Consider a system where a big chaotic dot is connected to two external reservoirs via two leads, cf. Fig. 5.11. We model the system by assigning a potential $V_{\rm M}$ to the dot and potentials $V_{\rm L}$ and $V_{\rm R}$ to the left and at the right

reservoirs, respectively. Let us consider the situation where the voltage drops $V_{\rm L}-V_{\rm M}$ and $V_{\rm M}-V_{\rm R}$ are much smaller than temperature Θ and suppose that the dot is large enough to consider it as an additional reservoir where the equilibrium distribution function for electrons is established.

Applying a bias voltage, current will start to flow. As we will show below, depending on the properties of the leads the dot can be both heated or cooled by current passing; this phenomena is called Peltier heating/cooling. The idea is that the heat current $I_{Q,\rm LM}$ from the left reservoir to the dot does not cancel with contribution $I_{Q,\rm MR}$ originating from the heat flow from the center to the right reservoir. To be more specific, we proceed with calculating

$$I_{Q,\rm MR} = \frac{2}{h}\int\limits_{-\infty}^{\infty}(E-\mu)\left\{\frac{1}{e^{(E-\mu+eV_{\rm M})/\Theta}+1}-\frac{1}{e^{(E-\mu+eV_{\rm R})/\Theta}+1}-\right\}T_{\rm R}(E)dE$$
$$= \frac{2eV_{\rm MR}}{h}\int(E-\mu)^2\frac{\partial n}{\partial E}\frac{\partial T_{\rm R}}{\partial E}dE, \tag{5.80}$$

and after expanding $T_{\rm R}(E)$ we obtain

$$I_{Q,\rm MR} = 2eV_{\rm MR}\frac{\partial T_{\rm R}}{\partial E}\bigg|_{E=\mu}2\Theta^2\int\limits_0^{+\infty}\zeta^2\frac{\partial n}{\partial\zeta}d\zeta = -\frac{2\pi^2}{3}\frac{eV_{\rm MR}k_{\rm B}^2\vartheta^2}{h}\frac{\partial T_{\rm R}}{\partial E}\bigg|_{E=\mu}, \tag{5.81}$$

where $V_{\rm MR}=V_{\rm M}-V_{\rm R}<0$. We see, if $\partial T_{\rm R}/\partial E\neq 0$, the answer is proportional to $V_{\rm MR}$. Here, we have omitted the part proportional to $V_{\rm MR}^2$, which gives the contribution from the Joule heat.

Consider now the situation where in the left point contact is in the plateau regime with $\partial T_{\rm L}/\partial E=0$ and only quadratic in $V_{\rm LM}$ terms will gives a contribution to $I_{Q,\rm LM}$; if the current and $V_{\rm LM}$ small we neglect this quadratic terms and $I_{Q,\rm LM}=0$. Let us calculate the "speed" of cooling of the dot $-\partial Q_{\rm M}/\partial t = I_{Q,\rm MR}$ where $Q_{\rm M}$ is a heat energy of the dot,

$$-\frac{\partial Q_{\rm M}}{\partial t} = -\frac{2\pi^2}{3}\frac{eV_{\rm MR}k_{\rm B}^2\vartheta^2}{h}\frac{\partial T}{\partial E} > 0; \tag{5.82}$$

note that $\partial Q_{\rm M}/\partial t$ is linear in current $I=(2e^2/h)V_{\rm MR}T(\mu)$ driven through the dot.

Now let us assume that transparency at the left is unity $T_{\rm L}=1$ and the right one is described by $T_{\rm R}(E)=1/(e^{2\pi(E-\mu)/\hbar\Gamma}+1)$. Noting that $T(\mu)=1/2$ and $\partial T_{\rm R}/\partial E|_{E=\mu}=\pi/2\hbar\Omega$ we obtain from (5.82)

$$-\frac{\partial Q_{\rm M}}{\partial t} = -\frac{\pi^3}{3}\frac{k_{\rm B}^2\vartheta^2}{e\hbar\Gamma}I. \tag{5.83}$$

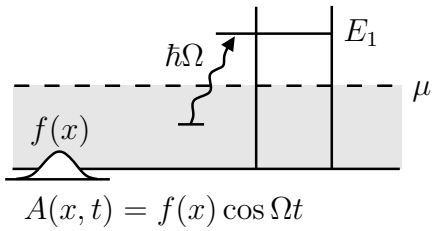

Figure 5.12: Photon-assisted tunneling.

The condition that the Peltier cooling should be stronger than Joule heating

$$IV_{\mathrm{B}} \ll \left| \frac{dQ_{\mathrm{M}}}{dt} \right| \tag{5.84}$$

should be satisfied in order that the dot is cooled in this setup; therefore, the bias voltage obeys the condition

$$|V_{\mathrm{B}}| \ll \frac{\pi^3}{3} \frac{k_{\mathrm{B}}^2 \vartheta^2}{e\hbar\Gamma}. \tag{5.85}$$

5.15 Photon-assisted tunneling

We consider the situation of applying an alternating electric potential on a 1D Fermi gas. The electric field can be modeled by an time-dependent vector potential along x of the form

$$A(x,t) = f(x)\sin\Omega t. \tag{5.86}$$

via $E(t) = -\partial_t A(x,t)/c$. Suppose that $f(x)$ is a smooth function such that $q = |\partial f/\partial x| \ll k_{\mathrm{F}}$ and the frequency Ω is smaller than inverted time of flight through the region where the field $A(x,t)$ is applied $\Omega \ll q v_{\mathrm{F}}$, cf Fig. 5.12. In this case, we can use the linear spectrum approximation for the interaction between the electrons and the electric field and obtain

$$\Psi_{\mathrm{L}}(x,t) = e^{2\pi i(\Phi/\Phi_0)\sin\{\Omega[t-(x-x_0)/v_{\mathrm{F}}]\}+ikx-i(\hbar k^2/2m)t}, \tag{5.87}$$

for the left-incoming Lippmann-Schwinger state, cf. Eq. (2.22), where $\Phi_0 = hc/e$, $\Phi = \int_{-\infty}^{\infty} f(x)dx$. Using the Jacobi-Anger identity

$$e^{iz\sin\theta} = \sum_{n=-\infty}^{\infty} J_n(z)e^{in\theta} \tag{5.88}$$

for the Bessel functions of the first kind $J_n(z)$, we rewrite (5.87) as

$$\Psi_{\rm L}(x,t) = e^{ikx - i(\hbar k^2/2m)t} \sum_{n=-\infty}^{\infty} J_n\Big(2\pi\frac{\Phi}{\Phi_0}\Big) e^{in\Omega[t-(x-x_0)/v_{\rm F}]}; \tag{5.89}$$

note that due to the applied field $A(x,t)$ (5.86) the plane wave which incident from the left is split into a coherent superposition of the plane waves propagating in the same direction (no back-reflection) but with new energies shifted by $n\hbar\Omega$ (with the amplitude J_{-n}). In a ballistic wire without applied electric field, the net current from each state is the same in the present approximation. Therefore no current flows without an additional scattering potential.

Consider now how the left-incoming Lippmann-Schwinger state (5.89) will behave when it impinges on a double-barrier potential. Suppose there is only one well-defined resonance at E_1 which is above $E_{\rm F}$, $E_1 > E_{\rm F}$. Applying a small time-independent voltage bias $eV_{\rm B} \ll E_1 - E_{\rm F}$, almost no current flows. On the other hand, applying an alternating voltage

$$V_\Omega(t) = V_\Omega \cos\Omega t, \tag{5.90}$$

which is modeled by an alternating vector potential $A(x,t)$ with

$$V_\Omega = \frac{\hbar\Omega}{e}\frac{\Phi}{\Phi_0}. \tag{5.91}$$

we chose the frequency Ω to be almost resonant, $\hbar\Omega \approx E_1 - E_{\rm F}$. The current through the resonance is then provided by the component of wave function

$$J_1(2\pi\Phi/\Phi_0) e^{ik_{\rm F}x - iE_{\rm F}t/\hbar - i\Omega[t-(x-x_0)/v_{\rm F}]} \tag{5.92}$$

proportional to $J_1(2\pi\Phi/\Phi_0)$. All other components with $n > 1$ are reflected, since the condition $eV_\Omega \ll E_1 - E_{\rm F}$ at $\hbar\Omega \approx E_1 - E_{\rm F}$ implies that $2\pi\Phi/\Phi_0 \ll 1$, see Eq (5.89), and therefore $J_{n>1}(2\pi\Phi/\Phi_0) \ll 1$. To observe "multi-photon" processes with $n \gg 1$, we need to have $2\pi\Phi/\Phi_0 \gg 1$, cf. Fig. 5.13; in order to still obey the relation $V_\Omega < E_1 - E_{\rm F}$, we keep $2\pi\Phi/\Phi_0 < (E_1 - E_{\rm F})/\hbar\Omega \approx n$.

The general formula for the current is given by

$$I = -\frac{2e}{h}\int_0^{E_{\rm F}} dE \Big\{ \sum_{n,n'} J_n\Big(2\pi\frac{\Phi}{\Phi_0}\Big) J_{n'}\Big(2\pi\frac{\Phi}{\Phi_0}\Big) e^{i(n-n')\Omega[t-(x-x_0)/v_{\rm F}]} \times t^*(E - n'\hbar\Omega) t(E - n\hbar\Omega) - T(E) \Big\}. \tag{5.93}$$

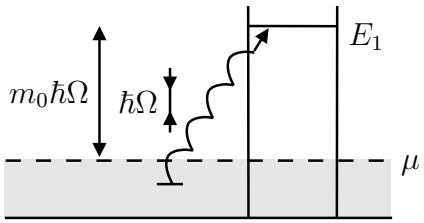

Figure 5.13: Multi-photon case. The number of photons with energy $\hbar\Omega$ is $m_0 = \lfloor (E_1 - E_{\rm F})/\hbar\Omega \rfloor + 1$.

where we can discuss the one and many photons cases in more details; here the second term proportional $T(E)$ originates from the electrons incoming from the right which are scattered at their original energies. The first term, originates from electrons incoming from the left which are promoted to new energies separated by $n\hbar\Omega$ by the alternating voltage applied. Without time-dependent voltage, the two contributions cancel and no current flows.

Consider the situation of a double barrier with sharp resonances. We want to calculate the component of the current which constant in time (dc-component, averaged over time),

$$I = -\frac{2e}{h}\int_0^{E_{\rm F}} dE \Big\{ \sum_{n=-\infty}^{\infty} J_n^2\Big(2\pi\frac{\Phi}{\Phi_0}\Big) T(E - n\hbar\Omega) - T(E) \Big\}. \tag{5.94}$$

The transparency $T(E)$ in this case is given by

$$T(E) = \sum_{m=1}^{\infty} \frac{\Gamma_m^2}{(E - E_m)^2 + \Gamma_m^2} T_m, \tag{5.95}$$

where sum runs over all resonances and T_m is the transmission probability at the mth resonance with $T_m \leq 1$. The first resonance $m = 1$ gives the largest contribution to the current and we estimate

$$I = -\frac{2e}{h} J_1^2\Big(2\pi\frac{\Phi}{\Phi_0}\Big) \pi\Gamma_1 T_1. \tag{5.96}$$

for the one-photon case.

In multi-photon case (the number of photons is $m_0 = \lfloor (E - E_{\rm F})/\hbar\Omega \rfloor + 1$) the current is given by

$$I = -\frac{2e}{h} \sum_{n=m_0}^{\infty} J_n^2\Big(2\pi\frac{\Phi}{\Phi_0}\Big) \pi\Gamma_1 T_1, \tag{5.97}$$

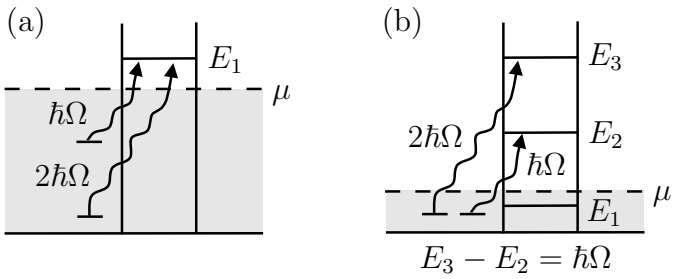

Figure 5.14: Special situations for the photon-assisted tunneling.

where, we assumed that J_n^2 at $n = E_{\rm F}/\hbar\Omega$ is already negligible. The above appearance of the constant current as a response to the alternating field corresponds to so-called "photovoltaic" effect [7]. Note that this sign of the induced current will be the opposite if we apply field from the right. Further possible cases (see e.g. Fig. 5.14(a,b)) can be analyzed in the similar way.

5.16 Oscillating bottom in the dot

Another situation with a time-dependent driving is when we modulate the bottom of a dot with a time dependent voltage (scalar potential), cf Fig. 5.15. To calculate the transmission amplitude, we use the same trick as in the Fabry-Perot interferometer. The new element is that during the presence of the electron in the dot, from $t_{\rm in}$ until time $t_{\rm out}$, the electron accumulate an extra phase

$$\phi(t_{\rm in}, t_{\rm out}) = e \int_{t_{\rm in}}^{t_{\rm out}} U(t)\, dt/\hbar. \tag{5.98}$$

For a plane wave with wave vector k incoming from the left, the transmitted part is given by

$$\begin{aligned}\Psi_{\rm L} &= e^{ik(x-v_{\rm F}t)}\, t_1 t_2 \Big\{ e^{-i\phi(t-x/v_{\rm F}-L/v_{\rm F},t-x/v_{\rm F})} \\ &\qquad + r_1 r_2 e^{2ikL-i\phi(t-x/v_{\rm F}-3L/v_{\rm F},t-x/v_{\rm F})} + \dots \Big\} \\ &= e^{ik(x-v_{\rm F}t)}\, t_1 t_2 \sum_{n=0}^{\infty} (r_1 r_2)^n e^{2nikL-i\phi(t-x/v_{\rm F}-(2n+1)L/v_{\rm F},t-x/v_{\rm F})}.\end{aligned} \tag{5.99}$$

In the case when the spacing between the resonances is large, we can sub-

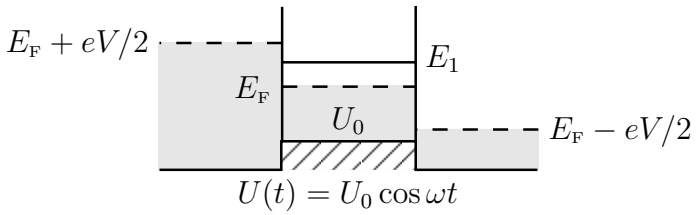

Figure 5.15: Oscillating bottom in the dot.

stitute the sum by an integral over n

$$\Psi_L = e^{ikx - ikv_F t}\, t_1 t_2 \int_0^\infty dn\, (r_1 r_2)^n e^{2nikL - i\phi(t - x/v_F - (2n+1)L/v_F, t - x/v_F)}. \quad (5.100)$$

For sharp resonances with $|T_{1,2}| \ll 1$, we can expand the product

$$(r_1 r_2)^n = e^{2in\chi^r + n \log |r_1 r_2|} = e^{2in\chi^r - n(T_1+T_2)/2},$$

with $\chi^r = (\chi_1^r + \chi_2^r)/2$ and $\chi_n^r = \arg r_k$ as before. Inserting this relation into (5.100), we obtain

$$\Psi_L = e^{ikx - ikv_F t}\, t_1 t_2 \int_0^\infty dn\, e^{i2n\delta kL - n(T_1+T_2)/2 - i\phi(t - x/v_F - (2n+1)L/v_F, t - x/v_F)}, \quad (5.101)$$

where $\delta k = k - k_m$, k_m is the position of the m-th resonance with $2k_m L + 2\chi^r = 2\pi m$. Using the relation $n(T_1 + T_2)/2 = 2\pi n \Gamma_n / \Delta_n$ [we use the expression for resonance width $\Gamma_n = (\Delta_n / 2\pi)(T_1 + T_2)/2$] and performing the substitution $s = 2nL/v_F$ in the integral yields

$$\Psi_L = e^{ikx - ikv_F t}\, t_1 t_2 \frac{\Delta_n}{h} \int_0^\infty ds\, e^{i\delta k v_F s - \Gamma s/\hbar - i\phi(t - x/v_F - L/v_F - s, t - x/v_F)}, \quad (5.102)$$

note that if $U(t)$ is slow, we can omit L/v_F in this formula.

For the situation when the band-bottom is harmonically modulated,

$$U = U_0 \cos \Omega t \quad (5.103)$$

we can expand the exponent into Bessel functions as before,

$$\begin{aligned} e^{-i\phi(t - x/v_F - L/v_F - s, t - x/v_F)} &= e^{-i(eU_0/\hbar\Omega)[\sin \Omega(t - x/v_F) - \sin \Omega(t - x/v_F - s)]} \quad (5.104) \\ &= \sum_{l,l'} J_l\left(\frac{eU_0}{\hbar\Omega}\right) J_{l'}\left(\frac{eU_0}{\hbar\Omega}\right) e^{-il'\Omega(t - x/v_F) + il\Omega(t - x/v_F - s)}. \end{aligned}$$

Performing the integration over s in (5.102) gives

$$\Psi_{\mathrm{L}} = e^{ikx-ikv_{\mathrm{F}}t}\, t_1 t_2 \sum_{l,l'} \frac{\Delta_n}{h}\, J_l\Big(\frac{eU_0}{\hbar\Omega}\Big) J_{l'}\Big(\frac{eU_0}{\hbar\Omega}\Big)\, \frac{-1}{i\delta k v_{\mathrm{F}} - \Gamma/\hbar - il\Omega}\, e^{-i(l-l')\Omega(t-x/v_{\mathrm{F}})}. \tag{5.105}$$

This result is quite similar to the case of photon-assisted tunneling, but now both left and right going states have transformed transmission amplitudes and there is no net current flow without bias, i.e., for $\mu_{\mathrm{L}} = \mu_{\mathrm{R}}$. Additionally, there are new phase factor in (5.104),

$$e^{-i(eU_0/\hbar\Omega)\sin\Omega(t-x/v_{\mathrm{F}})}, \tag{5.106}$$

as compared to the previous section. The formula (5.105) can be interpreted as if the electron first gets some energy quantum $n\hbar\Omega$, then tunnels through the double barrier with this additional energy, and afterwards obtaining (or loosing) an extra amount of the energy. Therefore, we do not know from the energy of the outgoing wave at which energy it was tunneling.

Bibliography

[1] R. Landauer, *Spatial variation of currents and fields due to localized scatterers in metallic conduction*, IBM J. Res. Dev. **1**, 223 (1957).

[2] R. Landauer, *Electrical resistance of disordered one-dimensional lattices*, Phil. Mag. **21**, 863 (1970).

[3] L. I. Glazman and A. V. Khaetskii, *Nonlinear quantum conductance of a point contact*, JETP Lett. **48**, 591 (1988).

[4] L. I. Glazman and A. V. Khaetskii, *Nonlinear quantum conductance of a lateral microsconstraint in a heterostructure*, Europhys. Lett. **9**, 263 (1989).

[5] R. J. Brown, M. J. Kelly, M. Pepper, H. Ahmed, D. G. Hasko, D. C. Peacock, J. E. F. Frost, D. A. Ritchie, and G. A. C. Jone, *Electronic instabilities in the hot-electron regime of the one-dimensional ballistic resistorelectronic instabilities in the hot-electron regime of the one-dimensional ballistic resistor*, J. Phys.: Condens. Matter **1**, 6285 (1989).

[6] L. D. Landau and E. M. Lifshitz, *Quantum Mechanics*, vol. 3 of *Course of Theoretical Physics* (Pergamon Press, London, 1958).

[7] V. I. Fal'ko and D. E. Khmelnitsky, *Mesoscopic photogalvanic effect in microjunctions*, Sov. Phys. JETP **68**, 186 (1989).

Chapter 6

Scattering matrix approach: the second-quantized formalism

6.1 Second-quantized formalism

In this chapter, we rederive Landauer's formula for mesoscopic conductors in the second-quantized formalism. The second quantized formalism replaces the state of one electron with the wave function $\varphi_k(x)$ by a creation operator $\hat{c}_k^\dagger$ acting on the vacuum $|0\rangle$. Its use is in the lies in the fact that for many-body states the symmetrization is already built in. As an example consider the many-body state of N electrons described by a Slater determinant

$$\hat{\Psi}(x_1, \ldots, x_N) = \frac{1}{\sqrt{N}} \begin{vmatrix} \varphi_1(x_1) & \cdots & \varphi_N(x_1) \\ \vdots & \ddots & \vdots \\ \varphi_1(x_N) & \cdots & \varphi_N(x_N) \end{vmatrix} \tag{6.1}$$

in the first-quantized description. In the second-quantized formalism, this state is replaced by product of the corresponding creation operators

$$\hat{c}_1^\dagger \ldots \hat{c}_N^\dagger |0\rangle \tag{6.2}$$

on the vacuum state $|0\rangle$. The anti-symmetry of the Slater-determinant is mapped on the fact that the creation operators $\hat{c}_k^\dagger$ anti-commute with each other.

In the second quantized formalism, we define current density operator as

$$\hat{J} = -\frac{ie\hbar}{2m}\big[(\nabla\hat{\Psi}^\dagger)\hat{\Psi} - \hat{\Psi}^\dagger\nabla\hat{\Psi}\big] \tag{6.3}$$

with the help of the field operators

$$\hat{\Psi}(x, \mathbf{r}_\perp) = \int \frac{dk}{2\pi} \sum_{n=1}^{N} \hat{c}_{n,k}\, \varphi_{n,k}(x, \mathbf{r}_\perp), \tag{6.4}$$

where $\mathbf{r}_\perp$ is a vector in the cross-section. One particle wave functions $\varphi_{n,k}$ represents itself the orthonormal set

$$\int dx\, d\mathbf{r}_\perp\, \varphi^*_{n',k'}(\mathbf{r})\, \varphi_{n,k}(\mathbf{r}) = 2\pi\delta_{n'n}\, \delta(k' - k). \tag{6.5}$$

and satisfy Schrödinger equation

$$\hat{H}\varphi_{n,k} = E_n(k)\varphi_{n,k}, \tag{6.6}$$

which also gives the dispersion $E_n(k)$. The normalization condition for annihilation $\hat{c}_{n,k}$ and creation $\hat{c}^\dagger_{n,k}$ operators then

$$\{\hat{c}^\dagger_{n',k'}\hat{c}_{n,k}\} = \hat{c}^\dagger_{n',k'}\hat{c}_{n,k} + \hat{c}_{n,k}\hat{c}^\dagger_{n',k'} = 2\pi\delta_{n'n}\, \delta(k' - k) \tag{6.7}$$

The total current operator can be found by integrating the current density $\hat{J}$ over cross-section

$$\hat{I} = \int d\mathbf{r}_\perp \hat{J}(x, \mathbf{r}_\perp). \tag{6.8}$$

The field operators $\hat{\Psi}$ are defined through creation and annihilation operators for the Lippmann-Schwinger scattering states (see formulas (3.6) and (3.7)) which form a complete orthonormal set of eigenstates of the Hamiltonian $\hat{H}$. Note that normalization in the formulas (6.5) and (6.7) should be consistent one with the other. One can redefine the normalization for the wave functions, e.g., to have δ-function in energy in the right hand side of formula (6.5), if one also redefines Eq. (6.7) to have the same δ-function on the right hand side.

We want to provide an explanation while the Lippmann-Schwinger scattering states are a complete orthonormal set of states in order to use them in the second-quantized formalism[1]. In order to prove that the Lippmann-Schwinger states are orthonormal, we can start by turning off the interaction potential where the solution to the Schrödinger equation is given by

[1]Note that Ya. Blanter and M. Büttiker in the review [1] use another set of states which are not orthonormal.

plain wave incoming from the left and from the right which form a complete orthonormal set. We then adiabatically switch on the scattering potential and the plain waves convert into the Lippmann-Schwinger states. Given this time-dependent Hamiltonian $\hat{\mathcal{H}}(t)$ (no-interaction for $t = 0$ and then adiabatically turning on the interaction potential), the evolution matrix $\hat{S}(t)$ is still unitary. Starting with a orthonormal set of states $|\alpha(0)\rangle$ with $\langle\alpha'(0)|\alpha(0)\rangle = \delta_{\alpha\alpha'}$ (e.g., plain waves), we will end up with a basis set which obeys the same orthonormality condition $|\alpha(t)\rangle = \hat{S}(t)|\alpha(0)\rangle$, $\langle\alpha'(t)|\alpha(t)\rangle = \langle\alpha'(0)|\hat{S}^\dagger(t)\hat{S}(t)|\alpha(0)\rangle = \delta_{\alpha\alpha'}$.

For pure state $|\alpha\rangle$ the average current is given by

$$I = \langle\alpha|\hat{I}|\alpha\rangle. \tag{6.9}$$

If a state described by density matrix $\hat{\rho}$ (an incoherent superposition of pure states), the expectation value of the current is given by the average

$$I = \sum_{\alpha,\beta}\langle\alpha|\hat{\rho}|\beta\rangle\langle\beta|\hat{I}|\alpha\rangle = \mathrm{Tr}\{\hat{\rho}\,\hat{I}\}. \tag{6.10}$$

where the current operator is multiplied with the density matrix and a trace is performed. For a system with Hamiltonian $\hat{H}$ at finite temperature ϑ and with chemical potential μ, the density matrix is given by

$$\hat{\rho} = e^{-(\hat{H}-\mu\hat{N})/k_\mathrm{B}\vartheta}; \tag{6.11}$$

experimentally average of the time[2].

It was suggested by Landauer that reservoirs are completely independent and that therefore the density matrices give independent contribution to the current. The total density matrix of the system can be written as the product of the density matrices describing left and right going electrons (in a two lead geometry). For a multilead geometry, each reservoir (which we label below by the Greek indices α and β) injects electrons into the corresponding lead independent on each other. The overall density matrix is then a product of all the individual density matrices. For a two lead device with reservoirs described by the density matrices,

$$\hat{\rho}_\mathrm{L} = e^{-\sum_\alpha \hat{c}^\dagger_{\mathrm{L},\alpha}\hat{c}_{\mathrm{L},\alpha}(\varepsilon_\alpha-\mu_\mathrm{L})/k_\mathrm{B}\vartheta_\mathrm{L}}, \quad \hat{\rho}_\mathrm{R} = e^{-\sum_\alpha \hat{c}^\dagger_{\mathrm{R},\alpha}\hat{c}_{\mathrm{R},\alpha}(\varepsilon_\alpha-\mu_\mathrm{R})/k_\mathrm{B}\vartheta_\mathrm{R}}. \tag{6.12}$$

[2]The believe that this average will coincide with the average over the time is the matter of ergodicity hypothesis. Note that only average over the time is experimentally accessible. So we calculate one value, measure another and ergodicity hypothesis promise us that the results do coincide. Yet it is still a hypothesis without rigorous proof.

the total density matrix has the form

$$\rho = e^{-\sum_\alpha \{\hat{c}^\dagger_{\mathrm{L},\alpha}\hat{c}_{\mathrm{L},\alpha}(\varepsilon_\alpha-\mu_\mathrm{L})-\hat{c}^\dagger_{\mathrm{R},\alpha}\hat{c}_{\mathrm{R},\alpha}(\varepsilon_\alpha-\mu_\mathrm{R})\}/k_\mathrm{B}\vartheta}. \tag{6.13}$$

Given the density matrix and knowing the form of the field operators $\hat{\Psi}$ (the basis in which the density matrix is given), it is easy obtain all the averages using $\langle \hat{c}^\dagger_{\mathrm{L},\alpha'}\hat{c}_{\mathrm{L},\alpha}\rangle = \delta_{\alpha'\alpha}n_{\alpha,\mathrm{L}}$ and $\langle \hat{c}^\dagger_{\mathrm{R},\alpha'}\hat{c}_{\mathrm{R},\alpha}\rangle = \delta_{\alpha'\alpha}n_{\alpha,\mathrm{R}}$[3]. The Fermi-Dirac distribution function $n_{\alpha,\mathrm{L}}$ and $n_{\alpha,\mathrm{R}}$ represent occupation numbers in left and right reservoir

$$n_{\alpha,\mathrm{L}} = \frac{1}{e^{(\varepsilon_\alpha-\mu_\mathrm{L})/k_\mathrm{B}\vartheta}+1}, \quad n_{\alpha,\mathrm{R}} = \frac{1}{e^{(\varepsilon_\alpha-\mu_\mathrm{R})/k_\mathrm{B}\vartheta}+1}. \tag{6.14}$$

assuming the situation when temperatures of the left and of the right electrons are equal $\vartheta_\mathrm{L} = \vartheta_\mathrm{R} = \vartheta$; otherwise, $\vartheta_{\mathrm{L/R}}$ has to be inserted in $n_{\alpha,\mathrm{L/R}}$ respectively.

Using this form of the density matrix, we will end up with the expression for the current

$$I_\beta = -\frac{2e}{h}\sum_\alpha\sum_{j,l}\int dE\,[n_\beta(\epsilon)-n_\alpha(E)]\,T_{\beta\alpha,lj}(E). \tag{6.15}$$

depending on the difference in the occupation function.

In 80th a lot of effort was devoted to justify the Landauer approach with the help of Kubo formula. We will show that the Landauer approach can be justified with the "poor man Keldysh technique" [2]. The Keldysh Green's function

$$iG^{-+}(\mathbf{r},\mathbf{r}') = \mathrm{Tr}\{\hat{\rho}\hat{\Psi}^\dagger(\mathbf{r}')\hat{\Psi}(\mathbf{r})\} = \langle\hat{\Psi}^\dagger(\mathbf{r}')\hat{\Psi}(\mathbf{r})\rangle \tag{6.16}$$

is an analog of the distribution function $f(q,p,t)$ in the classical kinetic equation. When we are solving the classical kinetic equation (Boltzmann) the boundary condition are that far away the distribution function should coincide with the equilibrium distribution function. The Keldysh Green's function has to satisfy similar boundary conditions at infinity, i.e., in the reservoirs

$$G^{-+}(\mathbf{r},\mathbf{r}')\big|_{\mathbf{r},\mathbf{r}'\in\mathrm{L(R)}} = G^{-+}_\mathrm{eq}(\mathbf{r},\mathbf{r}'), \tag{6.17}$$

where $\mathbf{r},\mathbf{r}' \in \mathrm{L(R)}$ denote both $\mathbf{r}$ and $\mathbf{r}'$ somewhere far in the left or right reservoirs, but never one of the in the left and the other in the right reservoir.

[3] By $\delta_{\alpha'\alpha}$, we denote the Kronecker symbol when α is a discrete parameter and $2\pi\delta(\alpha'-\alpha)$ when α is continuous. Here $\delta(x)$ is a usual Dirac δ-function.

The current can be express via Keldysh Green's function in the following way (note that we already used the average over $\hat{\Psi}^\dagger(\mathbf{r})\hat{\Psi}(\mathbf{r}')$ for calculating current):

$$\hat{J} = \frac{e\hbar}{2m}\left[\frac{\partial}{\partial \mathbf{r}'} - \frac{\partial}{\partial \mathbf{r}}\right] G^{-+}(\mathbf{r},\mathbf{r}')\Big|_{\mathbf{r}=\mathbf{r}'}. \tag{6.18}$$

Suppose now that we have quasi-1D quantum point contact, with the few open channels. Then far in the reservoir most of the electrons originate from the same reservoir and only few amount from some other reservoir. So, as soon as we have the small ratio of the number of open channels in quantum point contact to the number of open channels in the reservoir

$$\delta f \sim \frac{N_{\text{wire}}}{N_{\text{reservoir}}}. \tag{6.19}$$

Landauer's approach is justified, and the distribution function is almost equilibrium at the given μ_α.

6.2 Heisenberg representations of the operators

Usually in the Schrödinger representation of the operators of physical quantities $\hat{L}$ does not depend on time. The average value of the operator $\hat{L}$ in the state $|\alpha(t)\rangle$ is

$$\langle \hat{L}(t)\rangle = \langle \alpha(t)|\hat{L}|\alpha(t)\rangle \tag{6.20}$$

(here and below we omit the $\mathbf{r}$-dependence). Its time-dependence sit in the state $|\alpha(t)\rangle$. The evolution of the state is described by

$$|\alpha(t)\rangle = \hat{S}^\dagger(t)|\alpha\rangle. \tag{6.21}$$

Here $|\alpha\rangle \equiv |\alpha(0)\rangle$ and the evolution operator is

$$\hat{S}(t) = e^{-iE_{\mathbf{k}}t/\hbar}, \tag{6.22}$$

where $E_{\mathbf{k}}$ is a spectrum of the Hamiltonian of the system $\hat{H}$. We can rewrite the formula (6.20) as

$$\langle \hat{L}(t)\rangle = \langle \alpha|\hat{S}(t)\hat{L}\hat{S}^\dagger(t)|\alpha\rangle. \tag{6.23}$$

We can see to this relation as to the new operator

$$\hat{L}(t) = \hat{S}(t)\hat{L}\hat{S}^{\dagger}(t) \tag{6.24}$$

depending on time averaged over the initial state $|\alpha\rangle$. This notation is called Heisenberg representation of the operator.

Note that Heisenberg representation is valid for positive and negative t.

6.3 Interaction representation

Let us consider system with Hamiltonian

$$\hat{H} = \hat{H}_0 + \hat{H}_{\text{int}}. \tag{6.25}$$

We assume $\hat{H}_0$ to be noninteracting part and that we know everything about the system with this Hamiltonian. The time-dependent wave function

$$|\alpha(t)\rangle = e^{i[\hat{H}_0+\hat{H}_{\text{int}}]t/\hbar}|\alpha\rangle \tag{6.26}$$

should satisfy time-dependent Schrödinger equation

$$i\hbar\frac{\partial}{\partial t}|\alpha(t)\rangle = [\hat{H}_0 + \hat{H}_{\text{int}}]|\alpha(t)\rangle. \tag{6.27}$$

The interacting $\hat{H}_{\text{int}}(t)$ part we will consider as a perturbation. We will use the Heisenberg representation for the interaction part $\hat{H}_{\text{int}}(t) = e^{i\hat{H}_0 t/\hbar}\hat{H}_{\text{int}}e^{-i\hat{H}_0 t/\hbar}$. The Eq. (6.26) can be rewritten as

$$|\alpha(t)\rangle = e^{-i\hat{H}_0 t/\hbar}\hat{S}|\alpha\rangle \tag{6.28}$$

Here the $\hat{S}$-matrix according for the evolution due to interacting part is given by the time-ordered exponent

$$\hat{S} = \mathrm{T}e^{-(i/\hbar)\int_0^t d\tau \hat{H}_{\text{int}}(\tau)} = \sum_{n=0}^{\infty}\Big(-\frac{i}{\hbar}\Big)^n \int_0^t d\tau_1\, \hat{H}_{\text{int}}(\tau_1) \times \int_0^{\tau_1} d\tau_2\, \hat{H}_{\text{int}}(\tau_2)\ldots\int_0^{\tau_{n-1}} d\tau_n\, \hat{H}_{\text{int}}(\tau_n). \tag{6.29}$$

with ordered time $0 < \tau_n < \ldots < \tau_1 < t$. The inverse chronological exponent $\tilde{\mathrm{T}}$ and defined by the same relation but with $0 > \tau_n > \ldots > \tau_1 > t$. Note that

Let us proof the relation (6.28); we should check does such a state $|\alpha(t)\rangle$ satisfy (6.27). Lets do that

$$i\hbar\frac{\partial}{\partial t}|\alpha(t)\rangle = \hat{H}_0|\alpha(t)\rangle + e^{-i\hat{H}_0 t/\hbar}e^{i\hat{H}_0 t/\hbar}e^{-i\hat{H}_0 t/\hbar}\,\mathrm{T}e^{-(i/\hbar)\int_0^t d\tau \hat{H}_{\mathrm{int}}(\tau)}|\alpha\rangle = \\ = [\hat{H}_0 + \hat{H}_{\mathrm{int}}]|\alpha(t)\rangle. \quad (6.30)$$

The density matrix in interaction representation is defined in a similar way

$$\hat{\rho}(t) = e^{-i\hat{H}_0 t/\hbar}\hat{S}\hat{\rho}_0\hat{S}^\dagger e^{i\hat{H}_0 t/\hbar} = \\ = e^{-i\hat{H}_0 t/\hbar}\,\mathrm{T}e^{-(i/\hbar)\int_0^t d\tau \hat{H}_{\mathrm{int}}(\tau)}\hat{\rho}_0\tilde{\mathrm{T}}e^{(i/\hbar)\int_0^t d\tau \hat{H}_{\mathrm{int}}(\tau)}e^{i\hat{H}_0 t/\hbar}. \quad (6.31)$$

where $\hat{\rho}_0 = \hat{\rho}(0)$.

The average of current operator is[4]

$$I(t) \equiv \langle\hat{I}(t)\rangle = \mathrm{Tr}\{\hat{\rho}(t)\hat{I}\} = \\ = \mathrm{Tr}\Big\{\mathrm{T}e^{-(i/\hbar)\int_0^t d\tau \hat{H}_{\mathrm{int}}(\tau)}\,\hat{\rho}_0\,\tilde{\mathrm{T}}e^{(i/\hbar)\int_0^t d\tau \hat{H}_{\mathrm{int}}(\tau)}e^{i\hat{H}_0 t/\hbar}\hat{I}e^{-i\hat{H}_0 t/\hbar}\Big\}. \quad (6.32)$$

We can rewrite this expression, using current operator in Heisenberg representation

$$I(t) = \mathrm{Tr}\Big\{\hat{\rho}_0\,\tilde{\mathrm{T}}e^{(i/\hbar)\int_0^t d\tau \hat{H}_{\mathrm{int}}(\tau)}\hat{I}(t)\,\mathrm{T}e^{-(i/\hbar)\int_0^t d\tau \hat{H}_{\mathrm{int}}(\tau)}\Big\}. \quad (6.33)$$

6.4 Change of the current due to electron-electron interaction

In this chapter, we want to calculate the current through a symmetric quantum dot where electrons interacts if they are inside the confined area. The dot we model with the symmetric double of the length L barrier with transmission and reflection amplitudes t and r with rectangular interaction in between (each barrier has transmission and reflection amplitudes t_1 and r_1). The interaction Hamiltonian is

$$\hat{H}_{\mathrm{int}} = \frac{1}{2}\sum_{\sigma',\sigma}\int_{-\infty}^{\infty}dx\int_{-\infty}^{\infty}dx'\,\hat{\Psi}^\dagger_\sigma(x,t)\hat{\Psi}^\dagger_{\sigma'}(x',t)U(x,x')\hat{\Psi}_{\sigma'}(x',t)\hat{\Psi}_\sigma(x,t) \quad (6.34)$$

[4]Here and in the next formula we use the property of cyclic shift of operators in trace does not change its value, $\mathrm{Tr}\{\hat{A}\hat{B}\hat{C}\} = \mathrm{Tr}\{\hat{B}\hat{C}\hat{A}\}$.

with the interaction potential

$$U(x,x') = U_0\Theta(L/2-|x|)\Theta(L/2-|x'|); \tag{6.35}$$

which is nonzero on the square of dimension $L\times L$,[5] and σ the spin index, $\sigma =\uparrow,\downarrow$. The field operators in the interaction representation include the trivial time-dependence

$$\hat{\Psi}_\sigma(x,t) = \sum_{\alpha,k}\hat{c}_{\alpha\sigma k}\varphi_{\alpha k}(x)e^{-iE_k t/\hbar} \tag{6.36}$$

here, α distinguished between the left and right scattering states, $\alpha = \mathrm{L},\mathrm{R}$). In according with (6.33) the current is defined by the trace

$$I = \mathrm{Tr}\{\hat{\rho}_0\hat{S}^\dagger\hat{I}\hat{S}\}. \tag{6.37}$$

We are interested in the correction to the current δI due to the interaction (6.34) in first order perturbation theory. Expanding the exponent in $\hat{S}$, Eq. (6.37) yields

$$\delta\hat{I}(t) = \frac{i}{\hbar}\left[\hat{I},\int\limits_{-\infty}^{t}d\tau\,\hat{H}_{\mathrm{int}}(\tau)\right];\;\; \delta I(t) = \mathrm{Tr}\{\hat{\rho}\delta\hat{I}(t)\} \tag{6.38}$$

where t is the time where the current is measured. In order to be in the stationary regime, we let $t\to\infty$ and first perform the integration over time in (6.34)

$$\int\limits_{-\infty}^{\infty}\frac{d\tau}{\hbar}\,\hat{H}_{\mathrm{int}}(\tau) = \pi\sum_{\substack{\sigma',\sigma\\ k',q',k,q\\ \alpha,\beta,\theta,\delta}}U_{\alpha k,\beta q',\theta k,\delta q}\,\hat{c}^\dagger_{\alpha\sigma k'}\hat{c}^\dagger_{\beta\sigma' q'}\hat{c}_{\theta\sigma' k}\hat{c}_{\delta\sigma q}\delta(E_{k'}+E_{q'}-E_k-E_q),$$

with the interaction matrix elements

$$U_{\alpha k,\beta q',\theta k,\delta q} = U_0\int\limits_{-L/2}^{L/2}dx\int\limits_{-L/2}^{L/2}dx'\varphi^*_{\alpha k'}(x)\varphi^*_{\beta q'}(x')\varphi_{\theta k}(x')\varphi_{\delta q}(x). \tag{6.39}$$

Let us estimate U using the fact that wave function between two barriers near the resonance is coincides with the wave function in the box. For the

[5] We use the Heaviside step function $\Theta(x)$; $\Theta(x<0)=0$, $\Theta(x>0)=1$.

first resonance, we obtain [6]

$$\varphi^{(1)}_{\mathrm{L/R},k}(x) \approx \frac{2t_k}{t_1}\cos\frac{\pi x}{L}. \tag{6.40}$$

for both the left and the right scattering state. As the current has only an appreciable contribution close to the resonances, we can substitute (6.40) into U assuming that only the first resonance contributes to the transport. We obtain

$$U_{\alpha k,\beta q',\theta k,\delta q} = U_0\frac{4L^2}{T_1^2}t^*_{k'}t^*_{q'}t_k t_q. \tag{6.41}$$

Inserting U into the expression for the time integrated Hamiltonian and replacing the summation by an integration yields

$$\int_{-\infty}^{\infty}\frac{d\tau}{\hbar}\hat{H}_{\mathrm{int}}(\tau) = \pi U_0\frac{4L^2}{T_1^2}\sum_{\substack{\sigma',\sigma\\ \alpha,\beta,\theta,\delta}}\int_0^{\infty}\frac{dk'\,dq'\,dk\,dq}{(2\pi)^4}\hat{c}^\dagger_{\alpha\sigma k'}\hat{c}^\dagger_{\beta\sigma' q'}\hat{c}_{\theta\sigma' k}\hat{c}_{\delta\sigma q}$$
$$\times\, t^*_{k'}t^*_{q'}t_k t_q\delta(E_{k'}+E_{q'}-E_k-E_q). \tag{6.42}$$

In a next step, we express current operator $\hat{I}$ in terms of Lippmann-Schwinger scattering states. We substitute to the formula (6.3) the correspondent field operators (6.4)[7] and choose the position far at the right of the barrier. The asymptotic form is given by

$$\hat{\Psi}(x) = \sum_k\left[\hat{c}_{\mathrm{L}\sigma k}t_k e^{ikx} + \hat{c}_{\mathrm{R}\sigma k}(r_k e^{ikx}+e^{-ikx})\right]. \tag{6.43}$$

For simplicity assume symmetric barrier and zero magnetic field. We exchange the summation to an integration and obtain expression for current operator

$$\begin{aligned}\hat{I} = -\frac{e\hbar}{2m}\sum_\sigma\int_0^\infty\frac{dk'dk}{(2\pi)^2}\Big\{&\hat{c}^\dagger_{\mathrm{L}\sigma k'}\hat{c}_{\mathrm{L}\sigma k}(k'+k)t^*_{k'}t_{k'}e^{i(k-k')x}\\
&+\hat{c}^\dagger_{\mathrm{L}\sigma k'}\hat{c}_{\mathrm{R}\sigma k}\Big[k't^*_{k'}e^{-ik'x}(r_k e^{ikx}+e^{-ikx})+kt^*_{k'}e^{-ik'x}(r_k e^{ikx}-e^{-ikx})\Big]\\
&+\hat{c}^\dagger_{\mathrm{R}\sigma k'}\hat{c}_{\mathrm{L}\sigma k}\Big[k'(r^*_{k'}e^{-ik'x}-e^{ik'x})t_k e^{ikx}+k(r^*_{k'}e^{-ik'x}+e^{ik'x})t_k e^{ikx}\Big]\\
&+\hat{c}^\dagger_{\mathrm{R}\sigma k'}\hat{c}_{\mathrm{R}\sigma k}\Big[k'(r^*_{k'}e^{-ik'x}-e^{ik'x}(r_k e^{ikx}+e^{-ikx})\\
&\qquad+k(r^*_{k'}e^{-ik'x}+e^{ik'x})(r_k e^{ikx}-e^{-ikx})\Big]\Big\}.\end{aligned} \tag{6.44}$$

[6] The wave function near e.g. second resonance is $\varphi^{(2)}_{\mathrm{L/R},k}(x)\approx\mp\frac{2it_k}{t_1}\sin\frac{2\pi x}{L}$.

[7] We already performed the integration over $\mathbf{r}_\perp$.

Averaging of the current operator over the non-interacting density matrix gives the Landauer formula: the contribution from off-diagonal terms in L/R space vanishes. Furthermore, using the fact that $\langle \hat{c}^\dagger_{\alpha\sigma' k'} \hat{c}_{\beta\sigma k}\rangle = n_\alpha(k)\delta_{\alpha\beta}\delta_{\sigma'\sigma}\delta_{k'k}$ [where for continuos k, $\delta_{k'k} \equiv 2\pi\delta(k'-k)$] yields

$$\begin{aligned} I &= -\frac{e\hbar}{m}\int_0^\infty \frac{dk}{2\pi} k\big\{n_{\rm L}(k)T_k - n_{\rm R}(k)[1-R_k]\big\} \\ &= -\frac{e\hbar}{m}\int_0^\infty \frac{dk}{2\pi} kT_k[n_{\rm L}(k) - n_{\rm R}(k)]; \end{aligned} \tag{6.45}$$

after the substitution $k = \sqrt{2mE}/\hbar$, Landauer's formula is obtained.

needs to be corrected from here on

The contributions to δI is from current off-diagonal terms in L/R space. Let us define space part of current operator as $F(p',p) = (ik'e^{ik'x} - ik'r^*_{k'}e^{-ik'x})t_k e^{ikx} - (e^{ik'x} + r^*_{k'}e^{-ik'x})ikt_k e^{ikx}$ and $G(p',p) = (e^{-ikx} + r_k e^{ikx}) - (e^{ik'x} + r^*_{k'}e^{-ik'x})(-ike^{-ikx} + ikr_k e^{ikx})$. We calculate one of these terms as example, cioe term in Eq. (6.42) with $\alpha,\beta,\theta,\delta = {\rm L},{\rm R},{\rm L},{\rm L}$. The average value of the operators is

$$\begin{aligned} &\langle \hat{c}^\dagger_{{\rm L}\sigma k'}\hat{c}^\dagger_{{\rm R}\sigma' q'}\hat{c}_{{\rm L}\sigma' k}\hat{c}_{{\rm L}\sigma q}\hat{c}^\dagger_{{\rm L}\sigma'' p'}\hat{c}_{{\rm R}\sigma'' p}\rangle - \langle \hat{c}^\dagger_{{\rm L}\sigma'' p'}\hat{c}_{{\rm R}\sigma'' p}\hat{c}^\dagger_{{\rm L}\sigma k'}\hat{c}^\dagger_{{\rm R}\sigma' q'}\hat{c}_{{\rm L}\sigma' k}\hat{c}_{{\rm L}\sigma q}\rangle = \\ &= -\langle \hat{c}^\dagger_{{\rm R}\sigma' q'}\hat{c}_{{\rm R}\sigma'' p}\rangle\langle \hat{c}^\dagger_{{\rm L}\sigma k'}\hat{c}_{{\rm L}\sigma' k}\hat{c}_{{\rm L}\sigma q}\hat{c}^\dagger_{{\rm L}\sigma'' p'}\rangle + \langle \hat{c}_{{\rm R}\sigma'' p}\hat{c}^\dagger_{{\rm R}\sigma' q'}\rangle\langle \hat{c}^\dagger_{{\rm L}\sigma'' p'}\hat{c}^\dagger_{{\rm L}\sigma k'}\hat{c}_{{\rm L}\sigma' k}\hat{c}_{{\rm L}\sigma q}\rangle = \\ &\quad = -\langle \hat{c}^\dagger_{{\rm R}\sigma' q'}\hat{c}_{{\rm R}\sigma'' p}\rangle\Big[\langle \hat{c}^\dagger_{{\rm L}\sigma k'}\hat{c}_{{\rm L}\sigma' k}\rangle\langle \hat{c}_{{\rm L}\sigma q}\hat{c}^\dagger_{{\rm L}\sigma'' p'}\rangle - \langle \hat{c}^\dagger_{{\rm L}\sigma k'}\hat{c}_{{\rm L}\sigma q}\rangle\langle \hat{c}_{{\rm L}\sigma' k}\hat{c}^\dagger_{{\rm L}\sigma'' p'}\rangle\Big] + \\ &\quad + \langle \hat{c}_{{\rm R}\sigma'' p}\hat{c}^\dagger_{{\rm R}\sigma' q'}\rangle\Big[- \langle \hat{c}^\dagger_{{\rm L}\sigma'' p'}\hat{c}_{{\rm L}\sigma' k}\rangle\langle \hat{c}^\dagger_{{\rm L}\sigma k'}\hat{c}_{{\rm L}\sigma q}\rangle + \langle \hat{c}^\dagger_{{\rm L}\sigma'' p'}\hat{c}_{{\rm L}\sigma q}\rangle\langle \hat{c}^\dagger_{{\rm L}\sigma k'}\hat{c}_{{\rm L}\sigma' k}\rangle\Big] = \\ &\qquad = -n_{{\rm R}p}\delta_{\sigma'\sigma''}\delta_{q'p}\Big[1 - n_{{\rm L}k}\delta_{\sigma\sigma'}\delta_{k'k}(1-n_{{\rm L}q})\delta_{\sigma\sigma''}\delta_{qp'} - \\ &\qquad\qquad - n_{{\rm L}q}\delta_{\sigma\sigma}\delta_{k'q}(1-n_{{\rm L}k})\delta_{\sigma'\sigma''}\delta_{kp'}\Big] + \\ &\qquad + (1-n_{{\rm R}p})\delta_{\sigma''\sigma'}\delta_{pq'}\Big[- n_{{\rm L}k}\delta_{\sigma''\sigma'}\delta_{p'k}n_{{\rm L}q}\delta_{\sigma\sigma}\delta_{k'q} + \\ &\qquad\qquad + n_{{\rm L}q}\delta_{\sigma''\sigma}\delta_{p'q}n_{{\rm L}k}\delta_{\sigma\sigma'}\delta_{k'k}\Big] \end{aligned} \tag{6.46}$$

Making summation over spin indices and taking into account that

$$\sum_{\sigma,\sigma',\sigma''}\delta_{\sigma\sigma'}\delta_{\sigma'\sigma''}\delta_{\sigma''\sigma} = 2 \text{ and } \sum_{\sigma,\sigma',\sigma''}\delta_{\sigma\sigma}\delta_{\sigma'\sigma''}\delta_{\sigma''\sigma'} = 4$$

we rewrite (6.46) as

$$\begin{aligned} &- n_{{\rm R}p}\delta_{q'p}\big[2n_{{\rm L}k}\delta_{k'k}(1-n_{{\rm L}q})\delta_{qp'} - 4n_{{\rm L}q}\delta_{k'q}(1-n_{{\rm L}k})\delta_{kp'}\big] + \\ &\qquad + (1-n_{{\rm R}p})\delta_{pq'}\big[- 4\delta_{p'k}\delta_{k'q} + 2\delta_{p'q}\delta_{k'k}\big]n_{{\rm L}k}n_{{\rm L}q}. \end{aligned} \tag{6.47}$$

For continuous variables k and k' delta function $\delta_{k'k} \equiv 2\pi\delta(k'-k)$. Making integration over primes variables and taking into account δ-function of energies $\delta(k'^2+q'^2-k^2-q^2)$ and $F(p',p)$ we have

$$(2\pi)^3\Big\{-n_{\rm Rp}\big[2n_{\rm Lk}(1-n_{\rm Lq})\delta(p^2-q^2)F(q,p)-4n_{\rm Lq}(1-n_{\rm Lk})\delta(p^2-k^2)F(k,p)\big]+ \\ +(1-n_{\rm Rp})\big[-4\delta(p^2-k^2)F(k,p)+2\delta(p^2-q^2)F(q,p)\big]n_{\rm Lk}n_{\rm Lq}\Big\}. \quad (6.48)$$

Integration over p gives

$$(2\pi)^3\Big\{-2n_{\rm Rq}n_{\rm Lk}(1-n_{\rm Lq})\frac{F(q,q)}{2q}+4n_{\rm Rk}n_{\rm Lq}(1-n_{\rm Lk})\frac{F(k,k)}{2k}- \\ -4(1-n_{\rm Rk})n_{\rm Lk}n_{\rm Lq}\frac{F(k,k)}{2k}+2(1-n_{\rm Rq})n_{\rm Lk}n_{\rm Lq}\frac{F(q,q)}{2q}\Big\} \quad (6.49)$$

For equal arguments $F(q,q) = -2iqt_q^*r_q$ and $G(q,q) = -2iqt_qr_q^*$ and we obtain

$$-it_q^*r_q(2\pi)^3\Big\{-2n_{\rm Rq}n_{\rm Lk}(1-n_{\rm Lq})+4n_{\rm Rq}n_{\rm Lk}(1-n_{\rm Lq})- \\ -4(1-n_{\rm Rq})n_{\rm Lq}n_{\rm Lk}+2(1-n_{\rm Rq})n_{\rm Lk}n_{\rm Lq}\Big\}= \\ =-it_q^*r_q(2\pi)^3 2n_{\rm Lk}[n_{\rm Rq}-n_{\rm Lq}]. \quad (6.50)$$

The other terms are similar to this, summing up over all values of $\alpha,\beta,\theta,\delta$ we obtain the expression for all terms. Using the unitarity of the scattering matrix, i.e. $t_q^*r_q = -t_qr_q^*$ we obtain the expression for correction to the current

$$\delta I = \frac{\pi U_0}{2}\frac{4L^2}{T_1^2}\Big(-\frac{ie\hbar}{2m}\Big)\frac{2m}{\hbar^2}\int\limits_0^\infty\frac{dk\,dq}{(2\pi)^3}\,T_kT_q(-it_q^*r_q)\,8(n_{\rm Lk}+n_{\rm Rk})(n_{\rm Lq}-n_{\rm Rq}). \quad (6.51)$$

Simplifying it we obtain final result

$$\delta I = -\frac{2e}{h}\frac{8\pi U_0L^2}{T_1^2}\int\limits_0^\infty\frac{dk\,dq}{(2\pi)^2}\,T_kT_q\,t_q^*r_q(n_{\rm Lk}+n_{\rm Rk})(n_{\rm Lq}-n_{\rm Rq}). \quad (6.52)$$

The integration can be easily made, but we do not do that.

6.5 Time-dependent interaction

Let us define the density matrix $\hat{\rho}$ of the system with the time-dependent Hamiltonian

$$\hat{H}(t) = \hat{H}_0(t) + \hat{H}_{\rm int}(t) \tag{6.53}$$

by the usual equation

$$i\hbar\frac{\partial\hat{\rho}}{\partial t} = [\hat{H}_{\rm int}, \hat{\rho}] \equiv \hat{H}_{\rm int}\hat{\rho} - \hat{\rho}\hat{H}_{\rm int} \tag{6.54}$$

with the boundary condition

$$\hat{\rho}_0 = \hat{\rho}(-\infty) = e^{[F_0 - \hat{H}_0(-\infty)]/k_{\rm B}\vartheta}, \tag{6.55}$$

here F_0 is the initial free energy. The noninteracting term represents the energy of electrons in the external field with scalar $V = V(t)$ and $\mathbf{A} = \mathbf{A}(t)$ vector potential

$$\hat{H}_0(t) = \int d\mathbf{r}\, \hat{\Psi}_0^\dagger(t)\Big[E\Big(-i\nabla + \frac{e}{\hbar c}\mathbf{A}\Big) - eV\Big]\hat{\Psi}_0(t), \tag{6.56}$$

where $E(\mathbf{k})$ is a dispersion relation of the electrons. The field operators $\hat{\Psi}_0^\dagger(t)$ and $\hat{\Psi}_0(t)$ are defined in the following manner: let $\varphi_{\mathbf{k}}(t)$ be the complete system of functions determined by the equation

$$\Big[E\Big(-i\nabla + \frac{e}{\hbar c}\mathbf{A}\Big) - eV - i\hbar\frac{\partial}{\partial t}\Big]\varphi_{\mathbf{k}} = 0 \tag{6.57}$$

and boundary condition

$$\varphi_{\mathbf{k}}(t) \to e^{i\mathbf{kr} - iE(\mathbf{k})t/\hbar} \text{ as } t \to -\infty, \tag{6.58}$$

where we consider the external field the be switched off [$V \to 0$ and $\mathbf{A} \to 0$] at $t \to -\infty$. Than the field operators $\hat{\Psi}_0$ and $\hat{\Psi}_0^\dagger$ are defined by the relations

$$\hat{\Psi}(t) = \sum_{\mathbf{k}} \hat{c}_{\mathbf{k}}\varphi_{\mathbf{k}}(t) \tag{6.59}$$

and

$$\hat{\Psi}^\dagger(t) = \sum_{\mathbf{k}} \hat{c}_{\mathbf{k}}^\dagger\varphi_{\mathbf{k}}^*(t) \tag{6.60}$$

where $\hat{c}_{\mathbf{k}}$, $\hat{c}_{\mathbf{k}}^\dagger$ are usual Fermi annihilation and creation operators with commutation realtion

$$[\hat{c}_{\mathbf{k}}^\dagger, \hat{c}_{\mathbf{k}'}] \equiv \hat{c}_{\mathbf{k}}^\dagger\hat{c}_{\mathbf{k}'} + \hat{c}_{\mathbf{k}'}\hat{c}_{\mathbf{k}}^\dagger = \delta_{\mathbf{k}\mathbf{k}'}. \tag{6.61}$$

Utilizing the fact that the functions $\varphi_{\mathbf{k}}(t)$ form at arbitrary instant of time a complete orthogonal system and formulas (6.59), (6.60), and (6.61), it can be easily show that for coincident times we have

$$[\hat{\Psi}^{\dagger}_{\mathbf{k}}(t), \hat{\Psi}_{\mathbf{k}}(t)] = \delta(\mathbf{r} - \mathbf{r}'). \tag{6.62}$$

and in virtue of this operators $\hat{\Psi}_{\mathbf{k}}(t)$ satisfy the free equation of motion

$$i\hbar \frac{\partial \hat{\Psi}_{\mathbf{k}}}{\partial t} = \{\hat{\Psi}_{\mathbf{k}}, \hat{H}_0\} \equiv \hat{\Psi}_{\mathbf{k}} \hat{H}_0 - \hat{H}_0 \Psi_{\mathbf{k}}. \tag{6.63}$$

i.e., we have from the outset defined the field operators in the interaction representation.

We note that the operator $\hat{H}_0(t)$ differs from the Schrödinger representation and in the interaction representation in contrast to the usual case, when the external fields are independent of the time. Having in mind such a definition of the field operators we have from the outset written Eq. (6.54). In the interaction representation we leaving it only the operator for the interaction energy $\hat{H}_{\text{int}}$ which, for the sake of definiteness, we shall in future write in the form

$$\hat{H}_{\text{int}} = g \int d\mathbf{r}\, \hat{\Psi}^{\dagger}_{\mathbf{k}}(t) \hat{\Psi}_{\mathbf{k}}(t) \varphi(t). \tag{6.64}$$

where g is a dimensionless coupling constant. Such expression describes interaction between electrons and phonons in solids, and also can be utilized to describe Coulomb interaction of charged particles if we write a separate equation for the Coulomb field.

Eq. (6.54) for the density matrix $\hat{\rho}(t)$ can be formally solved by introducing S-matrix

$$\hat{S}(t) \equiv \hat{S}(t, -\infty) = \mathrm{T}\, e^{-(i/\hbar)\int_{-\infty}^{t} \hat{H}_{\text{int}}(\tau)\, d\tau}, \tag{6.65}$$

which satisfies the relation

$$i\hbar \frac{\partial \hat{S}(t)}{\partial t} = \hat{H}_{\text{int}}(t) \hat{S}(t). \tag{6.66}$$

Note that (6.65) is a formal solution of the differential equation (6.66). The symbol T in (6.65) denoted a time-ordered product defined in the usual manner. Than we have

$$\hat{\rho}(t) = \hat{S}(t) \hat{\rho}(t) \hat{S}^{\dagger}(t) = \hat{S}(t) \hat{\rho}(t) \hat{S}(t). \tag{6.67}$$

The density matrix defined in this manner depends explicitly on the time. The average value of an arbitrary operator $\hat{L}_0(t)$ at time t has the form

$$\langle \hat{L}_0(t) \rangle = \mathrm{Tr}\{\hat{\rho}(t)\hat{L}_0(t)\}, \tag{6.68}$$

where the subscript 0 in the operator $\hat{L}_0(t)$ shows that the operator is taken in interaction representation, i.e. its time dependence is determined by the free equation of motion in the external field

$$i\hbar \frac{\partial \hat{L}_0(t)}{\partial t} = \{\hat{L}_0, \hat{H}_0(t)\}, \tag{6.69}$$

since the density matrix $\hat{\rho}(t)$ itself was defined in the interaction representation.

Bibliography

[1] Ya. M. Blanter and M. Büttiker, *Shot noise in mesoscopic conductors*, Phys. Rep. **336**, 1 (2000).

[2] L. V. Keldysh, *Diagram technique for nonequilibrium processes*, Sov. Phys. JETP **20**, 1018 (1965).

Chapter 7

Noise review

7.1 Introduction

This chapter will provide a general overview about noise. First, we will discuss different types of classical noise together with general feature of noise. Then, we will apply a quantum approach to calculate noise. Probably, the first study about noise was done by Robert Brown in the context of Brownian motion [1] which was later explained by Albert Einstein as being due to random thermal motion of the fluid particles [2]. A different source of noise was put forward a bit later by Schottky. He concentrated his attention on the fact that the charge being transported by an electric current is not continuous but that electrons which constitute the current carry portion of charge. In this situation (shot-) noise appears which is due to the discrete nature of the electron charge [3]. An experiment performed by Johnson confirmed Schottky's idea [4] and thereby discovered flicker noise (also called $1/f$ noise, because its intensity grows like $1/f$ at small frequencies f). He observed flicker noise while trying to detect shot noise which is expected to be more or less constant as a function of frequency f; and he found an additional contribution to spectral density

$$S(\omega) \propto 1/\omega \tag{7.1}$$

(here $\omega \equiv 2\pi f$) which was "flickering" in time. Apart from shot noise and $1/f$ noise, Johnson measured also equilibrium noise (the so-called Nyquist-Johnson noise) [5, 6].

Some general remarks about noise: in classical mechanics, we can describe the motion of each individual particle to any accuracy. In quantum mechanics

this is in principle not possible (at least in the standard theory) and all we can hope is a statistical description is the world. However, even classical systems which are huge the motion of particles cannot be described it in all details. Thus, we study averages of quantities like $\langle I(t)\rangle$ which describes collective motion but not the properties of individual electrons. In order to obtain more detailed knowledge of the individual behavior, we can extend our study to include fluctuations $\langle \delta I^2\rangle$ and correlation functions like that $\langle \delta I(t_1)\delta I(t_2)\rangle$, where $\delta I(t)$ is a defined by

$$\delta I(t) = I(t) - \langle I(t)\rangle. \tag{7.2}$$

Theoretically, the average $\langle I(t)\rangle$ is taken over the ensembles, experimentally over the time. The deviation $\delta I(t)$ shows dynamics of system, which is not visible in $\langle I(t)\rangle$ which depends on time only in a case of collective motion of all the particle, e.g., in the presence of time-dependent potential.

The quantity describing noise is the second-order correlator $\langle \delta I(t_1)\delta I(t_2)\rangle$. When the process is stationary, this correlator depends only on time difference $t = t_2 - t_1$ and the spectral density is defined as the Fourier transformation of the correlator

$$S(\omega) = \int dt\, e^{i\omega t}\langle \delta I(0)\delta I(t)\rangle. \tag{7.3}$$

The correlator $\langle \delta I(t_1)\delta I(t_2)\rangle$ is called an irreducible correlator (denoted by double brackets),

$$\langle\langle I_1 I_2\rangle\rangle \equiv \langle \delta I_1 \delta I_2\rangle = \langle I_1 I_2\rangle - \langle I_1\rangle\langle I_2\rangle; \tag{7.4}$$

the lower index indicates the time at which the correlator has to be evaluated. Of course, it is also possible to study higher order correlators. In the following, we write down the decomposition of the higher order irreducible correlators into correlators and irreducible correlator of lower order. The third order irreducible correlator is given by

$$\langle\langle I_1 I_2 I_3\rangle\rangle \equiv \langle I_1 I_2 I_3\rangle - \langle I_1\rangle\langle\langle I_2 I_3\rangle\rangle - \langle I_2\rangle\langle\langle I_1 I_3\rangle\rangle - \langle I_3\rangle\langle\langle I_1 I_2\rangle\rangle - \langle I_1\rangle\langle I_2\rangle\langle I_3\rangle;$$

and the fourth-order irreducible correlator is

$$\begin{aligned}\langle\langle I_1 I_2 I_3 I_4\rangle\rangle \equiv{}& \langle I_1 I_2 I_3 I_4\rangle - \langle I_1\rangle\langle I_2\rangle\langle I_3\rangle\langle I_4\rangle - \\ & \langle I_1\rangle\langle\langle I_2 I_3 I_4\rangle\rangle - \langle I_2\rangle\langle\langle I_1 I_3 I_4\rangle\rangle - \langle I_3\rangle\langle\langle I_1 I_2 I_4\rangle\rangle - \langle I_4\rangle\langle\langle I_1 I_2 I_3\rangle\rangle - \\ & \langle\langle I_1 I_2\rangle\rangle\langle\langle I_3 I_4\rangle\rangle - \langle\langle I_1 I_3\rangle\rangle\langle\langle I_2 I_4\rangle\rangle - \langle\langle I_1 I_4\rangle\rangle\langle\langle I_2 I_3\rangle\rangle. \end{aligned} \tag{7.5}$$

These expressions for the correlators depend on the fact that the classical correlation functions are symmetric under interchange of their arguments. This is not the case for quantum mechanical correlators. The proper definition of quantum mechanical correlators, we will discuss later.

7.2 Shot noise[3]

Lets us first comment on shot noise; here, we follow the original work of Schottky. He discussed the charge transport of a vacuum tube and suggested that the process of emitting of electrons from the first electrode is the Poissonian, i.e., each electron has a probability to be emitted per unit time and this probability does not depend on what is happening to the other electrons — whether they emitted or not, see Figure 7.1. For a Poissonian process,

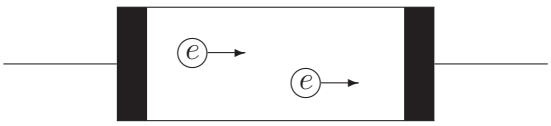

Figure 7.1: A vacuum tube. Biasing the capacitor place with a large voltage, electron are knocked out of the emitter plate, transverse the vacuum tube and are reabsorbed by the second plate. Due to the discreteness of the electron, the current cannot flow continuous and the current shows shot noise.

it is known that the variance is equal to the average,

$$\langle \delta N^2 \rangle = \langle N \rangle, \tag{7.6}$$

where N is a number of emitted electrons; even more all the higher order irreducible correlators are equal to the average,

$$\langle\langle N^k \rangle\rangle = \langle N \rangle, \tag{7.7}$$

here k is integer and $k > 0$. Correspondingly, the noise of the transmitted charge ($Q = -eN$) is given by

$$\langle\langle Q^2 \rangle\rangle = e^2 \langle N \rangle = e\langle Q \rangle = e\langle I \rangle t, \tag{7.8}$$

where $-e$ is the electron charge, $\langle I\rangle > 0$ is the average current, and t is the time of the observation. We want to relate this result to the spectral density $S(\omega)$ introduced above. Note that the transmitted charge Q is just the time-integrate current

$$Q = \int_0^t I(\tau)d\tau, \tag{7.9}$$

such that we can evaluate

$$\langle\langle Q^2\rangle\rangle = \int_0^t dt_1 \int_0^t dt_2 \, \langle\langle I(t_1)I(t_2)\rangle\rangle = \int_0^t dt_1 \int_0^t dt_2 \, \langle\langle I(0)I(t_2-t_1)\rangle\rangle. \tag{7.10}$$

in terms of the current. Next, we introduce the spectral density, cf. (7.3),

$$S(\omega) = \int dt \, e^{i\omega t}\langle\langle I(0)I(t)\rangle\rangle. \tag{7.11}$$

Substituting the Fourier transformed formula into (7.9) yields

$$\begin{aligned}\langle\langle Q^2\rangle\rangle &= \int_0^t dt_1 \int_0^t dt_2 \int \frac{d\omega}{2\pi} \, e^{-i\omega(t_2-t_1)} S(\omega) \\ &= \int \frac{d\omega}{2\pi} \, S(\omega) \int_0^t dt_1 \int_0^t dt_2 \, e^{-i\omega(t_2-t_1)}.\end{aligned} \tag{7.12}$$

Performing the integration over time, we arrive at the final result,

$$\langle\langle Q^2\rangle\rangle = \int \frac{d\omega}{2\pi} \, S(\omega) \frac{\sin^2 \omega t/2}{(\omega/2)^2}. \tag{7.13}$$

Remark. Now let us make a few notes about noise spectral density. For zero frequency $\omega = 0$ formula (7.11) gives

$$S(0) = \int_{-\infty}^{+\infty} \langle\langle I(0)I(t)\rangle\rangle \, dt.$$

$S(0)$ $\omega = 0$ is determined not just by long times.

Remark. $S(\omega)$. If $I(t_1)$ and $I(t_2)$ commutes $I(t_1)I(t_2) = I(t_2)I(t_1)$ and time invariant $\langle\langle I(t_1+\tau)I(t_2+\tau)\rangle\rangle = \langle\langle I(t_1)I(t_2)\rangle\rangle$ we can write $\langle\langle I(0)I(-|t|)\rangle\rangle = \langle\langle I(-|t|)I(0)\rangle\rangle = \langle\langle I(0)I(|t|)\rangle\rangle$ and perform the integration over the half space

$$S(0) = 2 \int_0^{+\infty} \langle\langle I(0)I(t)\rangle\rangle \, dt.$$

Remark. To replace

$$\int_{-\infty}^{+\infty} \frac{d\omega}{2\pi} S(\omega) \longrightarrow 2 \int_{0}^{+\infty} \frac{d\omega}{2\pi} S(\omega)$$

is wrong in general, since if $\omega > k_{\text{B}}T$ (or $\omega > eV$) the spectral density is not symmetric $S(-\omega) \neq S(\omega)$.

Remark. $S(\omega)$ is real in quantum and classical cases. In quantum (time-invariant case),

$$S^*(\omega) = \left(\int \langle I(0)I(t)\rangle e^{i\omega t} dt \right)^* = \int \langle I(t)I(0)\rangle e^{-i\omega t} dt = \int \langle I(0)I(-t)\rangle e^{-i\omega t} dt = \int \langle I(0)I(\tau)\rangle e^{-i\omega \tau} d\tau$$

so, we have

$$S^*(\omega) = S(\omega)$$

If $S(\omega)$ does not diverge at $\omega \lesssim 1/t$ we can use the representation of the δ-function in form [7]

$$\lim_{t\to\infty} \frac{\sin^2 \omega t}{\omega^2 t} = \pi\delta(\omega)$$

and obtain from (7.13)

$$\langle\langle Q^2 \rangle\rangle = t \int d\omega\, \delta(\omega) S(\omega) = tS(0). \tag{7.14}$$

This formula is valid for $t \gg \tau_{\text{corr}}$, where τ_{corr} is so-called correlation time.

Remark. Alternative to (7.12) and (7.13) we can write

$$\int_0^t dt_1 \int_0^t dt_2 \langle\langle I(0)I(t_2 - t_1)\rangle\rangle = \int_0^{+\infty} d\tau \int_0^t dT \langle\langle I(0)I(\tau)\rangle\rangle = t\, S(0),$$

where we have substituted $T = (t_1 + t_2)/2$ and $\tau = t_2 - t_1$.

Comparing (7.14) and (7.8), we finally obtain Schottky's formula

$$S(0) = e\langle I \rangle, \tag{7.15}$$

which is valid for all values of $\langle I \rangle$. The remarkable feature of this formula is that the charge quantum e appears in it. The vacuum tube experiment was used to measure charge of electron e. The accuracy was not very good (e.g. one of the reason was the flicker noise). Still it is some method which gives the charge of the electron with accuracy of about 10%. Recently, people used

this effect to demonstrate fractional charge in the fractional quantum Hall effect at $\nu = 1/3$ [8, 9]

$$S(0) = e^* \langle I \rangle, \tag{7.16}$$

double-charge of a Cooper pair in normall metall–superconductor system [ref]

$$S(0) = 2e \langle I \rangle. \tag{7.17}$$

For certain systems, the statistics is not Poissonian; for example, in a quasi one-dimensional quantum point contact the noise is given by [10]

$$S(0) = e\langle I \rangle (1 - T), \tag{7.18}$$

where T is the transmission probability. Let us give a hint, why the result is different: in a quantum mechanical system the reason for the fluctuations is different. For the vacuum tube the reason for fluctuations of emitted electrons is more or less classical. We can think that the occupation numbers of the electrons much less then unity, $n \ll 1$. And then just due to small fluctuations in occupation numbers you may have electrons in the electrode to emit or may have not; and this is the origin of current fluctuations. Now in quantum case it is more involved. Fermi statistics becomes important and the reason for the fluctuations is the probabilistic nature of quantum mechanics: whether an electron which is send to the obstacle is transmitted or not cannot be known and the outcome is purely random.

Remark. The "trick" $\langle\langle Q^2 \rangle\rangle = t\, S(0)$ works also for $\langle\langle Q^n \rangle\rangle = t\, \langle\langle I_0^n \rangle\rangle$, see later in Chapter 10 for full counting statistics.

7.3 Shot noise damping in a long wire

Later on, we will show more rigorously that Schottky answer (7.15) is valid for the noise in a tunnel junction with $T \ll 1$. Here, we model for long wire which is compose of two tunnel junctions with small transparencies T_1, $T_2 \ll 1$. Then if we have just one tunneling junction noise will be still

$$\langle \delta I^2 \rangle_\omega \equiv S(\omega) = e\langle I \rangle. \tag{7.19}$$

Now the question appear if in a conductor we have two tunneling junctions in series. First, we consider the situation where the region 2 in Figure 7.2 in between the tunneling junctions is large enough such that electrons are

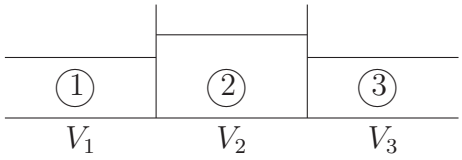

Figure 7.2: Tunneling elements (two junctions) with conductivities G_{12}, G_{23} and capacitances C_{12}, C_{23}. The voltage drop across left junction is $\delta V_{12} = V_2 - V_1$, $\delta V_{23} = V_3 - V_2$.

already thermalized.[1] Then because of a finite capacitance and the fluctuations of the charge, a time-dependent voltage δV builds up across the region 2: at zero frequency total noise is $S(\omega)/2$ for the identical junctions. We discuss this case to explain that in a long macroscopic wire shot noise will be damped. And roughly speaking the "strength" of damping will be some correlation length divided by the total length of the wire $L_{\rm corr}/L$; or, if we consider wire with N tunnel junctions this "strength" will be $1/N$. So, zero frequency noise of such a system consisting N tunneling junctions will be

$$S(0) = \frac{1}{N}\, e\langle I\rangle. \tag{7.20}$$

Next, let us write equations for the two tunneling junctions. We will do it in the framework of so-called quasi-stationary fluctuations and Langevin forces. In this approach first we write equation motion for the quantity we study. Second we say that it is not all and we shall add to it some random forces (Langevin forces), which are for example not included in kinetic (master) equation.

Fluctuations of the current in the contact between regions 1 and 2 (contact 12) is given by

$$\delta I_{12} = \delta V_{12} G_{12} + \delta j_{12}, \tag{7.21}$$

where G_{12} is a conductance of mentioned junction and δj_{12} is a random intrinsic shot noise appearing in it. The first term represents quasiclassical equation, the second one — Langevin force. We also can use the same equation for the contact between regions 2 and 3 (contact 23)

$$\delta I_{23} = \delta V_{23} G_{23} + \delta j_{23}. \tag{7.22}$$

[1] We considered such a model for describing the Peltier effect.

Then let us suppose that region 2 contains charge Q and we obtain for contact 12 and 23

$$-\delta V_{12} = \frac{\delta Q}{C_{12}} \tag{7.23}$$

and

$$\delta V_{23} = \frac{\delta Q}{C_{23}}, \tag{7.24}$$

where C_{12} and C_{23} are a capacities of the 12 and 23 junctions respectively. Here we suppose that voltages at the left and at the right are equal, $V_1 = V_3$ and only V_2 fluctuates. Then we can use the fact that $T_{1,2} \ll 1$ and write quasistationary differential equation for the charge on the island Q,

$$\frac{d}{dt}\delta Q = \delta I_{12} - \delta I_{23}. \tag{7.25}$$

Now we switch to the Fourier transformed values. Equation (7.25) transforms to

$$-i\omega\delta Q_\omega = \delta I_{12,\omega} - \delta I_{23,\omega}, \tag{7.26}$$

using (7.23) it can be rewritten in the form

$$-i\omega(-\delta V_{12,\omega}C_{12}) = \delta I_{12,\omega} - \delta I_{23,\omega} \tag{7.27}$$

and then

$$\delta V_{12,\omega} = \frac{1}{i\omega C_{12}}(\delta I_{12,\omega} - \delta I_{23,\omega}). \tag{7.28}$$

Here ω is a frequency which has arisen in the Fourier transformation. Substituting (7.28), (7.23), and (7.24) into (7.21) and (7.22) we have the system of two equations

$$\begin{cases} \delta I_{12,\omega} = \dfrac{G_{12}}{i\omega C_{12,\omega}}(\delta I_{12,\omega} - \delta I_{23,\omega}) + \delta j_{12,\omega}, \\ \delta I_{23,\omega} = -\dfrac{C_{12}}{C_{23}}\dfrac{G_{23}}{i\omega C_{12}}(\delta I_{12,\omega} - \delta I_{23,\omega}) + \delta j_{23,\omega}. \end{cases} \tag{7.29}$$

Solving this system of linear equations for I_{12} and denoting $\tau_{12} = C_{12}/G_{12}$, $\tau_{23} = C_{23}/G_{23}$ we obtain the answer

$$\delta I_{12,\omega} = \frac{\delta j_{23,\omega}\tau_{23} + \delta j_{12,\omega}\tau_{12}(1 - i\omega\tau_{23})}{\tau_{12} + \tau_{23} - i\omega\tau_{23}\tau_{12}}. \tag{7.30}$$

At zero frequency $\omega = 0$ the answer is

$$\delta I_{12,0} = \frac{\delta j_{23,0}\tau_{23} + \delta j_{12,0}\tau_{12}}{\tau_{12} + \tau_{23}}. \tag{7.31}$$

Now let us calculate Fourier transformed irreducible current-current correlator of two tunnel junctions system (this correlator is often called just "noise")

$$\langle \delta I_{12,-\omega} \delta I_{12,\omega} \rangle = \frac{\tau_{12}^2 \langle \delta j_{12,0}^2 \rangle + \tau_{23}^2 \langle \delta j_{23,0}^2 \rangle}{(\tau_{12} + \tau_{23})^2}. \tag{7.32}$$

Then note that for each junction Langevin forces give its own shot noise and $\langle \delta j_{12,0}^2 \rangle = \langle \delta j_{23,0}^2 \rangle = e\langle I \rangle$. We obtain

$$\langle \delta I_{12,-\omega} \delta I_{12,\omega} \rangle = e\langle I \rangle \frac{\tau_{12}^2 + \tau_{23}^2}{(\tau_{12} + \tau_{23})^2}. \tag{7.33}$$

Also we can rewrite this result via resistivity of each junction $R_{12} = 1/G_{12}$ and $R_{23} = 1/G_{23}$

$$\langle \delta I_{12,-\omega} \delta I_{12,\omega} \rangle = e\langle I \rangle \frac{R_{12}^2 C_{12}^2 + R_{23}^2 C_{23}^2}{(R_{12} C_{23} + R_{23} C_{23})^2}. \tag{7.34}$$

In case $\tau_{12} = \tau_{23}$ we have

$$\langle \delta I_{12,0}^2 \rangle = \frac{1}{2} e\langle I \rangle. \tag{7.35}$$

In case of $\tau_{12} \gg \tau_{23}$ we approach the limit of one tunnel junction

$$\langle \delta I_{12,0}^2 \rangle = e\langle I \rangle. \tag{7.36}$$

For high-frequency limit $\omega \gg 1/\tau$ where $\tau = \min\{\tau_{12}, \tau_{23}\}$ from (7.30) we have

$$\delta I_{12,\omega} \simeq \delta_{12,\omega}, \tag{7.37}$$

therefore is we suppose that $\langle \delta j_{12,\omega}^2 \rangle = \text{const}$ (white noise) and $\langle \delta j_{12,\omega}^2 \rangle = e\langle I \rangle$

$$\langle \delta I_{12,\omega}^2 \rangle = e\langle I \rangle. \tag{7.38}$$

For the N identical junctions and zero frequency similarly to (7.31) we have

$$\delta I = \frac{1}{N} \sum_{i=1}^{N} j_i \tag{7.39}$$

and for the noise

$$\langle \delta I^2 \rangle_{\omega=0} = \frac{1}{N^2} \sum_{i=1}^{N} \langle j_i^2 \rangle_{\omega=0} = \frac{N}{N^2} e\langle I \rangle = \frac{1}{N} e\langle I \rangle. \tag{7.40}$$

This formula coincides with the predicted result (7.20).

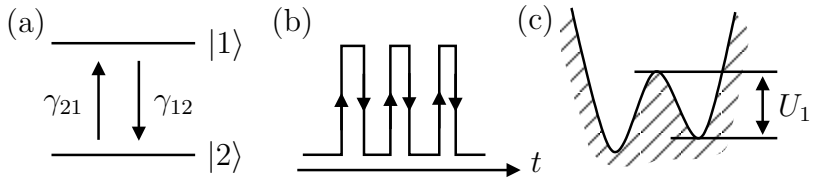

Figure 7.3: (a)&(b) Telegraph noise is random jumping between two states with probabilities γ_{12} and γ_{21}. (c) Double well potential. E.g. the probability of jump from state $|1\rangle$ to $|2\rangle$ is due to the finite temperature and is about $\gamma_{12} \sim e^{-U_1/k_B\vartheta}$.

7.4 Telegraph noise

The reason to present telegraph noise is two fold. First, there are noise sources which produce telegraph noise in many materials (e.g., charge impurities). Second, telegraph noise is the basic ingredient in order to discuss $1/f$ noise which we will do in the next section. The main idea to explain $1/f$ (flicker) noise is the following: In (almost) all large system there are a large set of relaxation times present. Taking into account all these relaxation times can lead to a $1/f$ dependence of the noise power (we will see how it work).

Telegraph noise is a quantity $x(t)$ which fluctuates in time between two values x_1, x_2, see Figure 7.3(b). Physically this can by an impurity in a double-well potential like Fig. 7.3(c). As was shown by Altshuler [ref] and independently by Stone [ref] that in coherent conductor if one impurity changes its position by a distance L much larger than the Fermi wavelength λ_F ($L \gg \lambda_F$) the conductance changes by

$$\delta G \sim \frac{e^2}{h} \frac{1}{(Gh/e^2)^\alpha}. \tag{7.41}$$

(find the power α). That an impurity jumps between two stable positions happens often in mesoscopic systems, e.g., in heterostructures in the Coulomb blockade regime or in qubits. These impurities are one of the reason why the devices do not operate perfectly; the impurity jumps and induces some uncontrollable fluctuations. Lets consider a simple example. We have a quasi one-dimensional channel forming a QPC. As mentioned in Chapter 3.3 transport there is dominated by the top of the effective potential. If the top of the potential is near the Fermi energy, then small fluctuations of the

potential due to the different position of the impurity change the transmission probability considerably.

The first experiment on noise of a quantum point contact was performed by Tsui [ref] (who also discovered the fractional quantum Hall effect [11]). He mostly observe this flicker noise. Partly he observe shot noise damping in a sense that at plato he had low noise; lower than Shottky value. But nevertheless the dominant was telegraph signal due to impurity. *???*

At the moment suppose that impurity jumps between two states and the process can be described classically. Then, we have a fluctuating conductance $G(t)$ as a function of time which can be equal to G_1 or G_2 for $x = x_1, x_2$, respectively. The current through contact is given by $I(t) = VG(t)$. Again suppose that probability to find the impurity in position $|1\rangle$ in state and conductance G_1 is $P_1(t)$; to find impurity in state $|2\rangle$ and conductance G_1 is $P_2(t)$. Naturally

$$P_1(t) + P_2(t) = 1. \tag{7.42}$$

If we know the rates γ_{12} and γ_{21} we can write down a master equations for probabilities $P_1(t)$ and $P_2(t)$

$$\frac{\partial P_1}{\partial t} = -\gamma_{12}P_1 + \gamma_{21}P_2, \tag{7.43}$$

using (7.42), we can rewrite it

$$\frac{\partial P_1}{\partial t} = -(\gamma_{12} + \gamma_{21})P_1 + \gamma_{21}. \tag{7.44}$$

Let us consider the case when at $t = 0$ the impurity was in state $|1\rangle$,

$$P_1(0) = 1. \tag{7.45}$$

Let us call the solution for probability $P_1(t)$ of the (7.44) with the condition (7.45) $\tilde{P}_1(t)$. This conditional probability is

$$\tilde{P}_1(t) = \frac{\gamma_{12}}{\Gamma}e^{-\Gamma t} + \frac{\gamma_{21}}{\Gamma}, \tag{7.46}$$

where $\Gamma = \gamma_{12} + \gamma_{21}$. The same conditional probability (with the condition $P_2(0) = 1$) for the second state is

$$\tilde{P}_2(t) = \frac{\gamma_{21}}{\Gamma}e^{-\Gamma t} + \frac{\gamma_{12}}{\Gamma}. \tag{7.47}$$

If we go to infinity we should say that the probabilities $P_1(t)$ and $P_2(t)$ are saturated and left part of the equation (7.44) is zero. We have

$$P_1(+\infty) = \frac{\gamma_{21}}{\Gamma},\ P_2(+\infty) = \frac{\gamma_{12}}{\Gamma}. \tag{7.48}$$

The averages of the probabilities are defined by their relaxed values, $\langle P_1(t)\rangle = P_1(+\infty)$, $\langle P_2(t)\rangle = P_2(+\infty)$.

Now we are equipped to calculate the current-current (or, what is the same, conductance-conductance) correlator

$$\langle I(0)I(t)\rangle = V^2\langle G(0)G(t)\rangle. \tag{7.49}$$

Sometimes correlator $\langle G(0)G(t)\rangle$ is called conductance fluctuations. Now let us use the expression for $G(t)$

$$G(t) = G_1P_1(t) + G_2P_2(t) \tag{7.50}$$

and calculate the correlator

$$\langle G(0)G(t)\rangle = \langle P_1\rangle G_1\big\{G_1\tilde{P}_1(t) + G_2(1-\tilde{P}_1(t))\big\}+ \\ \langle P_2\rangle G_2\big\{G_2\tilde{P}_2(t) + G_1(1-\tilde{P}_2(t))\big\}. \tag{7.51}$$

Let us explain this formula. In the first term $\langle P_1\rangle$ is the probability to find system in the initial state $|1\rangle$. We should multiply it by conductance in this state G_1 and by the conductance $G(t)$ under assumption (7.45). And then add the same term for opposite initial term. Formula (7.51) can be rewritten by introducing $\Delta G = G_1 - G_2$ and we have

$$\langle G(0)G(t)\rangle = \langle P_1\rangle G_1\big\{G_2 + \tilde{P}_1(t)\Delta G\big\} + \langle P_2\rangle G_2\big\{G_1 - \tilde{P}_2(t)\Delta G\big\}. \tag{7.52}$$

Now lets use expressions for conditional probabilities (7.46) and (7.47)

$$\langle G(0)G(t)\rangle = \langle P_1\rangle G_1\left\{G_2 + \left(\frac{\gamma_{12}}{\Gamma}e^{-\Gamma t} + \frac{\gamma_{21}}{\Gamma}\right)\Delta G\right\} + \langle P_2\rangle G_2\left\{G_1 - \right. \\ \left.\left(\frac{\gamma_{21}}{\Gamma}e^{-\Gamma t} + \frac{\gamma_{12}}{\Gamma}\right)\Delta G\right\} = \langle P_1\rangle G_1\left\{\frac{\gamma_{21}}{\Gamma}G_1 + \frac{\gamma_{12}}{\Gamma}G_2 + \Delta G\frac{\gamma_{12}}{\Gamma}e^{-\Gamma t}\right\}+ \\ \langle P_2\rangle G_2\left\{\frac{\gamma_{21}}{\Gamma}G_1 + \frac{\gamma_{12}}{\Gamma}G_2 - \Delta G\frac{\gamma_{21}}{\Gamma}e^{-\Gamma t}\right\}. \tag{7.53}$$

Taking into account that

$$\frac{\gamma_{21}}{\Gamma}G_1 + \frac{\gamma_{12}}{\Gamma}G_2 = \langle P_1\rangle G_1 + \langle P_2\rangle G_2 = \langle G\rangle$$

we obtain for $t > 0$

$$\begin{aligned}\langle G(0)G(t)\rangle &= \langle G\rangle^2 + \Delta G\left(\langle P_1\rangle G_1\frac{\gamma_{12}}{\Gamma} - \langle P_2\rangle G_2\frac{\gamma_{21}}{\Gamma}\right)e^{-\Gamma t}\\ &= \langle G\rangle^2 + \Delta G^2\langle P_1\rangle\langle P_2\rangle e^{-\Gamma t}.\end{aligned} \tag{7.54}$$

The irreducible correlator is

$$\langle\langle G(0)G(t)\rangle\rangle = \Delta G^2\langle P_1\rangle\langle P_2\rangle e^{-\Gamma t}. \tag{7.55}$$

For $t < 0$ we can write

$$\langle\langle G(0)G(t)\rangle\rangle = \langle\langle G(t)G(0)\rangle\rangle = \langle\langle G(0)G(-t)\rangle\rangle.$$

So, for any time

$$\langle\langle G(0)G(t)\rangle\rangle = \Delta G^2\langle P_1\rangle\langle P_2\rangle e^{-\Gamma|t|}. \tag{7.56}$$

The spectral density for conductance fluctuations

$$S_G(\omega) = \int dt\, e^{i\omega t}\langle\langle G(0)G(t)\rangle\rangle \tag{7.57}$$

can be easily calculated. We have standard Lorentzian shape

$$S_G(\omega) = \Delta G^2\langle P_1\rangle\langle P_2\rangle\frac{2\Gamma}{\Gamma^2+\omega^2}. \tag{7.58}$$

And the same answer for current fluctuations in telegraph regime

$$S_I(\omega) = V^2\Delta G^2\langle P_1\rangle\langle P_2\rangle\frac{2\Gamma}{\Gamma^2+\omega^2}. \tag{7.59}$$

7.5 Flicker noise

Soon after discovering flicker noise, the idea was presented that the origin of flicker noise are two-level fluctuators (impurities) producing telegraph noise with different relaxation times. If we sum up it all this individual noise sources, we get a $1/f$ dependence. The total spectral density $S(\omega)$ is a sum of the spectral densities from the impurities (this statement is equivalent to the fact that the individual telegraph processes are independent of each other). The relaxation rates Γ_i of the impurities are distributed with the distribution function $f(\Gamma)$. For simplicity let us assume that ΔG is the same for each object. The spectral density of the flicker noise can be written in the form

$$S(\omega) = V^2\Delta G^2\int\limits_0^{+\infty}\frac{2\Gamma}{\Gamma^2+\omega^2}\,f(\Gamma)\,d\Gamma. \tag{7.60}$$

Q: What is the maximal value of Γ in the formula for spectral density (7.60)?

A: To be more realistic in the expression for the total spectral density, we have to introduce an upper limit of integration, $\Gamma_{\max}$. The rate $\Gamma_{\max}$ corresponds to the fastest relaxation in the system which is of course not infinite. All our considerations is correct only if $\omega \ll \Gamma_{\max}$.

Now we can assume a distribution function $f(\Gamma)$ such as to get a $1/\omega$ dependence in (7.60).

Remark. By the way in experiment its not exactly $1/\omega$, but $1/\omega^{\alpha}$. The power α can be less than unity, or can be even little bit more which indicates that process is already nonstationary.

Assuming that

$$f(\Gamma) = \frac{f_0}{\Gamma}, \tag{7.61}$$

where f_0 is some constant, we obtain a $1/\omega$ dependence from (7.60)

$$S(\omega) = V^2 \Delta G^2 \, \frac{\pi f_0}{\omega}. \tag{7.62}$$

The question remains which the fluctuators are distributed according to Eq. (7.61) work. The jumping rate Γ is due to thermal excitations given by Arrhenius law

$$\Gamma = \Gamma_0 \, e^{-U_0/k_{\mathrm{B}}\vartheta}, \tag{7.63}$$

where Γ_0 is some constant and U_0 is the height of the barrier between the two minima in the potential, see Fig. 7.3(c). The number of two-level systems in the interval $[\Gamma, \Gamma + d\Gamma]$ can be rewritten as the number of objects in the corresponding interval in barrier height $[U_0, U_0 + dU_0]$ via

$$f(\Gamma)\, d\Gamma = f(\Gamma) \, \frac{\Gamma_0}{k_{\mathrm{B}}\vartheta} \, e^{-U_0/k_{\mathrm{B}}\vartheta} |dU_0| = n(U_0)\, |dU_0|. \tag{7.64}$$

with a distribution

$$n(U_0) = \frac{\Gamma_0}{k_{\mathrm{B}}\vartheta} \, e^{-U_0/k_{\mathrm{B}}\vartheta} \, f\left[\Gamma_0 \, e^{-U_0/k_{\mathrm{B}}\vartheta}\right] = \frac{\Gamma}{k_{\mathrm{B}}\vartheta} f(\Gamma), \tag{7.65}$$

of the potential barriers heights U_0.

If we now suppose that distribution (7.65) of the barrier heights is constant $n(U_0) = n_0$, we obtain the distribution (7.61) for the relaxation rates with $f_0 = n_0 k_{\mathrm{B}} \vartheta$.

In general case we have

$$f(\Gamma)\frac{\Gamma}{k_{\mathrm{B}}\vartheta} = n(U_0). \tag{7.66}$$

Suppose the distribution $n(U_0)$ is powerlike

$$n(U_0) \propto \frac{1}{U_0^n}. \tag{7.67}$$

Using Eq. (7.63) and expressing U_0 in terms of Γ,

$$n(U_0) = k_{\mathrm{B}}\vartheta \log\frac{\Gamma}{\Gamma_0} \tag{7.68}$$

we obtain only the logarithmic deviation from (7.61)

$$f(\Gamma) = \frac{k_{\mathrm{B}}\vartheta}{\Gamma}\frac{1}{\log^n(\Gamma/\Gamma_0)} \tag{7.69}$$

In the case of exponential distribution of barrier heights U_0

$$n(U_0) \propto e^{-U_0/E}. \tag{7.70}$$

(E is some constant) we obtain power distribution for Γ

$$f(\Gamma) = \frac{k_{\mathrm{B}}\vartheta}{\Gamma}\left(\frac{\Gamma}{\Gamma_0}\right)^{k_{\mathrm{B}}\vartheta/E}. \tag{7.71}$$

The flicker noise is an enormously general phenomena and its origin is not understood on a more fundamental basis than the reasoning above. More elaborate calculations have been performed taking into account electron-electron interaction [12]. The authors found a noise spectrum proportional to $1/\omega$ for a 2D system.

Flicker noise can be observed everywhere: if you observe current flow, or count cars on a street, ... People analyze music in this sense (e.g., no $1/f$-noise is observed in modern (rock) music which is close white noise plus couple of frequencies while classical music produces $1/f$ noise).

7.6 Nyquist theorem (Nyquist-Johnson thermal noise)

Next we discuss Nyquist-Johnson or thermal noise. We will perform the calculation for classical noise at zero frequency; in Chapter 7.7, we will general

this to the quantum mechanical case. Here we present a simplest way to derive Nyquist-Johnson noise [6].

Consider the system which contains resistor with resistance R and capacitor with capacitance C shown at the Figure 7.4. At a finite temperature ϑ, there are current fluctuation for which we want to calculate the power spectrum. We know from the equipartition theorem in classical statistical

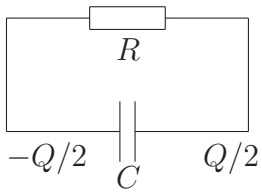

Figure 7.4: Scheme for Nyquist-Johnson thermal noise.

mechanics that in thermal equilibrium the average energy in the capacitor is defined by the temperature ϑ and given by

$$\langle E_C \rangle = \frac{\langle Q^2 \rangle}{2C} = \frac{k_{\text{B}}\vartheta}{2}, \tag{7.72}$$

where Q is a charge at the capacitor. We are interested in the current I. This current I is connected with voltage drop at capacitor $V = Q/C$ by the Ohm law, so we have

$$I = \frac{Q}{CR}. \tag{7.73}$$

The speed of capacitor discharging dQ/dt is determined by this current and we can write the differential equation for charge

$$-\frac{dQ}{dt} = \frac{Q}{CR}. \tag{7.74}$$

If we suppose that at $t = 0$ the charge at capacitor was Q_0 this equation has the solution

$$Q = Q_0\, e^{-t/RC}, \tag{7.75}$$

i.e., the capacitor is discharged with the RC time constant. In the theory of quasistationary fluctuations one assumes that the correlator $\langle\langle Q(0)Q(t)\rangle\rangle$ satisfies the same differential equation as $Q(t)$ itself. Therefore, we have

$$\frac{\partial}{\partial t}\langle\langle Q(0)Q(t)\rangle\rangle = -\frac{1}{RC}\,\langle\langle Q(0)Q(t)\rangle\rangle \tag{7.76}$$

with the solution

$$\langle\langle Q(0)Q(t)\rangle\rangle = \langle\langle Q^2(0)\rangle\rangle\, e^{-t/RC}. \tag{7.77}$$

Remark. This approach is different from the Langevin approach which we introduced before (see 7.3). Here, the treatment is the following: if we know what is the fluctuations in the coincident times $\langle\langle Q^2(0)\rangle\rangle$ from somewhere (e.g. here from thermodynamics) then we can find out how the correlator $\langle\langle Q(0)Q(t)\rangle\rangle$ behaves in time. For the quasistationary fluctuations with $\hat{L}_1 Q_1 = 0$ (where $\hat{L}$ is some operator acting only on Q_1 and is not acting on Q_0), we require $\hat{L}_1\langle Q_0 Q_1\rangle = 0$.

The frequency dependence of the power spectrum can be obtained by Fourier transforming Eq. (7.77). The spectral density is given by

$$S_Q(\omega) = \langle\langle Q^2\rangle\rangle \frac{2(RC)^{-1}}{(RC)^{-2} + \omega^2}. \tag{7.78}$$

Note that $\langle\langle Q^2\rangle\rangle$ is completely determined by equation (7.72) since $\langle Q\rangle = 0$. The zero frequency fluctuations are given by

$$S_Q(0) = 2k_{\mathrm{B}}\vartheta RC^2. \tag{7.79}$$

The voltage correlator can be obtained by dividing Eq. (7.79) by C^2. This yields

$$S_V(0) = 2k_{\mathrm{B}}\vartheta R. \tag{7.80}$$

For the spectral density of current-current fluctuations, we introduce conductance $G = 1/R$ and have

$$S_I(0) = 2k_{\mathrm{B}}\vartheta G. \tag{7.81}$$

Equations (7.80) and (7.81) are called the Nyquist theorem for zero frequency thermal noise. The analysis for finite frequency can be performed in the same way but as soon as you go to the frequency higher than the temperature this approach will break down because at $\hbar\omega > k_{\mathrm{B}}\vartheta$ the system is not longer only determined by its thermodynamic properties.

7.7 The fluctuation-dissipation theorem

In the study of noise (e.g. see the original paper of Callen and Welton [13] or Landau and Lifshitz [14]) it is customary to consider the symmetrized current-current correlator

$$\frac{1}{2}\langle I_\omega I_{-\omega} + I_{-\omega} I_\omega\rangle.$$

The reason for this is that it is a real quantity. In fact it was shown by Lesovik and Loosen [15] and then by Gavish *et al* [16], that at low temperatures in a natural setup where one measure finite frequency noise the experimentally measurable quantity is $\langle I_{-\omega} I_{\omega} \rangle$ taken at $\omega > 0$.

First, let us calculate linear response of a system to an external driving field. The fluctuation-dissipation theorem connects the linear response coefficients with the fluctuations in the equilibrium. We will calculate linear response in framework of the many-body perturbation theory. Suppose we have a vector potential A such that the interaction part of the Hamiltonian can be written as

$$\hat{V}(t) = -\frac{1}{c} \int dx\, A(x,t) \hat{I}(x,t), \tag{7.82}$$

where c is the speed of light (in the following, we will set $c = 1$).

Of course also other quantities can be studied, e.g., the response of density to some potential and so on. Now we will calculate current in the presence of the time-dependent flux

$$A(x,t) = A_{\omega}(x) e^{-i\omega t} \tag{7.83}$$

and we will search for the linear response coefficient $\alpha_{\omega}(x,x')$ in the relation

$$I_{\omega}(x) = \int dx'\, A_{\omega}(x') \alpha_{\omega}(x,x') e^{-i\omega t} \tag{7.84}$$

In fact, as $A(x,t)$ is a real quantity, Eq. (7.83) should in fact read $A(x,t) = [A_{\omega}(x)e^{-i\omega t} + A_{-\omega}(x)e^{i\omega t}]/2$; we can always add up the negative and positive frequency components at the end. As we have already shown before, the average current is equal to

$$\langle \hat{I}(t) \rangle = \mathrm{Tr}\big\{ \hat{\rho}\, \hat{S}^{\dagger}(-\infty, t) \hat{I}(t) \hat{S}(-\infty, t) \big\}, \tag{7.85}$$

where $\hat{\rho}$ is the initial density matrix at time $t \to -\infty$ and $\hat{S}$ is the evolution operator given by

$$\hat{S}(-\infty, t) = \mathcal{T} e^{(i/\hbar) \int_{-\infty}^{t} dt' \int dx\, \hat{I}(x,t') A(x,t')} \tag{7.86}$$

Using (7.86) the formula (7.85) can be rewritten as

$$\langle \hat{I}(t) \rangle = \mathrm{Tr} \Big\{ \hat{\rho}\, \mathcal{T} e^{(i/\hbar) \int_{-\infty}^{t} dt' \int dx\, \hat{I}(x,t') A(x,t')}\, \hat{I}(t) \times \tilde{\mathcal{T}} e^{-(i/\hbar) \int_{-\infty}^{t} dt' \int dx\, \hat{I}(x,t') A(x,t')} \Big\}. \tag{7.87}$$

Expanding to first order in A yields

$$\langle \hat{I}(x,t)\rangle = \frac{i}{\hbar}\int\limits_{-\infty}^{t} dt' \int dx'\, A(x',t')\langle \hat{I}(x,t)\hat{I}(x',t') - \hat{I}(x',t')\hat{I}(x,t)\rangle. \quad (7.88)$$

Here, the first term $\hat{I}(x,t)\hat{I}(x',t')$ originates from the expansion of $\hat{S}$ and the second $\hat{I}(x',t')\hat{I}(x,t)$ from the expansion of $\hat{S}^{\dagger}$. Plugging in the harmonic time-dependent for $A(t)$, we obtain

$$\langle \hat{I}(x,t)\rangle = \frac{i}{\hbar}\int\limits_{-\infty}^{t} dt' \int dx'\, A_{\omega}(x')\, e^{-i\omega t'} \times \langle \hat{I}(x,t)\hat{I}(x',t') - \hat{I}(x',t')\hat{I}(x,t)\rangle. \quad (7.89)$$

Now, we go over to frequency space. Here we suppose that the process is stationary and therfore $\langle \hat{I}(0)\hat{I}(t) - \hat{I}(t)\hat{I}(0)\rangle = \langle \hat{I}(0)\hat{I}(t) - \hat{I}(t)\hat{I}(0)\rangle = \langle\langle \hat{I}(0)\hat{I}(t) - \hat{I}(t)\hat{I}(0)\rangle\rangle + \langle\langle \hat{I}(0)\hat{I}(t) - \hat{I}(t)\hat{I}(0)\rangle\rangle$. If the process is non-stationary, we can still continue in the same fashion but we should be careful with introducing two frequency for the correlator. Equation (7.89) transforms into

$$I_{\omega}(x) = \frac{i}{\hbar}\int \frac{d\Omega}{2\pi}\int\limits_{-\infty}^{t} e^{-i\omega t'} dt' \int dx'\, A_{\omega}(x') \times \times \left\{ e^{-i\Omega(t'-t)}\langle \hat{I}_{-\Omega}\hat{I}_{\Omega}\rangle - e^{-i\Omega(t-t')}\langle \hat{I}_{\Omega}\hat{I}_{-\Omega}\rangle \right\}. \quad (7.90)$$

After performing the integration over time, we obtain

$$I_{\omega}(x) = \frac{i}{\hbar}\int \frac{d\Omega}{2\pi} \int dx'\, A_{\omega}(x') e^{-i\omega t} \frac{i(\omega+\Omega)+\gamma}{(\omega+\Omega)^2+\gamma^2} \left\{ \langle \hat{I}_{-\Omega}\hat{I}_{\Omega}\rangle - \langle \hat{I}_{\Omega}\hat{I}_{-\Omega}\rangle \right\}, \quad (7.91)$$

with $\gamma \to 0^{+}$. Now we have to convert this expression to the δ-function plus something and make the integration over Ω. For the real part of the fraction in the (7.91) we can write

$$\lim_{\gamma\to 0} \frac{\gamma}{(\omega+\Omega)^2+\gamma^2} = \pi\delta(\omega+\Omega).$$

The another part give the non-dissipative part of the response and it is some labour to consider what to do with it because in addition to this contribution

to current there appears the term which is proportional to ρA i.e. diamagnetic response. In normal system there is a cancelation of this diamagnetic term which come from the Fermi surface contribution of namely this part. We will not do this because in fluctuation-dissipation theorem only important part is the dissipative part of response. Therefore we take away this imaginary part and obtain

$$I_\omega(x) = \frac{i}{2\hbar}\int dx'\, A_\omega(x')e^{-i\omega t}\left\{\langle \hat{I}_{-\omega}(x)\hat{I}_\omega(x')\rangle - \langle \hat{I}_\omega(x')\hat{I}_{-\omega}(x)\rangle\right\}. \quad (7.92)$$

This is the answer.

Now let us write the expression for dissipative part of response. We subtract from total $\alpha_\omega(x,x')$ the non-dissipative (reactive) term

$$\tilde{\alpha}_\omega(x,x') = \alpha_\omega(x,x') - \alpha'_\omega(x,x') \quad (7.93)$$

and for $\tilde{\alpha}_\omega(x,x')$, we obtain

$$\tilde{\alpha}_\omega(x,x') = \frac{i}{2\hbar}\left\{\langle \hat{I}_{-\omega}(x)\hat{I}_\omega(x')\rangle - \langle \hat{I}_\omega(x')\hat{I}_{-\omega}(x)\rangle\right\} \quad (7.94)$$

We switch now to the electric field

$$E = -\frac{\partial A}{\partial t} \quad (7.95)$$

if we substitute here time-dependent A from (7.83)

$$E_\omega = i\omega A_\omega e^{-i\omega t}. \quad (7.96)$$

The current is expressed in terms of the conductance G as

$$I_\omega(x) = \int dx' G_\omega(x,x')E_\omega(x'). \quad (7.97)$$

As $\omega \to 0$ the kernel in the last formula is constant and we have

$$I_\omega = G_\omega \int dx\, E_\omega(x) = G_\omega V_\omega. \quad (7.98)$$

Using formulae (7.92), (7.96), and (7.98) we have

$$S(-\omega) - S(\omega) = 2\hbar\omega G_\omega. \quad (7.99)$$

This is Kubo's formula. *The* fluctuation-dissipation relation we will consider below. As a matter of the fact, Kubo's formula is also valid in a nonequilibrium situation, as was recently pointed out by Gavish *et al.* [17].

Now we will obtain *the* fluctuation-dissipation theorem. The idea is to connect $S(\omega)$ and $S(-\omega)$ by knowing the properties of density matrix and substitute it to the Kubo formula (7.99).

First we calculate current-current correlator in quite general form

$$\langle \hat{I}(x_1,t_1)\hat{I}(x_2,t_2)\rangle = \mathrm{Tr}\big\{\hat{\rho}\,\hat{S}^\dagger(t_1)\hat{I}(x_1)\hat{S}(t_1)\,\hat{S}^\dagger(t_2)\hat{I}(x_2)\hat{S}(t_2)\big\}, \qquad (7.100)$$

where $\hat{S}(t) = e^{-i\hat{H}_0 t/\hbar}$ is an evolution operator which is connecting time-dependent and time-independent current operators $\hat{I}(t) = \hat{S}^\dagger(t)\hat{I}\hat{S}(t)$ and $\hat{\rho}$ is a density matrix operator. Since it is a stationary problem and we suppose to know Hamiltonian in general form we can rewrite it in matrix form. So we go to some representation which diagonalize Hamiltonian and the density matrix

$$\langle \hat{I}(x_1,t_1)\hat{I}(x_2,t_2)\rangle = \sum_{n,m}\langle n|\rho|n\rangle\langle n|\hat{I}(x_1,t_1)|m\rangle\langle m|\hat{I}(x_2,t_2)|n\rangle, \qquad (7.101)$$

here indices n and m cover everything (wave vectors, spin, ...). Introducing $\rho_{nm} = \langle n|\hat{\rho}|m\rangle$ and substituting evolution operators we have

$$\begin{aligned}
\langle \hat{I}(x_1,t_1)\hat{I}(x_2,t_2)\rangle &= \sum_{n,m}\rho_{nn}\langle n|e^{i\hat{H}_0 t_1/\hbar}\hat{I}(x_1)e^{-i\hat{H}_0 t_1/\hbar}|m\rangle\times \\
\langle m|e^{i\hat{H}_0 t_2/\hbar}\hat{I}(x_2)e^{-i\hat{H}_0 t_2/\hbar}|n\rangle &= \sum_{n,m}\rho_{nn}\langle n|\hat{I}(x_1)|m\rangle\langle m|\hat{I}(x_2)|n\rangle\, e^{iE_n t_1/\hbar - iE_m t_1/\hbar}\times \\
e^{iE_m t_2/\hbar - iE_n t_2/\hbar} &= \sum_{n,m}\rho_{nn}\langle n|\hat{I}(x_1)|m\rangle\langle m|\hat{I}(x_2)|n\rangle\, e^{i(E_m-E_n)(t_2-t_1)/\hbar}. \qquad (7.102)
\end{aligned}$$

Now lets go on to the frequency representation. In most general form

$$\begin{aligned}
\langle \hat{I}_{\omega_1}(x_1)\hat{I}_{\omega_2}(x_2)\rangle &= \int dt_1 e^{i\omega_1 t_1}\int dt_2\, e^{i\omega_2 t_2}\langle \hat{I}(x_1,t_1)\hat{I}(x_2,t_2)\rangle = \\
&\sum_{n,m}\rho_{nn}\langle n|\hat{I}(x_1)|m\rangle\langle m|\hat{I}(x_2)|n\rangle\,(2\pi)^2\,\delta\Big[\omega_1 - \frac{E_m-E_n}{\hbar}\Big]\times \\
\delta\Big[\omega_2 - \frac{E_n-E_m}{\hbar}\Big] &= (2\pi)^2\sum_{n,m}\rho_{nn}\langle n|\hat{I}(x_1)|m\rangle\langle m|\hat{I}(x_2)|n\rangle\times \\
\delta\big[\omega_1+\omega_2\big]\,\delta\Big[\omega_1 - \frac{E_m-E_n}{\hbar}\Big] &= 2\pi\delta\left(\omega_1+\omega_2\right)\langle \hat{I}_{\omega_1}(x_1)\hat{I}_{-\omega_1}(x_2)\rangle. \qquad (7.103)
\end{aligned}$$

$$S(x_1,x_2;\omega)=\langle\hat{I}_\omega(x_1)\hat{I}_{-\omega}(x_2)\rangle=\int dt\,e^{i\omega t}\langle\hat{I}(x_1,0)\hat{I}(x_2,t)\rangle= 2\pi\sum_{n,m}\rho_{nn}\langle n|\hat{I}(x_1)|m\rangle\langle m|\hat{I}(x_2)|n\rangle\,\delta\Big[\omega-\frac{E_m-E_n}{\hbar}\Big]. \quad (7.104)$$

This expression is non-zero only at energies $E_m-E_n=\hbar\omega$. The diagonal elements of density matrix are $\rho_{nn}\sim e^{-E_n/k_{\mathrm{B}}\vartheta}$ and $\rho_{mm}\sim e^{-E_m/k_{\mathrm{B}}\vartheta}$, where ϑ is a temperature and k_{B} is a Boltzmann constant. Thus

$$\rho_{mm}=e^{-\hbar\omega/k_{\mathrm{B}}\vartheta}\rho_{nn}. \quad (7.105)$$

Now let us change $n\leftrightarrow m$ in the sum in formula (7.104) and then substitute the expression (7.105) for ρ_{mm}, we have

$$S(x_1,x_2;\omega)=2\pi\sum_{m,n}\rho_{mm}\langle m|\hat{I}(x_1)|n\rangle\langle n|\hat{I}(x_2)|m\rangle\,\delta\Big[\omega-\frac{E_n-E_m}{\hbar}\Big]= 2\pi\sum_{m,n}\rho_{mm}\langle m|\hat{I}(x_1)|n\rangle\langle n|\hat{I}(x_2)|m\rangle\,\delta\Big[-\omega-\frac{E_m-E_n}{\hbar}\Big]= 2\pi\sum_{m,n}e^{-\hbar\omega/k_{\mathrm{B}}\vartheta}\rho_{nn}\langle m|\hat{I}(x_1)|n\rangle\langle n|\hat{I}(x_2)|m\rangle\,\delta\Big[-\omega-\frac{E_m-E_n}{\hbar}\Big]= e^{-\hbar\omega/k_{\mathrm{B}}\vartheta}S(x_2,x_1;-\omega). \quad (7.106)$$

This formula connects $S(x_1,x_2;\omega)$ and $S(x_1,x_2;-\omega)$. By substituting this relation to formula (7.99) we get the fluctuation-dissipation relation

$$(e^{\hbar\omega/k_{\mathrm{B}}\vartheta}-1)\,S(x_1,x_2,\omega)=2\hbar\omega G_\omega(x_1,x_2). \quad (7.107)$$

The standard formulation of the fluctuation-dissipation theorem is for symmetrized current-current correlator. Let us modify our result. Let us rewrite the expression for the symmetrized current-current using (7.106)

$$\frac{1}{2}\langle\hat{I}_\omega(x_1)\hat{I}_{-\omega}(x_2)+\hat{I}_{-\omega}(x_1)\hat{I}_\omega(x_2)\rangle=\frac{e^{\hbar\omega/k_{\mathrm{B}}\vartheta}+1}{2}\,S(x_1,x_2,\omega).$$

After that we can substitute the expression for $S(x_1,x_2;\omega)$ from (7.107) and obtain

$$\frac{1}{2}\langle\hat{I}_\omega(x_1)\hat{I}_{-\omega}(x_2)+\hat{I}_{-\omega}(x_1)\hat{I}_\omega(x_2)\rangle=2\hbar\omega G(x_1,x_2;\omega)\coth\Big(\frac{\hbar\omega}{2k_{\mathrm{B}}\vartheta}\Big). \quad (7.108)$$

Similar, we obtain for Bosons the Bose-Einstein occupation numbers $N(\varepsilon) = 1/(e^{\varepsilon/k_{\rm B}\vartheta} - 1)$. The fluctuation-dissipation theorem in its standard form reads

$$\frac{1}{4}\langle \hat{I}_\omega(x_1)\hat{I}_{-\omega}(x_2) + \hat{I}_{-\omega}(x_1)\hat{I}_\omega(x_2)\rangle = \hbar\omega[G(x_1,x_2;\omega) + G(x_2,x_1;\omega)]\Big\{\frac{1}{2} + N(\hbar\omega)\Big\}. \quad (7.109)$$

7.8 Theory of measurements of the noise

In recording high frequencies it is suitable to use a resonance circuit (RC) as a detector coupled by inductance with the investigated conductor so that the RC is not affected by dc.

In this case the detector can be described by the equation of motion

$$\ddot{\phi} = -\Omega^2\phi - \gamma\dot{\phi} - \lambda\dot{I}(t), \quad (7.110)$$

where the external force is proportional to the derivative of the measured current $\lambda\dot{I}(t)$, and the circuit quality should be high, so $\gamma \ll \Omega$. Then the detector response is a changed charge at the capacitor, $\phi \to Q$,

$$Q^2 = \int d\omega\, \frac{\lambda^2\omega^2 I_\omega I_\omega}{(\Omega-\omega)^2 + \omega^2\gamma^2}. \quad (7.111)$$

We have considered the same system in quantum-mechanical terms [15], assuming the circuit to have a certain temperature $\vartheta_{\rm LC}$. Treating the RC as an oscillator with infinitely small damping η, we have found the correction to squared charge fluctuations, which is of second order with respect to the inductance coupling constant. The result can be formulated as follows: the measurable response of the considered detector at the resonance frequency Ω is expressed via current correlators as:

$$S_{\rm meas} = K\Big\{S(\Omega) + N_\Omega\big[S(\Omega) - S(-\Omega)\big]\Big\}. \quad (7.112)$$

where

$$S(\Omega) = \int dt\, \langle \hat{I}(0)\hat{I}(t)\rangle\, e^{i\Omega t}. \quad (7.113)$$

The frequency Ω is assumed to be positive in the expressions, N_Ω are the Bose occupation numbers of the oscillator, i.e.,

$$N_\Omega = \frac{1}{e^{\hbar\Omega/k_{\rm B}\vartheta_{\rm LC}} - 1}, \quad (7.114)$$

K is an effective constant of coupling between the quantum wire and the RC, $\langle A\rangle = \mathrm{Tr}\{\hat{\rho}\hat{A}\}$, where $\hat{\rho}$ is the electron density matrix, and the time-dependent current operators are determined in the ordinary way as $I(t) = e^{i\hat{H}t}\hat{I}e^{-i\hat{H}t}$. The derived expression should be compared with the widely used formula [14]

$$S(\omega) = \int d\omega\, e^{i\omega t}\Big\langle \frac{\hat{I}(0)\hat{I}(t) + \hat{I}(t)\hat{I}(0)}{2}\Big\rangle. \tag{7.115}$$

Note that the formula includes the symmetrized current correlator. The symmetrization results from the fact that the current operators at different times are not commutative, the symmetrization guarantees the correlators to be reals, and is likely similar to the corresponding classical expression [14]. It is easy to check that the quantity

$$\int dt\, \hat{I}(0)\hat{I}(t)\, e^{i\Omega t}.$$

is Hermitian and $S(\Omega)$ is real [under the condition of time homogeneity $\langle \hat{I}(t_1)\hat{I}(t_2)\rangle = f(t_1 - t_2)$, as was assumed in the derivation of Eq. (7.112)][2] Formula (7.115) leads to the well known expression for the spectral density of fluctuations in an equilibrium conductor [6]:

$$S(\Omega) = 2G\hbar\Omega\Big[\frac{1}{2} + \frac{1}{e^{\hbar\Omega/k_{\mathrm{B}}\vartheta} - 1}\Big] \tag{7.116}$$

This means that at zero temperature the fluctuations should be proportional to frequency, which is usually interpreted as an analog of zero (vacuum) oscillations in an electromagnetic field.

However, as is known from optical measurement, normal photodetectors do not record zero oscillations, because the energy required to excite an atom in the detector cannot be extracted from the vacuum (see, e.g., Ref. [19]. At the same time, zero-point oscillations can be observed (although by a more complicated way than for usual fluctuations) in the Lamb shift of levels [20], in the Casimir effect [20], or with the use of the so-called Mandel quantum counter [21], which is initially prepared in an excited state and hence can record zero oscillations.

Analyzing Eq. (7.112), we will show that the RC can operate as a photodetector, which is not affected by zero-point oscillations, or a quantum

[2] For the case we study correlations at different points the measurable (and real) quantity is $[S(x_1, x_2; \omega) + S(x_2, x_1; \omega)]/2$, see Ref. [18].

counter, but its response is never described by the standard Nyquist expression (7.116) as would be expected.

When the detected frequency greatly exceeds the temperature of the LC-detector, N_Ω is exponentially small, and the only non-vanishing term in Eq. (7.112) is the positive part of the spectral density $S(\Omega)$, which describes the energy emission from the conductor to the RC. In this case the LC-detector works as a normal photoreceiver. As an example, we express $S(\Omega)$ in a coherent conductor with transmission coefficient T at zero temperature and finite voltage as

$$S(\Omega) = \frac{2e^2}{h} T(1-T)(eV - \hbar\Omega), \tag{7.117}$$

when $\hbar\Omega < eV$, and $S(\Omega) = 0$ in the opposite case. Here we ignore the energy dependence of the transmission coefficient. Expression (7.117) coincides with the excess spectral density calculated by the symmetrized correlator (7.115).

If the frequency is much less than the temperature of the RC, i.e. $\hbar\Omega \ll k_{\mathrm{B}}\vartheta_{\mathrm{LC}}$, the Bose numbers N_Ω can be replaced by $K_{\mathrm{B}}\vartheta_{\mathrm{LC}}/\hbar\Omega$. The difference $S(\Omega) - S(-\Omega)$ is negative, and for a quantum conductor with a transmission coefficient weakly dependent on energy we obtain

$$S(\Omega) - S(-\Omega) = -2\hbar\Omega G, \tag{7.118}$$

where $G = (2e^2/h)\sum_n T_n$ is the conductance.

Note that the singular behaviour of the spectral density at $\hbar\Omega = eV$, which was found in Ref. [22] for the symmetrized expression $S(\Omega) + S(-\Omega)$, does not take place for $S(\Omega) - S(-\Omega)$, therefore we can conclude that the only singularity which can be measured at zero temperature and finite voltage is determined by frequency cut-off of voltage in $S(\Omega)$.

Now we have for $\hbar\Omega \ll k_{\mathrm{B}}\vartheta_{\mathrm{LC}}$:

$$S_{\mathrm{meas}} = K(S(\Omega) - 2Gk_{\mathrm{B}}\vartheta_{\mathrm{LC}}), \tag{7.119}$$

The meaning of the negative term is clear: the LC-detector is "cooled", emitting energy into the conductor. Thus, in this limit the zero-point oscillations presented by $S(-\Omega)$ can be observed in some sense, but the final result includes an expression different from the Nyquist formula (7.116).

If the conductor is in equilibrium (to an accuracy of a weak interaction with the RC), we have at low frequencies: $S_{\mathrm{meas}} \propto 2G(\vartheta_{\mathrm{e}} - \vartheta_{\mathrm{LC}})$. This expression is equal to zero, when the electron temperature ϑ_{e} is equal to

the temperature $\vartheta_{\rm LC}$ of the LC-detector, as was to be expected for the total equilibrium of the system.

At intermediate frequencies $k_{\rm B}\vartheta_{\rm e}, eV \ll \hbar\Omega \ll k_{\rm B}\vartheta_{\rm LC}$, the measuring response is negative: $S_{\rm meas} = -2Gk_{\rm B}\vartheta_{\rm LC}$.

When the low-frequency limit $\hbar\Omega \ll eV_{\rm bias}k_{\rm B}\vartheta_{\rm LC}$ is considered, it makes no difference whether we use $S(\Omega)$ or $S(-\Omega)$ or the Fourier transform of the symmetrized expression (7.115) to determine the spectral density, since the result will be the same with the accuracy of small corrections of the order of $\hbar\Omega/ev, k_{\rm B}\vartheta$.

Bibliography

[1] R. Brown, *A brief account of microscopical observations made in the months of June, July and August, 1827, on the particles contained in the pollen of plants; and on the general existence of active molecules in organic and inorganic bodies.*, Phil. Mag. **4**, 161 (1828).

[2] A. Einstein, *Über die von der molekularkinetischen Theorie der Wärme geforderte Bewegung von in ruhenden Flüssigkeiten suspendierten Teilchen.*, Ann. Phys. (Leipzig) **17**, 549 (1905).

[3] W. Schottky, *Über spontane Stromschwankungen in verschiedenen Elektrizitätsleitern*, Ann. Phys. (Leipzig) **57**, 541 (1918).

[4] J. B. Johnson, *The Schottky effect in low frequency circuits*, Phys. Rev. **26**, 71 (1925).

[5] J. B. Johnson, *Thermal agitation of electricity in conductors*, Phys. Rev. **32**, 97 (1928).

[6] H. Nyquist, *Thermal agitation of electricity in conductors*, Phys. Rev. **32**, 110 (1928).

[7] L. D. Landau and E. M. Lifshitz, *Quantum Mechanics*, vol. 3 of *Course of Theoretical Physics* (Pergamon Press, London, 1958).

[8] R. de-Picciotto, M. Reznikov, M. Heiblum, V. Umansky, G. Bunin, and D. Mahalu, *Direct observation of a fractional charge*, Nature **389**, 162 (1997).

[9] L. Saminadayar, D. C. Glattli, Y. Jin, and B. Etienne, *Observation of the e/3 fractionally charged Laughlin quasiparticles*, Phys. Rev. Lett. **79**, 2526 (1997).

[10] G. B. Lesovik, *Excess quantum noise in 2D ballistic point contacts*, JETP Lett. **49**, 592 (1989).

[11] D. C. Tsui, H. L. Stormer, and A. C. Gossard, *Two-dimensional magnetotransport in the extreme quantum limit*, Phys. Rev. Lett. **48**, 1559 (1982).

[12] F. Von Oppen and A. Stern, *Electron-electron interaction, conductance fluctuations, and current noise*, Phys. Rev. Lett. **79**, 1114 (2007).

[13] H. B. Callen and T. A. Welton, *Irreversibility and generalized noise*, Phys. Rev. **83**, 34 (1951).

[14] L. D. Landau and E. M. Lifshitz, *Statistical Physics*, vol. 5 of *Course of Theoretical Physics* (Pergamon Press, London, 1958).

[15] G. B. Lesovik and R. Loosen, *On the detection of finite-frequency current fluctuations*, JETP Lett. **65**, 295 (1997).

[16] U. Gavish, Y. Levinson, and Y. Imry, *Detection of quantum noise*, Phys. Rev. B **62**, R10637 (2000).

[17] U. Gavish, Y. Imry, and Y. Levinson, *Quantum noise, detailed balance and Kubo formula in nonequilibrium quantum systems*, cond-mat/0211681 (2002).

[18] G. B. Lesovik, A. V. Lebedev, and G. Blatter, *Wave function collapse in a mesoscopic device*, Phys. Rev. B **71**, 125313 (2005).

[19] J. Perina, *Coherence of Light* (D. Reidel Publ. Co., Dordrecht, 1985).

[20] W. E. Lamb and R. C. Retherford, *Fine structure of the hydrogen atom by a microwave method*, Phys. Rev. **72**, 241 (1947).

[21] L. Mandel, *Antinormally ordered correlations and quantum counters*, Phys. Rev. **152**, 438 (1966).

[22] S.-R. E. Yang, *Quantum shot noise spectrum of a point contact*, Solid State Commun. **81**, 375 (1992).

Chapter 8

Noise: the second-quantized formalism

8.1 Noise in non-equilibrium systems

In this chapter we will be interested in current noise in the mesoscopic conductors and use scattering matrix approach more formally, in framework of second quantization. To describe this noise we need second-order correlators of the current operator $\hat{I}(x,t)$. The most general formula for it is

$$\langle \hat{I}(x_1,t_1)\hat{I}(x_2,t_2)\rangle = \mathrm{Tr}\big\{\hat{\rho}\,\hat{I}(x_1,t_1)\hat{I}(x_2,t_2)\big\}, \tag{8.1}$$

where $\hat{\rho}$ is a density matrix of the system. For the time-independent Hamiltonian of the system $\hat{H}_0$ we can write down current operator in Heisenberg representation (see section 6.2)

$$\hat{I}(x,t) = e^{i\hat{H}_0 t/\hbar}\,\hat{I}(x)\,e^{-i\hat{H}_0 t/\hbar}. \tag{8.2}$$

Here

$$\hat{I} = -\frac{ie\hbar}{2m}\sum_{\sigma}\int_0^{\infty}\frac{dk'dk}{(2\pi)^2}\Big\{\hat{c}^{\dagger}_{\mathrm{L}\sigma k'}\hat{c}_{\mathrm{L}\sigma k}(-ik'-ik)t^{*}_{k'}t_k e^{i(k-k')x}+$$
$$+\hat{c}^{\dagger}_{\mathrm{L}\sigma k'}\hat{c}_{\mathrm{R}\sigma k}\Big[(-ik')t^{*}_{k'}e^{-ik'x}(e^{-ikx}+r_k e^{ikx})-t^{*}_{k'}e^{-ik'x}(-ike^{-ikx}+$$
$$+ikr_k e^{ikx})\Big]+\hat{c}^{\dagger}_{\mathrm{R}\sigma k'}\hat{c}_{\mathrm{L}\sigma k}\Big[(ik'e^{ik'x}-ik'r^{*}_{k'}e^{-ik'x})t_k e^{ikx}-$$
$$-(e^{ik'x}+r^{*}_{k'}e^{-ik'x})ikt_k e^{ikx}\Big]+\hat{c}^{\dagger}_{\mathrm{R}\sigma k'}\hat{c}_{\mathrm{R}\sigma k}\Big[(ik'e^{ik'x}-ik'r^{*}_{k'}e^{-ik'x})\times$$
$$\times(e^{-ikx}+r_k e^{ikx})-(e^{ik'x}+r^{*}_{k'}e^{-ik'x})(-ike^{-ikx}+ikr_k e^{ikx})\Big]\Big\} \quad (8.3)$$

is a current operator (6.44) which can be obtain by solving time-independent Shödinger equation; the equation (8.2) describes its evolution.

Let's start with simple one-channel problem for simplicity. Later we will discuss how it was in n-channel case with $n \times n$ scattering matrix. But now we have a simple problem — scattering on the potential. It has a solution in the form of Lippman-Swinger scattering states (see section 2.4 for more details): incident state from the left $|\mathrm{L}\rangle$ or vice-versa incident state from the right $|\mathrm{R}\rangle$. In the first case the transmission and reflection amplitudes will be t_{LR} and r_{LL} respectively; in the second case they are t_{RL} and r_{RR}. In the absence of magnetic field $H = 0$ transmission amplitudes from left to right and from right to left are equal, $t_{\mathrm{RL}} = t_{\mathrm{LR}}$. In general for $H \neq 0$ these amplitudes are not equal $t_{\mathrm{RL}} \neq t_{\mathrm{LR}}$ and due to the time reversal symmetry $t_{\mathrm{RL}}(H) = t_{\mathrm{LR}}(-H)$. In quite general case $r_{\mathrm{LL}} \neq r_{\mathrm{RR}}$ (even for $H = 0$) but for the symmetric barrier $r_{\mathrm{LL}} = r_{\mathrm{RR}}$. Let's suppose the symmetric potential to simplify our notations.

Using the same technic as in section 6.4 we obtain the answer for corre-

lator (8.1) and then, making Fourier transformation for the spectral density

$$\langle\langle \hat{I}_{-\omega}(x_1)\hat{I}_{\omega}(x_2)\rangle\rangle = \frac{2e^2\hbar^2}{(2m)^2}\int\limits_0^\infty \frac{d\varepsilon}{h v_{\varepsilon'} v_\varepsilon}\Big[$$
$$n_{\rm L}(\varepsilon')[1-n_{\rm L}(\varepsilon)](k+k')^2\, T_{\varepsilon'}T_\varepsilon\, e^{i(k-k')(x_1-x_2)} +$$
$$+\, n_{\rm L}(\varepsilon')[1-n_{\rm R}(\varepsilon)]\Big\{(k+k')^2 T_{\varepsilon'}(1-T_\varepsilon)e^{i(k-k')(x_1-x_2)} +$$
$$(k'^2-k^2)T_{\varepsilon'}e^{-ik'(x_1-x_2)}(r_\varepsilon e^{ik(x_1+x_2)}+r_\varepsilon^* e^{-ik(x_1+x_2)})+(k'-k)^2 T_{\varepsilon'}e^{-i(k+k')(x_1-x_2)}\Big\}+$$
$$+\, n_{\rm R}(\varepsilon')[1-n_{\rm L}(\varepsilon)]\Big\{(k+k')^2 T_{\varepsilon}(1-T_{\varepsilon'})e^{i(k-k')(x_1-x_2)} +$$
$$+(k^2-k'^2)T_{\varepsilon}e^{ik(x_1-x_2)}\big(r_{\varepsilon'}e^{ik'(x_1+x_2)}+r_{\varepsilon'}^* e^{-ik'(x_1+x_2)}\big)+(k'-k)^2 T_{\varepsilon}e^{i(k+k')(x_1-x_2)}\Big\}+$$
$$+\, n_{\rm R}(\varepsilon')[1-n_{\rm R}(\varepsilon)]\Big\{(k+k')^2 e^{-i(k-k')(x_1-x_2)} + (k+k')^2 R_{\varepsilon'}R_\varepsilon e^{i(k-k')(x_1-x_2)} -$$
$$-\,(k+k')^2\big[r_{\varepsilon'}^* r_\varepsilon e^{i(k-k')(x_1+x_2)} + r_\varepsilon^* r_{\varepsilon'} e^{-i(k-k')(x_1+x_2)}\big] +$$
$$(k^2-k'^2)\big[r_\varepsilon^* e^{-i(k-k')x_1-i(k+k')x_2} - r_{\varepsilon'}e^{i(k+k')x_2} + r_{\varepsilon'}^* e^{i(k-k')x_2}e^{-i(k+k')x_1} - r_\varepsilon e^{i(k+k')x_1}\big] +$$
$$(k^2-k'^2)\big[r_{\varepsilon'}^* R_\varepsilon e^{i(k-k')x_1-i(k+k')x_2} - r_\varepsilon R_{\varepsilon'}e^{i(k+k')x_2} -$$
$$R_{\varepsilon'}r_\varepsilon^* e^{-i(k-k')x_2-i(k+k')x_1} - R_\varepsilon r_{\varepsilon'}e^{i(k+k')x_1}\big] -$$
$$(k-k')^2\big[r_{\varepsilon'}^* e^{-i(k+k')x_1} - r_\varepsilon e^{i(k+k')x_1}\big]\big[r_\varepsilon^* e^{-i(k+k')x_2} - r_{\varepsilon'}e^{i(k+k')x_2}\big]\Big\}\Big], \quad (8.4)$$

here $\varepsilon' = \varepsilon + \hbar\omega$, electron velocity $v_\varepsilon = \sqrt{2\varepsilon/m}$, and electron wave vector $k = \sqrt{2m\varepsilon}/\hbar$.

For zero frequency $\omega = 0$ spectral density (8.4) does not depend on coordinates and we have

$$S(0) \equiv \langle\langle \hat{I}_{-\omega}\hat{I}_{\omega}\rangle\rangle\big|_{\omega=0} = \frac{2e^2}{h}\int\limits_0^{+\infty} d\varepsilon\,\Big[n_{\rm L}(\varepsilon)[1-n_{\rm L}(\varepsilon)]T_\varepsilon^2 +$$
$$n_{\rm R}(\varepsilon)[1-n_{\rm R}(\varepsilon)]T_\varepsilon^2 + T_\varepsilon[1-T_\varepsilon]\big\{n_{\rm L}(\varepsilon)(1-n_{\rm R}(\varepsilon)) + n_{\rm R}(\varepsilon)(1-n_{\rm L}(\varepsilon))\big\}\Big]. \quad (8.5)$$

Now let us consider some limits of the Eq. (8.5).

Zero temperature limit. In case of zero temperature $n_{\rm L/R}(\varepsilon) = \Theta(\mu_{\rm L/R} - \varepsilon)$ and nonzero voltage V the formula for the spectral density (8.5) simplifies and we obtain

$$S(0) = \frac{2e^2}{h}\int\limits_{\mu-eV/2}^{\mu+eV/2} d\varepsilon\, T_\varepsilon[1-T_\varepsilon]. \quad (8.6)$$

If in addition we suppose that transmission probability T does not depend on energy dramatically, then we can replace the expression in the integral to the its value at Fermi energy, $T_\varepsilon \approx T_\mu \equiv T$,

$$S(0) = \frac{2e^3 V}{h} T[1-T]. \tag{8.7}$$

This limit is gives us quantum shot noise. The source of this noise is the choice of quantum alternative: to tunnel or neglect.

Equilibrium limit. Now let us consider the case with nonzero temperature and zero bias voltage $V = 0$. In this case $n_{\mathrm{L}} = n_{\mathrm{R}} \equiv n$.

$$S(0) = \frac{2e^2}{h} \int_0^{+\infty} d\varepsilon \, 2n(\varepsilon)[1-n(\varepsilon)]T_\varepsilon. \tag{8.8}$$

If we assume T_ε to be constant and taking into account that $\int_0^\infty d\varepsilon n(\varepsilon)[1-n(\varepsilon)] = k_{\mathrm{B}}\vartheta$ we recovered Nyquwest result for the noise

$$S(0) = 2k_{\mathrm{B}}\vartheta G, \tag{8.9}$$

where G is a conductance per spin.

In the Shottky limit of we assume $n_{\mathrm{R}} = 0$ and $n_{\mathrm{L}} \ll 1$. In this limit the spectral noise

$$S(0) = \frac{2e^2}{h} \int_0^{+\infty} d\varepsilon \, n_{\mathrm{L}}(\varepsilon) T_\varepsilon \tag{8.10}$$

is proportional to the average current

$$\langle \hat{I} \rangle = \frac{2e}{h} \int_0^{+\infty} d\varepsilon \, n_{\mathrm{L}}(\varepsilon) T_\varepsilon \tag{8.11}$$

with coefficient which is exactly equals to the electron charge e,

$$S(0) = e\langle \hat{I} \rangle. \tag{8.12}$$

8.2 Beam splitter

Let us consider the symmetric bean splitter represented at Fig. 8.1. The electrons comes from the reservoir 1 and can tunnel to the reservoirs 3 (with

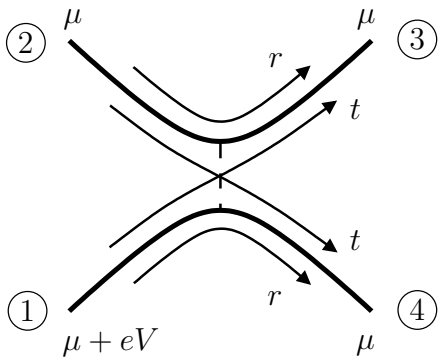

Figure 8.1: Symmetric splitter. The voltage V is applied to the lead 1; the leads 2-4 are at zero potential. The probability to tunnel from the lead 1 to 4 is r, to 3 is t and there is no backscattering at all.

amplitude r) and 4 (with amplitude t) and does not reflect to back and to the reservoir 2. Let us calculate the spectral density at zero frequency of the current-current correlator $\langle\langle \hat{I}_3 \hat{I}_4 \rangle\rangle$ between current in the 3rd and 4th reservoirs. The definition of this kind of correlator

$$S_{34}(\omega) = \int dt \, \langle\langle \hat{I}_3 \hat{I}_4 \rangle\rangle e^{i\omega t}. \tag{8.13}$$

Due to the absence of the backscattering we can take only the term in (8.3) which is proportional to the $\hat{c}^\dagger_{\mathrm{L}\sigma k'} \hat{c}_{\mathrm{L}\sigma k}$ (Lippman-Scwhinger state coming from the left = from 1st lead), e.g. for the 3rd lead

$$\hat{I}_3 = -\frac{ie\hbar}{2m} \sum_\sigma \int_0^\infty \frac{dk' dk}{(2\pi)^2} (-ik - ik') \left[\hat{c}^\dagger_{1\sigma k'} t^* + \hat{c}^\dagger_{2\sigma k'} r^*\right] \left[\hat{c}_{1\sigma k} t + \hat{c}_{2\sigma k} r\right] e^{i(k-k')x}. \tag{8.14}$$

The current in the 4th lead can be obtained by replacing $t \leftrightarrow r$ in (8.14),

$$\hat{I}_4 = -\frac{ie\hbar}{2m} \sum_\sigma \int_0^\infty \frac{dq' dq}{(2\pi)^2} (-iq - iq') \left[\hat{c}^\dagger_{1\sigma q'} r^* + \hat{c}^\dagger_{2\sigma q'} t^*\right] \left[\hat{c}_{1\sigma q} r + \hat{c}_{2\sigma q} t\right] e^{i(q-q')x}. \tag{8.15}$$

The irreducible correlator for zero temperature and zero frequency is given by the term proportional to $\langle \hat{c}^\dagger_{1\sigma k'} \hat{c}_{1\sigma q} \rangle \langle \hat{c}_{2\sigma k} \hat{c}^\dagger_{2\sigma q'} \rangle \propto n_1(\varepsilon)[1 - n_2(\varepsilon)]$.[1] Here

[1] The similar term $\langle \hat{c}^\dagger_{1\sigma k'} \hat{c}_{1\sigma q} \rangle \langle \hat{c}_{2\sigma k} \hat{c}^\dagger_{2\sigma q'} \rangle \propto n_2(\varepsilon)[1 - n_1(\varepsilon)]$ is zero because the nonzero regions of the functions $n_2(\varepsilon)$ and $1 - n_1(\varepsilon)$ do not intersect.

$n_1(\varepsilon)$ and $n_2(\varepsilon)$ are Fermi occupation numbers in 1st and 2nd leads. The corresponding spectral density is

$$S_{34}(0) = \frac{2e^2\hbar^2}{(2m)^2} \int_0^\infty \frac{d\varepsilon}{hv_\varepsilon^2} n_1(\varepsilon)[1 - n_2(\varepsilon)] 4k^2\, t_\varepsilon^* r_\varepsilon t_\varepsilon^* r_\varepsilon. \tag{8.16}$$

Note, that due to unitarity of the scattering matrix of the splitter we have $t_\varepsilon^* r_\varepsilon = -t_\varepsilon r_\varepsilon^*$, so $t_{\varepsilon'}^* t_\varepsilon r_\varepsilon^* r_{\varepsilon'} = -T_{\varepsilon'} R_\varepsilon$ (here $T_\varepsilon = |t_\varepsilon|^2$ and $R_\varepsilon = |r_\varepsilon|^2 = 1 - T_\varepsilon$). Therefore, the formula (8.16) transforms to

$$S_{34}(0) = -\frac{2e^2}{h} \int_0^\infty d\varepsilon\, n_1(\varepsilon)[1 - n_2(\varepsilon)]\, T_\varepsilon R_\varepsilon. \tag{8.17}$$

And assuming T_ε and R_ε to be constant in the interval $[\mu \dots \mu + eV]$ we obtain the answer

$$S_{34}(0) = -\frac{2e^3 V}{h} T_\varepsilon R_\varepsilon. \tag{8.18}$$

The $S_{34}(0)$ is negative; this reflects the fact that although the wave function is splitted, the electron can be found in only one arm.

Chapter 9

Entanglement and Bell's inequality

9.1 Pure and entangled states

Le us consider the two noninteracting quantum mechanical subsystems, which are described by wave functions $|\psi_1\rangle$ and $|\psi_2\rangle$. The state of the composite system which can be presented in a tensor product of its subsystems states

$$|\psi(x_1, x_2)\rangle = |\psi_1(x_1)\rangle \otimes |\psi_2(x_2)\rangle. \tag{9.1}$$

is called *product* state of the system.

But all states of the system can not be described by (9.1). For example the state

$$|\psi(x_1, x_2)\rangle = \frac{1}{\sqrt{2}}\Big[|\psi_1(x_1)\rangle|\psi_2(x_2)\rangle - |\psi_1(x_2)\rangle|\psi_2(x_1)\rangle\Big] \tag{9.2}$$

can not be written as a product of the (orthonormal) states $|\psi_1\rangle$ and $|\psi_2\rangle$ of the subsystems . All states of the system, which can not be written in form (9.1) are called *entangled*. For the state (9.1) each particle 1 and 2 is in pure state. Their density matrices are

$$\hat{\rho}_1 = |\psi_1\rangle\langle\psi_1|, \quad \hat{\rho}_2 = |\psi_2\rangle\langle\psi_2|. \tag{9.3}$$

For them $\mathrm{Tr}\{\hat{\rho}^2_{1,2}\} = \mathrm{Tr}\{\hat{\rho}_{1,2}\} = 1$ as must be for pure states [1]. In other hand, density matrix of the 1st particle for the state (9.2) is

$$\hat{\rho}_1(x_1) = \mathrm{Tr}_2\big\{|\psi\rangle\langle\psi|\big\} = \frac{1}{2}\Big[|\psi_1(x_1)\rangle\langle\psi_1(x_1)| + |\psi_2(x_1)\rangle\langle\psi_2(x_1)|\Big], \tag{9.4}$$

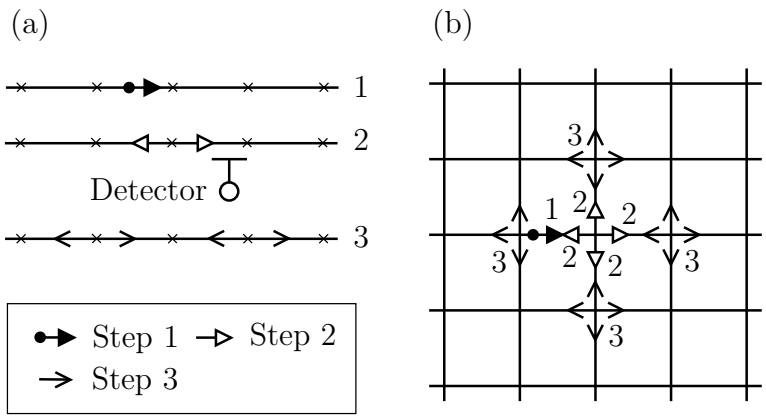

Figure 9.1: Quantum random walk at 1D lattice (a) and at 2D lattice (b).

where Tr_2 is a trace over degrees of freedom of the 2nd particle. Then

$$\mathrm{Tr}\{\hat{\rho}_1^2\} = \frac{1}{2} < 1 \tag{9.5}$$

and thus, particle 1 is not in *pure* but in a *mixed* state, due to entanglement with particle 2.

9.2 Entropy growth due to entanglement

In this section we discuss which path detector and will be interested in the entropy of the system S with entanglement. The entropy is defined by usual formula

$$S = -\mathrm{Tr}\{\hat{\rho}\log_2\hat{\rho}\}. \tag{9.6}$$

In the case the detector works perfectly and detect passed particle without perturbing its motion, one can use the master equation to describe the probability to find particle after step number n in (symmetric) random walk, cf. Fig. 9.1. In 1D case Fig. 9.1(a) the master equation is

$$P_{j,\rightarrow}(n) = \frac{1}{2}P_{j-1,\rightarrow}(n-1) + \frac{1}{2}P_{j+1,\leftarrow}(n-1), \tag{9.7}$$

where j is a number of segment between the scatterer, arrows show in which direction the particle travels. And similar equation for opposite direction

$$P_{j,\leftarrow}(n) = \frac{1}{2}P_{j+1,\leftarrow}(n-1) + \frac{1}{2}P_{j-1,\rightarrow}(n-1). \tag{9.8}$$

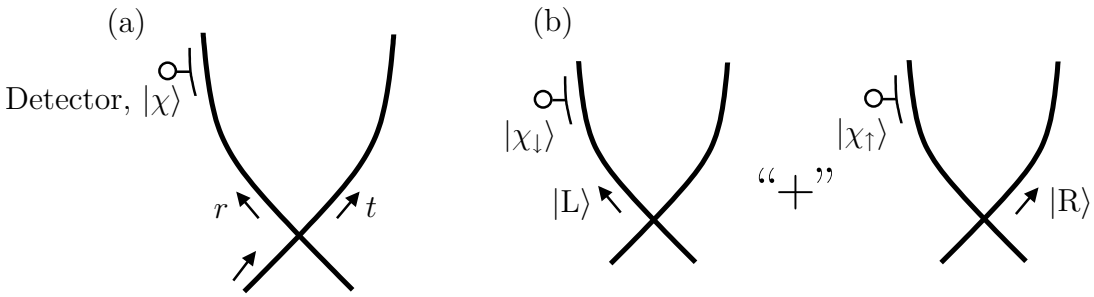

Figure 9.2: Entropy growing due to entanglement. (a) Scheme of the which path detector setup; the state of the detector is characterized by spinor function $|\chi\rangle$ (states $|\chi_\uparrow\rangle$ or $|\chi_\downarrow\rangle$) and the sate of the electron — by left $|\mathrm{L}\rangle$ or right $|\mathrm{R}\rangle$ arm. (b) The states of electron and detector are entangled: $r|\chi_\downarrow\rangle|\mathrm{L}\rangle - t|\chi_\uparrow\rangle|\mathrm{R}\rangle$, where $|r|^2 + |t|^2 = 1$.

Using (9.7), (9.8), and convexity of the function $-x\log_2 x$ one can prove, that entropy grows $S(n+1) \geq S(n)$. (In fact $S(n+1) > S(n)$ striclty.)

Consider now in details a which path detector. At the entrance of it electron splitter is placed. The electron can propagate to the left arm (state $|\mathrm{L}\rangle$) with probability $R = |r|^2$ and to the right arm (state $|\mathrm{R}\rangle$) with probability $T = |t|^2$; $T + R = 1$. The transmission amplitudes t and r characterize splitter, we assume that no backscattering takes place.

The state of detector is described by spinor function $|\chi\rangle$ with basis states "up" $|\chi_\uparrow\rangle$ and "down" $|\chi_\downarrow\rangle$. The initial state of the spinor is in the direction of z axe

$$|\chi(0)\rangle = |\chi_\uparrow\rangle \equiv \begin{bmatrix} 1 \\ 0 \end{bmatrix}. \tag{9.9}$$

The operator which rotates spinor $|\chi\rangle$ around axe x to the angle φ is

$$\hat{U}(\varphi) = \cos\frac{\varphi}{2} + i\sigma_x \sin\frac{\varphi}{2} = \begin{bmatrix} \cos(\varphi/2) & i\sin(\varphi/2) \\ i\sin(\varphi/2) & \cos(\varphi/2) \end{bmatrix}. \tag{9.10}$$

The state of the spinor rotated around axe x to the angle φ is

$$|\chi(\varphi)\rangle = \hat{U}(\varphi)|\chi(0)\rangle = \begin{bmatrix} \cos(\varphi/2) \\ i\sin(\varphi/2) \end{bmatrix}. \tag{9.11}$$

The density matrix, projected to the state when the particle is found in

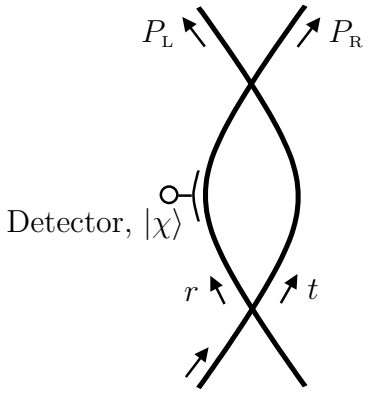

Figure 9.3: The detector has initial state $|\chi_\uparrow\rangle$ and change it to $|\chi_\downarrow\rangle$ if electron moves through the left arm (state of the electron $|\mathrm{L}\rangle$) and does not change if electron moves through the right arm (state of the electron $|\mathrm{R}\rangle$).

the lead L is

$$\hat{\rho} = R^2|\chi(\varphi)\rangle\langle\chi(\varphi)| + T^2|\chi(0)\rangle\langle\chi(0)| \\ - RTe^{-i\phi_{\rm LR}}|\chi(0)\rangle\langle\chi(\varphi)| - RTe^{i\phi_{\rm LR}}|\chi(\varphi)\rangle\langle\chi(0)|, \quad (9.12)$$

where $\phi_{\rm LR} = \phi_{\rm L} - \phi_{\rm R}$ is a difference between phases accumulated in left and right arms.

The probability to find electron in the left after second splitter is a sum of probabilities which correspond to the different states of the detector, $|\chi_\uparrow\rangle$ and $|\chi_\downarrow\rangle$

$$P_{\rm L} = \langle\chi_\uparrow|\hat{\rho}|\chi_\uparrow\rangle + \langle\chi_\downarrow|\hat{\rho}|\chi_\downarrow\rangle. \quad (9.13)$$

Usung (9.11) and (9.13) we obtain

$$P_{\rm L} = R^2 + T^2 - 2RT\cos\frac{\varphi}{2}\cos\phi_{\rm LR}. \quad (9.14)$$

Let us calculate the *visibility* of the interference in the left arm

$$V = \frac{\max\{P_{\rm L}\} - \min\{P_{\rm L}\}}{\max\{P_{\rm L}\} + \min\{P_{\rm L}\}} = \frac{2RT|\cos(\varphi/2)|}{R^2 + T^2}. \quad (9.15)$$

For the symmetric splitter $R = T$ the visibility is

$$V = \left|\cos\frac{\varphi}{2}\right|. \quad (9.16)$$

Interference decrease due to entanglement of the particle with the detector

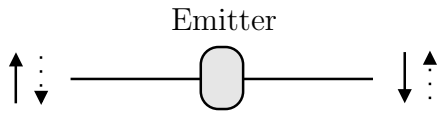

Figure 9.4: Bohm emitter emits two particles in opposite directions with opposite spins (possible realizations are marked with solid and dashed lines).

9.3 Bohm state

For product state

$$\hat{a}^{\dagger}_{1\uparrow}\hat{a}^{\dagger}_{2\downarrow}|0\rangle. \tag{9.17}$$

Wave function in first quantize formalism is

$$\frac{1}{\sqrt{2}}\big\{\varphi_1(x_1)\chi_{\uparrow}(\xi_1)\varphi_2(x_2)\chi_{\downarrow}(\xi_2)-\varphi_1(x_2)\chi_{\uparrow}(\xi_2)\varphi_2(x_1)\chi_{\downarrow}(\xi_1)\big\}. \tag{9.18}$$

Entangled state in second quantize formalism is

$$\frac{1}{\sqrt{2}}\big\{\hat{a}^{\dagger}_{1\uparrow}\hat{a}^{\dagger}_{2\downarrow}-\hat{a}^{\dagger}_{1\downarrow}\hat{a}^{\dagger}_{2\uparrow}\big\}|0\rangle \tag{9.19}$$

and in first quantize formalism

$$\frac{1}{\sqrt{2}}\big\{\varphi_1(x_1)\chi_{\uparrow}(\xi_1)\varphi_2(x_2)\chi_{\downarrow}(\xi_2)-\varphi_1(x_2)\chi_{\uparrow}(\xi_2)\varphi_2(x_1)\chi_{\downarrow}(\xi_1)- \\ \varphi_1(x_1)\chi_{\downarrow}(\xi_1)\varphi_2(x_2)\chi_{\uparrow}(\xi_2)+\varphi_1(x_2)\chi_{\downarrow}(\xi_2)\varphi_2(x_1)\chi_{\uparrow}(\xi_1)\big\}. \tag{9.20}$$

We take here

$$\int dx\varphi_1^*(x)\varphi_2(x)=0. \tag{9.21}$$

Compare (9.18) to usual

$$\big[\varphi_1(x_1)\varphi_2(x_2)\pm\varphi_1(x_2)\varphi_2(x_1)\big]\big[\chi_{\uparrow}(\xi_1)\chi_{\downarrow}(\xi_2)\mp\chi_{\uparrow}(\xi_2)\chi_{\downarrow}(\xi_1)\big]. \tag{9.22}$$

9.4 Bell type inequality

If x, x', y, y' are arbitrary variables and the conditions $|x|\leq 1$, $|x'|\leq 1$, $|y|\leq 1$, $|y'|\leq 1$ are valid. Let us calculate the limitations for the absolute value of $(x-x')y+(x+x')y'$. The modulus of the sum is equal or smaller then sum of modulus

$$|(x-x')y+(x+x')y'|\leq|(x-x')y|+|(x+x')y'|\leq|x-x'|+|x+x'|. \tag{9.23}$$

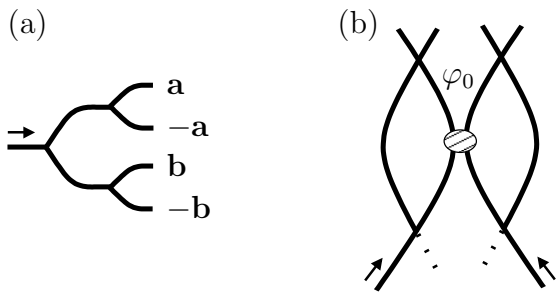

Figure 9.5: Entanglement in solid state physics: examples. (a) Setup 1. (b) Setup 2.

Due to symmetries $x \to -x$ and $x' \to -x'$ we can analyze last expression for positive x and x'. For $x > x'$ it is equal to $2x$, otherwise it is equal to $2x'$. Therefore it less or equal 2 and we have

$$|(x - x')y + (x + x')y'| \leq 2. \tag{9.24}$$

Now let us suppose that

$$x = x(\mathbf{a}, \lambda), \quad x' = x'(\mathbf{a}, \lambda), \quad y = y(\mathbf{a}, \lambda), \text{ and } y' = y'(\mathbf{a}, \lambda). \tag{9.25}$$

Distribution $\rho(\lambda)$, $\int d\lambda\, \rho(\lambda) = 1$. State of the detector is described by $\mathbf{a}$, and the state of the particle is described by λ.

Determine the result of measurements $x(\mathbf{a}, \lambda)$ in local hidden variables theory (LHVT) averaging with $\rho(\lambda)$ over (9.24), have

$$-2 \leq \langle xy \rangle - \langle x'y \rangle + \langle xy' \rangle + \langle x'y' \rangle \leq 2. \tag{9.26}$$

9.5 Entanglement in solid state physics: examples

Here we presented a few solid states setups, where Bell's inequality violates, cf Fig. 9.5.

9.6 Entanglement in solid state physics: one more example

Let us consider one more violation of Bell's inequality example (cf Fig. 9.6) in more details. We should construct variables x and y which are in range

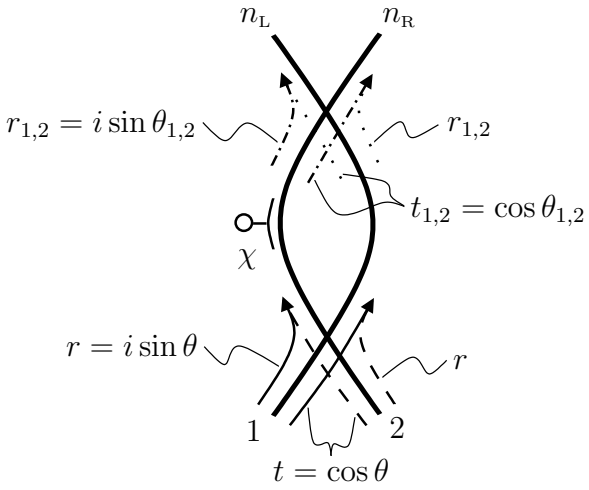

Figure 9.6: Violation of Bell's inequality setup is formed by two splitters [first one with r and t; second is controllable with $r_{1,2}$ and $t_{1,2}$] and detector in the left arm.

$[-1 \ldots 1]$; it is possible in the following way

$$x = n_{\mathrm{L}} - n_{\mathrm{R}}, \quad y = N_{\mathrm{L}} - N_{\mathrm{R}}. \tag{9.27}$$

Then the first term in Bell's inequality looks like

$$\langle xy \rangle = \langle n_{\mathrm{L}} N_{\mathrm{L}} \rangle + \langle n_{\mathrm{R}} N_{\mathrm{R}} \rangle - \langle n_{\mathrm{L}} N_{\mathrm{R}} \rangle - \langle n_{\mathrm{R}} N_{\mathrm{L}} \rangle. \tag{9.28}$$

Now we postselect the state, when spin flipped due to one particle passed

$$|\chi_{\downarrow}\rangle \big(r^2 |\mathrm{L}\rangle |\mathrm{R}\rangle + t^2 |\mathrm{R}\rangle |\mathrm{L}\rangle \big) \tag{9.29}$$

Let us calculate the averages in (9.28), the first one is

$$\begin{aligned} \langle n_{\mathrm{L}} N_{\mathrm{L}} \rangle &= \frac{1}{2} \big| i \sin\theta_1 \cos\theta_2 - i \cos\theta_1 \sin\theta_2 \big|^2 \\ &= \frac{1}{2} \big[\sin^2\theta_1 \cos^2\theta_2 + \cos^2\theta_1 \sin^2\theta_2 - 2 \sin\theta_1 \cos\theta_1 \sin\theta_2 \cos\theta_2 \big] = \frac{1}{2} \sin^2(\theta_1 - \theta_2) \end{aligned} \tag{9.30}$$

In the same way we calculate

$$\langle n_{\mathrm{L}} N_{\mathrm{R}} \rangle = \frac{1}{2} \big| i \sin\theta_1 i \sin\theta_2 - \cos\theta_1 \cos\theta_2 \big|^2 = \frac{1}{2} \cos^2(\theta_1 - \theta_2) \tag{9.31}$$

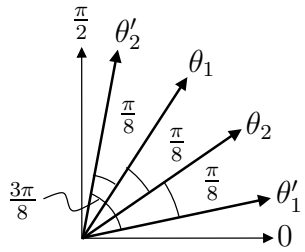

Figure 9.7: Violations of Bell inequalities: optimal angles for pseudo-spin which are violated of Bell's inequality.

and

$$\langle n_{\rm R} N_{\rm R}\rangle = \frac{1}{2}\sin^2(\theta_1-\theta_2),\quad \langle n_{\rm R} N_{\rm L}\rangle = \frac{1}{2}\cos^2(\theta_1-\theta_2). \tag{9.32}$$

Using these answers we obtain the average

$$\langle xy\rangle = -\cos 2(\theta_1-\theta_2). \tag{9.33}$$

Now we construct the Bell's inequality (9.26),

$$\big|\cos 2(\theta_1-\theta_2)+\cos 2(\theta_1'-\theta_2)+\cos 2(\theta_1-\theta_2')-\cos 2(\theta_1'-\theta_2')\big|\le 2. \tag{9.34}$$

The maximal value of the left side of the last relation reaches at angles

$$\theta_2'-\theta_1=\frac{\pi}{8},\quad \theta_1-\theta_2=\frac{\pi}{8},\quad \theta_2-\theta_1'=\frac{\pi}{8}, \tag{9.35}$$

cf Fig. 9.7 and equal to

$$\max\big|\cos 2(\theta_1-\theta_2)+\cos 2(\theta_1'-\theta_2)+ \\ \cos 2(\theta_1-\theta_2')-\cos 2(\theta_1'-\theta_2')\big| = 2\sqrt{2}>2. \tag{9.36}$$

This is the theoretical maximal violation of the Bell's inequality. For the state

$$|\chi_\downarrow\rangle\big(rt|{\rm L}\rangle|{\rm R}\rangle + rt|{\rm R}\rangle|{\rm L}\rangle\big) \tag{9.37}$$

we have to substitute $\theta_2\to-\theta_2$.

Bibliography

[1] L. D. Landau and E. M. Lifshitz, *Quantum Mechanics*, vol. 3 of *Course of Theoretical Physics* (Pergamon Press, London, 1958).

Chapter 10

Full Counting Statistics

10.1 Introduction

In general, it is not only interesting to measure the average current through a quantum wire but also higher moments,

$$\langle Q^n \rangle = \int_0^t dt_1 \cdots dt_n \, \langle I(t_1) \cdots I(t_n) \rangle. \tag{10.1}$$

Given the knowledge of all the cumulants, one can infer the noise such a quantum wire would induce on a nearby quantum system without using the assumption of Gaussian noise [1–3]. Furthermore, it allows for a precise discussion of the detector properties of a quantum point contact coupled to a nearby quantum bit [4]. Customary, all the information of the moments is combined in the generating function

$$\chi(\lambda) = \sum_n \frac{\langle (-Q/e)^n \rangle}{n!} (i\lambda)^n = \langle e^{-i\lambda Q/e} \rangle; \tag{10.2}$$

called the characteristic function of the "full counting statistics"; the arbitrary factor of $-e$ has been introduced to render λ dimensionless. The characteristic function provides all the information about the charge transport and enables an easy determination of the moments via taking derivatives

$$\langle (-Q/e)^n \rangle = \frac{d^n}{d(i\lambda)^n} \chi(\lambda) \bigg|_{\lambda=0}. \tag{10.3}$$

However, cumulants defined via

$$\langle\langle (-Q/e)^n \rangle\rangle = \frac{d^n}{d(i\lambda)^n} \log \chi(\lambda) \bigg|_{\lambda=0} \tag{10.4}$$

are usually better suited than moments to characterize a random process. They have the following important properties: (i) if the random variable is shifted by an amount c then all cumulants $n \leq 2$ remain invariant, $\langle\langle (Q+c)^n \rangle\rangle = \langle\langle Q^n \rangle\rangle$. (ii) they are homogeneous of degree n, $\langle\langle (cQ)^n \rangle\rangle = c^n \langle\langle Q^n \rangle\rangle$. (iii) given two independent random variables Q and $\tilde{Q}$, the cumulants are additive, $\langle\langle (Q+\tilde{Q})^n \rangle\rangle = \langle\langle Q^n \rangle\rangle + \langle\langle \tilde{Q}^n \rangle\rangle$. From the last property, one deduce that $\langle\langle Q^n \rangle\rangle \propto t$ for large times t larger than any correlation time in the system. The argument goes as follows: for large times, the process can be thought as being composed of many subprocesses which are independent on each other (each of them being larger than the correlation time) and add up to the total answer. As the number of subprocesses grows linear in t so does the total cumulant.

Next, we want to introduce the notion of the number n of electrons transfered in the time t which is related to the charge via $Q = -en$. The random process is determined by the probabilities P_n that exactly n electrons are transmitted in the time t, i.e.,

$$\chi(\lambda) = \langle e^{-i\lambda Q/e} \rangle = \sum_n P_n e^{i\lambda n}. \tag{10.5}$$

Note, that the assumption that n is an integer leads to the fact that $\chi(\lambda)$ is periodic with period 2π. Given the characteristic function, the P_n can be obtained by a Fourier transformation

$$P_n = \int_0^{2\pi} \frac{d\lambda}{2\pi} e^{-i\lambda n} \chi(\lambda). \tag{10.6}$$

In quantum mechanics, the problem of assigning a rigorous definition to $\chi(\lambda)$ appears. There are at least two ways to define $\chi(\lambda)$. (a) we can use the definition of the current operator

$$I(t) = \frac{ie\hbar}{2m}[\Psi(x;t)^* \Psi'(x;t) - \Psi'(x;t)^* \Psi(x;t)] \tag{10.7}$$

to calculate (10.1) which defines $\chi_I(\lambda)$. (b) we can calculate P_n using a projection of the wave function on the part describing the event of n transmitted particles; in this case $\chi(\lambda)$ is by construction 2π periodic. It turns out that the two approaches lead to different results and we have to model the specific counter together with the quantum wire in order to obtain an unambiguous result. The ambiguity can be traced back to the fact that in the quantum

version of Eq. (10.1) no recipe for the ordering of the noncommuting current operators is given. Taking (10.1) literally, the current operators should be symmetrized. On the other hand, one could think about time ordering them or any arbitrary other choice. In the following, the different approaches pursued in the literature will be outlined.

Full counting statistics was first introduced in a pioneering paper by Levitov and Lesovik in 1992 [5]. They used the definition (*a*) for a setup where a single-mode quantum wire with transmission probability T is biased by a voltage V at zero temperature. Their result

$$\begin{aligned}\chi(\lambda) &= \left\langle e^{-i\lambda \int_0^t dt' I(t')/e} \right\rangle \\ &= \left[\cos(\lambda\sqrt{T}) + i\sqrt{T}\sin(\lambda\sqrt{T})\right]^N, \end{aligned} \tag{10.8}$$

with the number of attempts $N = 2eVt/h \gg 1$, is periodic with periodicity $2\pi/\sqrt{T}$ which admits the interpretation that the charge is quantized in units of $e^* = e\sqrt{T}$. Measuring (10.1) would imply to be able to monitor the current operator instantaneously; thereby, making it essentially a classical random variable. However, any realistic measurement device averages the current operator over a small time interval so that up to our knowledge no measurement apparatus is expected to retrieve the full counting statistics given by Eq. (10.8).

Having realized the necessity to include a realistic counting procedure in the description of the full counting statistics, Levitov and Lesovik put forward the idea of counting the electrons by an auxiliary spin 1/2 degree of freedom [6, 7]; the procession frequency of the spin is proportional to the magnetic field which itself is proportional to the current. Therefore, the precession angle of the spin directly measures the transmitted charge Q. More precisely, we the interaction between the spin and electrons in the wire is given by

$$H_{\text{int}} = -\frac{1}{c}\int dx\, I(x)A(x) \tag{10.9}$$

with $A(x)$ the component along the wire of the vector potential generated by the spin 1/2. In general, the interaction is long-ranged dipole interaction. For simplicity (and to keep the charge quantization exact), we model the interaction as a point interaction with a vector potential of the form

$$A(x) = A_0\,\delta(x - x_0)\sigma_z \tag{10.10}$$

where σ_z denotes a Pauli matrix, x_0 is the position of the spin counter and A_0 is its interaction strength with the electrons in the wire. Accordingly, the interaction Hamiltonian assumes the form $H_{\rm int} = H_{{\rm int},+}|\uparrow\rangle\langle\uparrow| + H_{{\rm int},-}|\downarrow\rangle\langle\downarrow|$ with

$$H_{{\rm int},\pm} = \mp\lambda\frac{\hbar I(x_0)}{2e} \tag{10.11}$$

and $\lambda = 2eA_0/\hbar c$. Given an initial position of the spin counter described by the density matrix $\rho^{\rm s}(0)$ at time $t = 0$, the counting statistics is expected the reveal itself in the rotation angle of the spin (off-diagonal element of the density matrix) after a time t. The time evolution of the off-diagonal element of the spin density matrix is given by (assuming the density matrix at time $t = 0$ to be separable with $\rho^{\rm w}(0)$ the density matrix of the electronic subsystem)

$$\begin{aligned}\rho^{\rm s}_{\downarrow\uparrow}(t) &= {\rm Tr}_{\rm w}\left[e^{-i(H_{\rm w}+H_{{\rm int},-})t/\hbar}\,\rho_e(0)\,e^{i(H_{\rm w}+H_{{\rm int},+}/\hbar)}\right]\rho^{\rm s}_{\downarrow\uparrow}(0) \\ &= {\rm Tr}_{\rm w}\Big(\left[e^{-i\lambda\int_0^t dt' I(x_0,t')/2e}\right]_-\rho^{\rm w}(0)\left[e^{-i\lambda\int_0^t dt' I(x_0,t')/2e}\right]_+\Big)\rho^{\rm s}_{\downarrow\uparrow}(0)\end{aligned} \tag{10.12}$$

where the trace ${\rm Tr}_{\rm w}$ is taken over the electronic degrees of freedom, $H_{\rm w}$ denotes the Hamiltonian of the electronic subsystem. In going from the first to the second line in (10.12), we went from the Schrödinger to the interaction picture where the free evolution operator $H_{\rm w}$ dictates the time evolution of the current operator $I(x_0, t)$; furthermore, $[\cdot]_\pm$ denote time- and antitime-ordering of the operators enclosed, respectively. Defining $\chi(\lambda)$ to be $\rho^{\rm s}_{\downarrow\uparrow}(t)/\rho^{\rm s}_{\downarrow\uparrow}(0)$, the generating function of the full counting statistics for a spin counter assumes the form

$$\chi(\lambda) = \left\langle\left[e^{-i\lambda\int_0^t dt' I(t')/2e}\right]_+\left[e^{-i\lambda\int_0^t dt' I(t')/2e}\right]_-\right\rangle. \tag{10.13}$$

The difference to (10.8) is due to the distinct ordering of the current operators. Given the definition (10.13), the characteristic function of the full counting statistics for the constant voltage setup

$$\chi(\lambda) = \left[1 - T + Te^{i\lambda}\right]^N \tag{10.14}$$

is 2π periodic, which infers a quantization of the charge in units of e. Even though for the constant voltage case the spin 1/2 definition of the full counting statistics turns out to be 2π periodic there is no argument why this should be the case for general setups, i.e., for general H_e and $\rho_e(0)$. Even

more, Shelankov and Rammer [8] have constructed an example where the initial state is a superposition of electrons incoming from the left and from the right where the generating function is only 4π periodic; note that even though the spin counter does not always provide an answer where the charge is quantized in units of e, the generating function is measurable and corresponds to the dephasing of a qubit coupled to the quantum wire, cf. Ch. **??**. Shelankov and Rammer provided an alternative definition of $\chi(\lambda)$ which is 2π periodic and where the associated P_n can be proven to be positive. This new definition matches the idea to measure P_n directly, definition (b), proposed by Muzykantskii and Adamov [9] and used by others [10, 11]. Performing a measurement modeled by the operator $\mathcal{Q} = \int_{x_0}^{\infty} dx\, |x\rangle\langle x|$ which measures the charge to the right of the counter at time $t = 0$ and comparing it to the charge residing there at time t we can infer the number of electrons which passed the counter during the time t. This measurement setup yields the characteristic function

$$\chi(\lambda) = \langle e^{-i\lambda U^\dagger \mathcal{Q} U/e} e^{i\lambda \mathcal{Q}/e} \rangle, \tag{10.15}$$

where $U = \exp(-iH_{\rm w}t)$ is the (unitary) evolution operator and $\langle\cdot\rangle$ is an average over an eigenstate of the operator $\mathcal{Q}$, i.e., the particles are initially either to the left or to the right of the scatterer thereby avoiding the states which lead to a 4π periodic generating function in the case of the spin counter. A different definition of $\chi(\lambda)$ was put forward by Nazarov using the Keldysh formalism in a system without physical analogue which involves different Hamiltonians $H_{\rm w} + H_{{\rm int},\pm}$ on the forward and backward time contour, cf. Eq. (10.12) [12].

10.2 Full counting statistics of one single electron

Consider a wave packet (for $t \to -\infty$ and traveling to the right)

$$\Psi_{\rm in}(x,t) \equiv \Psi_f(x,t) = \int \frac{dk}{2\pi} f(k)\, e^{i(kx - \omega_k t)}, \tag{10.16}$$

centered around $k_0 > 0$ with quadratic dispersion $\omega_k = \hbar k^2/2m$ and normalization $\int (dk/2\pi)|f(k)|^2 = 1$, incident on a scatterer characterized by transmission and reflection amplitudes t_k and r_k. We place the qubit behind the

scatterer to have it interact with the transmitted part of the wave function. The transmitted wave packet then acquires an additional phase due to the interaction with the qubit: for a magnetic interaction the extra phase accumulated up to the position x amounts to $\delta\phi_A(x) = 2\pi \int^x dx'\, A_x(x')/\Phi_0$, independent of k; as $x \to \infty$ this adds up to a total phase $\lambda/2 = 2\pi \int_{-\infty}^{\infty} dx\, A_x(x)/\Phi_0$, cf. (**??**). For an electric interaction, cf. (**??**), the situation is slightly more involved: the extra phase can be easily determined for a slowly varying (quasiclassical) potential of small magnitude, i.e., $e|\varphi| \ll \hbar^2 k_0^2/2m$. Expanding the quasiclassical phase $\int^x dx'\, p(x')/\hbar$ with $p(x) = \sqrt{2m(E + e\varphi(x))}$ to first order in the potential $\varphi(x)$ yields the phase $\delta\phi_\varphi(x) = (e/\hbar v)\int^x dx'\, \varphi(x')$ which asymptotically accumulates to the value $\lambda/2$; its v-dependence is due to the particle's acceleration in the scalar potential and will be discussed in more detail below. Moreover, note that ϕ_A changes sign for a particle moving in the opposite direction ($k \to -k$) (i.e., under time reversal) whereas ϕ_φ does not. For a qubit placed behind the scatterer both magnetic and electric couplings produce equivalent phase shifts. Depending on the state $|\pm\rangle$ of the qubit, the outgoing wave (for $t \to \infty$)

$$\Psi^{\pm}_{\text{out}}(x,t) = \int \frac{dk}{2\pi} f(k) e^{-i\omega_k t}\left[r_k e^{-ikx}\Theta(-x) + e^{\pm i\lambda/2} t_k e^{ikx}\Theta(x)\right]$$

acquires a different asymptotic phase on its transmitted part. The fidelity is given by the overlap of the two outgoing waves,

$$\begin{aligned}\chi(\lambda,t) &= \int dx \Psi^{-}_{\text{out}}{}^{*}(x,t)\Psi^{+}_{\text{out}}(x,t) = \int \frac{dk}{2\pi}(R_k + e^{i\lambda}T_k)|f(k)|^2 \\ &= \langle R\rangle_f + e^{i\lambda}\langle T\rangle_f, \end{aligned} \tag{10.17}$$

where $R_k = |r_k|^2$ and $T_k = |t_k|^2$ denote the probabilities for reflection and transmission, respectively, and we have neglected exponentially small off-diagonal terms involving products $\int dk f(-k)^* f(k)$. The result (10.17) applies to both magnetic and electric couplings; its interpretation as the generating function of the charge counting statistics provides us with the two nonzero Fourier coefficients $P_0 = \langle R\rangle_f$ and $P_1 = \langle T\rangle_f$ which are simply the probabilities for reflection and transmission of the particle. This result agrees with the usual notion of 'counting' those particles which have passed the qubit behind the scatterer. When, instead, the interest is in the system's sensitivity, we observe that the fidelity $\chi(\lambda,t)$ lies on the unit circle only for the 'trivial' cases of zero or full transmission $T = 0,\ 1$, i.e., in the absence of

partitioning, or for $\lambda = 2\pi\mathbb{Z}$; the latter condition corresponds to no counting or the periodic vanishing of decoherence in the qubit. On the contrary, in the case of maximal partitioning with $\langle R\rangle_f = \langle T\rangle_f = 1/2$, a simple phase shift by $\lambda = \pi$ makes the fidelity vanish altogether. Hence, partitioning has to be considered as a (purely quantum) source of sensitivity towards small changes, as chaoticity generates sensitivity in a quantum system with a classical analogue.

The result (10.17) also applies for a qubit placed in front of the scattering region provided the coupling is of magnetic nature (for the reflected wave, the additional phases picked up in the interaction region cancel, while the phase in the transmitted part remains uncompensated). However, an electric coupling behaves differently under time reversal and the fidelity acquires the new form

$$\chi(\lambda, t) = e^{i\lambda}\big(e^{i\lambda}\langle R\rangle_f + \langle T\rangle_f\big). \tag{10.18}$$

Next, we comment on the (velocity) dispersion in the electric coupling λ: the different components in the wave packet then acquire different phases. To make this point more explicit consider a Gaussian wave packet centered around k_0 with a small spreading $\delta k \ll k_0$ and denote with λ_0 the phase associated with the k_0 mode. The spreading δk in k generates a corresponding spreading in $\delta\lambda \approx \lambda_0(\delta k/k_0)$ which leads to a reduced fidelity

$$\chi(\lambda, t) = \langle R\rangle_f + \langle e^{i\lambda}T\rangle_f \approx R_{k_0} + e^{i\lambda_0 - \frac{\lambda_0^2(\delta k)^2}{2k_0^2}} T_{k_0}, \tag{10.19}$$

where we have assumed a smooth dependence of T_k over δk in the last equation. The reduced fidelity for $T = 1$ is due to the acceleration and deceleration produced by the two states of the qubit.[1] The wave packets passing the qubit then acquire a different time delay depending on the qubit's state. As a result, the wave packets become separated in space with an exponentially small residual overlap for the Gaussian shaped packets.

Bibliography

[1] G. Falci, E. Paladino, and R. Fazio, *Decoherence in Josephson qubits*, in *Quantum Phenomena in Mesoscopic Systems*, edited by B. Al'tshuler, A. Tagliacozzo, and V. Tognetti (IOS Press, Amsterdam, 2003).

[1] The fidelity involves the matrix element of wave functions perturbed by opposite states of the qubit.

[2] Yu. M. Galperin, B. L. Al'tshuler, and D. V. Shantsev, *Low-frequency noise as a source of dephasing of a qubit*, Phys. Rev. Lett. **96**, 097009 (2006).

[3] I. Neder, F. Marquardt, M. Heiblum, D. Mahalu, and V. Umansky, *Controlled dephasing of electrons by non-gaussian shot noise*, Nature Physics **3**, 534 (2007).

[4] D. V. Averin and E. V. Sukhorukov, *Counting statistics and detector properties of quantum point contacts*, Phys. Rev. Lett. **95**, 126803 (2005).

[5] L. S. Levitov and G. B. Lesovik, *Charge-transport statistics in quantum conductors*, JETP Lett. **55**, 555 (1992).

[6] L. S. Levitov and G. B. Lesovik, *Quantum measurement in electric circuit*, cond-mat/9401004 (1994).

[7] L. S. Levitov, H. W. Lee, and G. B. Lesovik, *Electron counting statistics and coherent states of electric current*, J. Math. Phys. **37**, 4845 (1996).

[8] A. Shelankov and J. Rammer, *Charge transfer counting statistics revisited*, Europhys. Lett. **63**, 485 (2003).

[9] B. A. Muzykantskii and Y. Adamov, *Scattering approach to counting statistics in quantum pumps*, Phys. Rev. B **68**, 155304 (2003).

[10] K. Schönhammer, *Full counting statistics for noninteracting fermions: Exact results and the Levitov-Lesovik formula*, Phys. Rev. B **75**, 205329 (2007).

[11] J. E. Avron, S. Bachmann, G. M. Graf, and I. Klich, *Fredholm determinants and the statistics of charge transport*, Commun. Math. Phys. **280**, 807 (2008).

[12] Yu. V. Nazarov, *Universalities of weak localization*, cond-mat/9908143 (1999).